CORRELATION OF LOCALLY-BASED PERFORMANCE OF ASPHALTS WITH THEIR PHYSICOCHEMICAL PARAMETERS

TASK 1 REPORT
JANUARY 1988

IOWA DOT PROJECT HR-298
ERI PROJECT 1942

Sponsored by the Highway Division of the Iowa Department of Transporatation and the Iowa Highway Research Board.

ENGINEERING RESEARCH INSTITUTE
iowa state university

eri 88-408

CORRELATION OF LOCALLY-BASED PERFORMANCE OF ASPHALTS WITH THEIR PHYSICOCHEMICAL PARAMETERS

TASK 1 REPORT
JANUARY 1988

D. Y. LEE
B. V. ENUSTUN

IOWA DOT PROJECT HR-298
ERI PROJECT 1942

Sponsored by the Highway Division of the Iowa Department of Transportation and the Iowa Highway Research Board.

TABLE OF CONTENTS

LIST OF TABLES

LIST OF FIGURES

LIST OF FIGURES (Cont'd.)

I. INTRODUCTION

1.1. Background

Current specifications for asphalt cement contain limits on physical properties based on correlations established in the past with field performance of asphalt pavements. Recently, however, concerns have arisen that although current asphalts in use meet these specifications, they are not consistently providing the long service life once achieved.

There are a number of logically possible explanations of this situation:

[1] A considerable concern is associated with the recent world crude oil supply and the economic climate after the 1973 oil embargo which may have affected the properties of asphalt of certain origin (Hodgson, 1984). Blending several crudes, as routinely practiced in refineries to produce asphalts meeting current specifications, may have upset certain delicate balances of compatibility between various asphaltic constitutents, which may manifest itself in their long-term field performance but not in original physical properties specified in the specifications (Goodrich et al., 1985; and Petersen, 1984).

[2] The increased volume and loads of traffic on highways, which have occurred over the decades, may have shortened the life span of pavements, indicating the necessity of revising specification limits and/or imposing new provisions to maintain desired durability.

[3] Inadequate mixture design, particularly poor gradation of aggregates, changing construction practices and improper use of additives may also be responsible for early deterioration of asphalt pavements (Anderson and Dukatz, 1985; and Hodgson, 1984).

[4] Specifications based only on physical properties of asphalts do not guarantee adequate performance.

While the performance of the asphalt pavements could be improved by judicious application of improved mix design techniques, more rational thickness design procedures, better construction methods and quality control measures, selection of asphalts based on performance-related properties, tests, and specifications is the key to durable asphalt pavements.

Highway Research Project HR-298 was approved by the Iowa Highway Research Board on December 2, 1986 to study the relationships between the performance of locally available asphalts and their physicochemical properties under Iowa conditions with the ultimate objective of development of locally and performance-based asphalt specifications for durable pavements; funding for Task 1 (year 1) of the three-year study was authorized in January 1987. This Task 1 report describes work performed and findings resulted during the first year of the study.

1.2. Objectives

The objective of this study was to establish locally-based quality and performance criteria for asphalts, and ultimately to develop performance-related specifications based on simple physicochemical methods. Three of the most promising chemical methods (high performance liquid chromatography or HPLC, thermal analysis or TA and X-ray diffraction or XRD) were selected to analyze samples of:

a. Virgin asphalts from local suppliers.

b. Virgin asphalts subjected to thin film oven test.

c. Asphalts extracted from laboratory mixes prepared using the virgin asphalts after they are artifically aged in chambers under accelerated environmental conditions (exposures to ultraviolet and infrared radiations, temperature and moisture extremes).

d. Asphalts extracted from pavements with known performance records.

The results obtained will be analyzed to find the fundamental asphalt property variables (such as viscosity, molecular size, micelle size, transition temperatures, temperature susceptibility, resistance to oxidative hardening, reactivity with environment, etc.) which directly affect the field performance in Iowa.

On the basis of the laboratory-field-property-performance correlations, we expect to formulate specifications and establish testing procedures which can be performed in the transportation materials laboratories of the Iowa DOT and ISU.

1.3. Program of Study

The ultimate objective of this study is to establish locally-based quality and performance criteria as a basis for asphalt specifications, in other words, the development of performance-based specifications for the state of Iowa.

This research will be carried out in six tasks completed in three years. The specific tasks to be performed were presented in the research proposal and are shown in Figure 1.

2. EXPERIMENTAL

2.1 Materials

Asphalt cement samples representing those commonly used in Iowa were obtained from Koch Asphalt Co., St. Paul and Jebro, Inc., Sioux City, Iowa. Two sets of asphalt samples were supplied by each of the two suppliers: each set of samples consisted of one AC-5, one AC-10 and one AC-20. The two sets of samples from Jebro were received in February and September 1987; those obtained from Koch were received in June and October 1987. A total of 12 virgin asphalt cement samples were tested in Task 1. They were identified as J0501, J0502, J1001, J1002, J2001, J2002, K0501, K0502, K1001, K1002, K2001 and K2002.

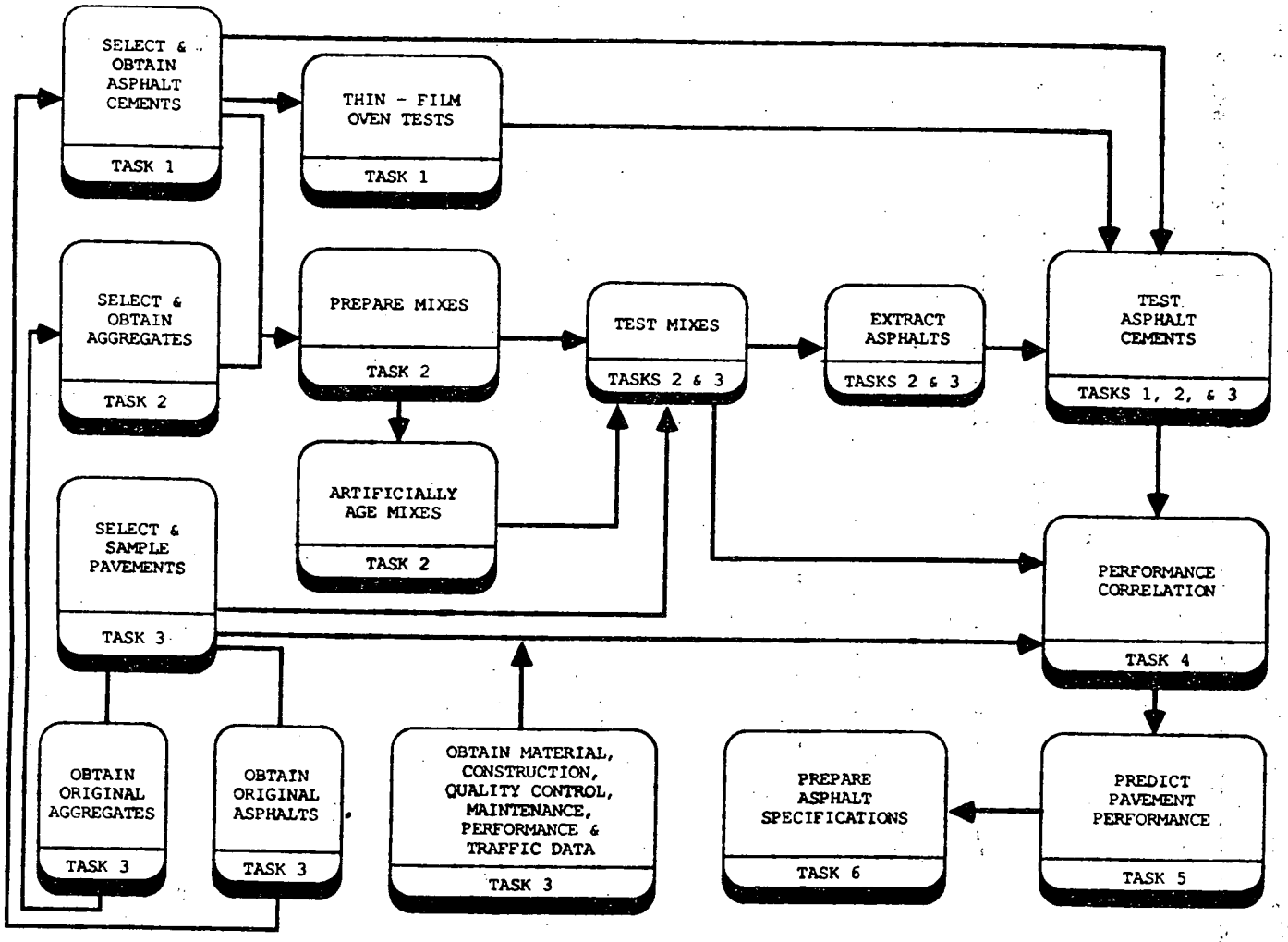

FIGURE 1. SUMMARY OF PROPOSED RESEARCH

In addition, two sets of asphalt samples recovered from pavement cores taken in April 1987 were provided by the Materials Laboratory, Iowa DOT. These samples were taken from seven-year old pavements of known performance with respect to cracking (Marks and Huisman, 1985). They were identified as Sugar Creek (surface, binder and base) and Wood River (surface, binder and base), respectively.

Furthermore, 25 reference asphalt samples with extensive data from FHWA and a reference asphalt from Montana State University were also obtained and will be evaluated in Tasks 4 to 6.

2.2. Procedures

The 12 virgin asphalts (O samples) were first aged following thin-film oven test procedure (ASTM D 1754) and identified as R samples. The 12 original (O) and 12 aged (R) samples were then characterized by physical and chemical tests as described in the following sections:

2.2.1. Rheological properties : Penetration at 41 and 77°F, viscosity at 77, 140 and 275°F, and ring-and-ball softening point tests were performed on both original and TFOT aged residue asphalts. From these data penetration index (PI), pen-vis number (PVN), viscosity temperature susceptibility, cracking temperature, critical stiffness and critical stiffness temperature were calculated.

In addition to the above mentioned standard tests, certain rheological properties of a few samples were studied in greater depth at a moderately low temperature, which might have some bearing on their low temperature performance in the field. They were the samples J05-01-0, J10-01-0, J20-01-0, SC-S (Sugar Creek surface) and WR-S (Wood River surface). The primary purpose of these experiments was to see how the low temperature transformations revealed by thermal analysis, to be described later, reflect on rheological properties.

The secondary purpose was to study the time dependence of these properties at a low temperature.

A review of the relevant literature reveals that a considerable effort has been made by the researchers sponsored by asphalt producers to establish a universal relationship to describe rheological properties of all asphalts (Brodnyan et al., 1960; Sisko and Brunstrun, 1968; Jongepiev and Kuilman, 1969; and Dobson, 1969). However, the question of how fast an asphalt sample acquires these properties when brought to a given temperature from a different temperature, or whether these properties are indeed single valued functions of temperature for practical purposes, seems to have received little attention. The lower the temperature, the more valid become these questions due to sluggish behavior of asphalts. The contributions of many authors in this field were confined to their in-passing remarks that rheological properties of asphalts depend on their thermal history.

Hoping to get some discriminating information on asphalts possibly related to thermal cracking of pavements, we studied viscoelastic properties of a few samples at +5°C as a function of their thermal history and time. The reasons for choosing this temperature were the following:

(1) It was the lowest temperature at which rheological tests were manageable with the equipment on hand.

(2) It may reasonably be considered as an intermediate winter temperature which prevails after a warm spell or after a severe cold.

(3) It is within a temperature range in which most asphalts suffer a thermal (endothermic) transformation upon heating (Noel and Corbett, 1970; Albert et al., 1985; and Brule et al., 1986).

Experiments were designed to estimate the elastic shear modulus of the samples, as well as their Newtonian viscosities at +5°C, using a cone and plate viscometer.

To provide Newtonian conditions, the samples had to be sheared at extremely low rates. This requirement coupled with shortening the testing time made it necessary to increase the accuracy of displacement measurements by two orders of magnitude. This was achieved by an optical method of measurement of the rotation of the cone. For this purpose a replaceable reflecting mirror was fastened on the cone axle as shown in Figure 2. A focusable beam of light from a projection pointer was directed to the mirror, and its reflection on a graduated screen was used to measure the rotation of the cone with an accuracy of better than $\pm$ 0.005 degree. With this modification of the cone and plate instrument, it was possible to work at an angular velocity of as low as 2×10^{-5} degree/sec.

An analysis of the experimental results has shown that the rheological behavior of asphalts under Newtonian conditions at low temperatures can be described reasonably well by the equation

$$x = Lt/_{\beta} + L(1 - e^{-\varepsilon_1 t/\beta_1})/_{\varepsilon_1} + L(1 - e^{-\varepsilon_2 t/\beta_2})/_{\varepsilon_2} \qquad (1)$$

where x is the angle of rotation of the cone under an applied load L, t is time; β, β_1, β_2, ε_1 and ε_2 are constants. Equation (1) is known to describe the motion of the viscoelastic system shown in Fig. 3 where the dashpots represent Newtonian viscous elements and the springs represent Hookeian elastic elements (Pagen, 1964). β characterizes the viscous behavior of the left-hand-side dashpot, and is proportional to the true (steady) viscosity of the asphalt sample. The proportionality constant is known as the "cone constant". β_1 and β_2 are similarly associated with the second and the third dashpots, respectively. ε_1 and ε_2 are the force constants of the first and the second springs, respectively. They are proportional to the shear moduli of elasticity of the sample. A typical plot of experimental x vs. t data is given in Fig. 4.

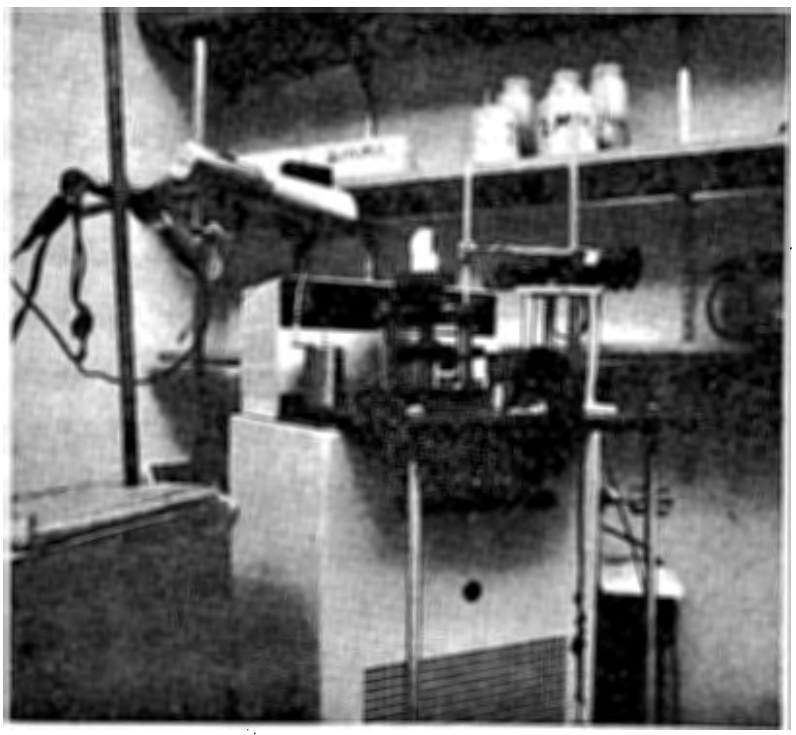

Figure 2. Modified cone and plate viscometer.

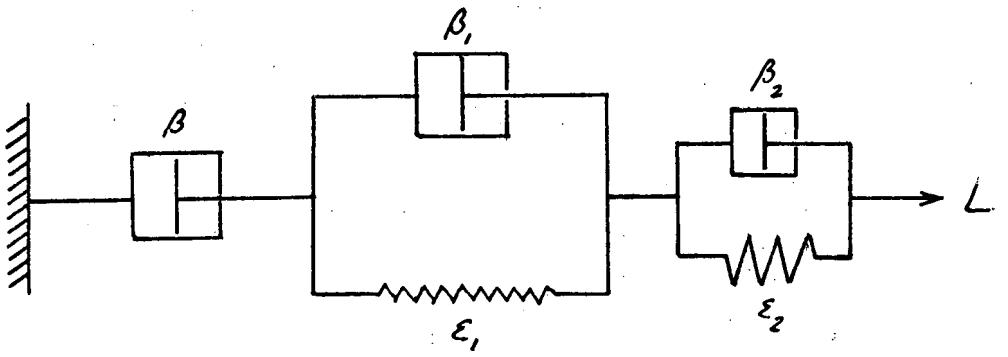

Figure 3. Mechanical model corresponding to asphalts at a low-temperature.

A detailed analysis of the experimental results shows, in general, that at +5 °C, $\beta \cong \beta_1 > \beta_2$ and $\varepsilon_1 < \varepsilon_2$.

Therefore

$$\varepsilon_1/\beta_1 \ll \varepsilon_2/\beta_2 \tag{2}$$

These make the third term in Eq. (1) negligible for most purposes.

An analytic examination of Eq. (1) in its exact form reveals that if shearing continues long enough the experimental points on a x vs. t plot fall on a straight line with a slope of L/β, and an intercept of $L\,(1/\varepsilon_1+1/\varepsilon_2)$ as indicated in Fig. 4. Therefore, it was possible to estimate the viscosity index β and an equivalent shear modulus index $\bar{\varepsilon}$ defined by

$$1/\bar{\varepsilon} = 1/\varepsilon_1 + 1/\varepsilon_2 \tag{3}$$

from the slope and the intercept, respectively, of the experimental straight line for a given set of data.

The viscoelastic properties of all five samples were investigated at +5 °C as a function of time by this method after mounting each sample on the cone and plate assembly and keeping at 25°C for 24 hours.

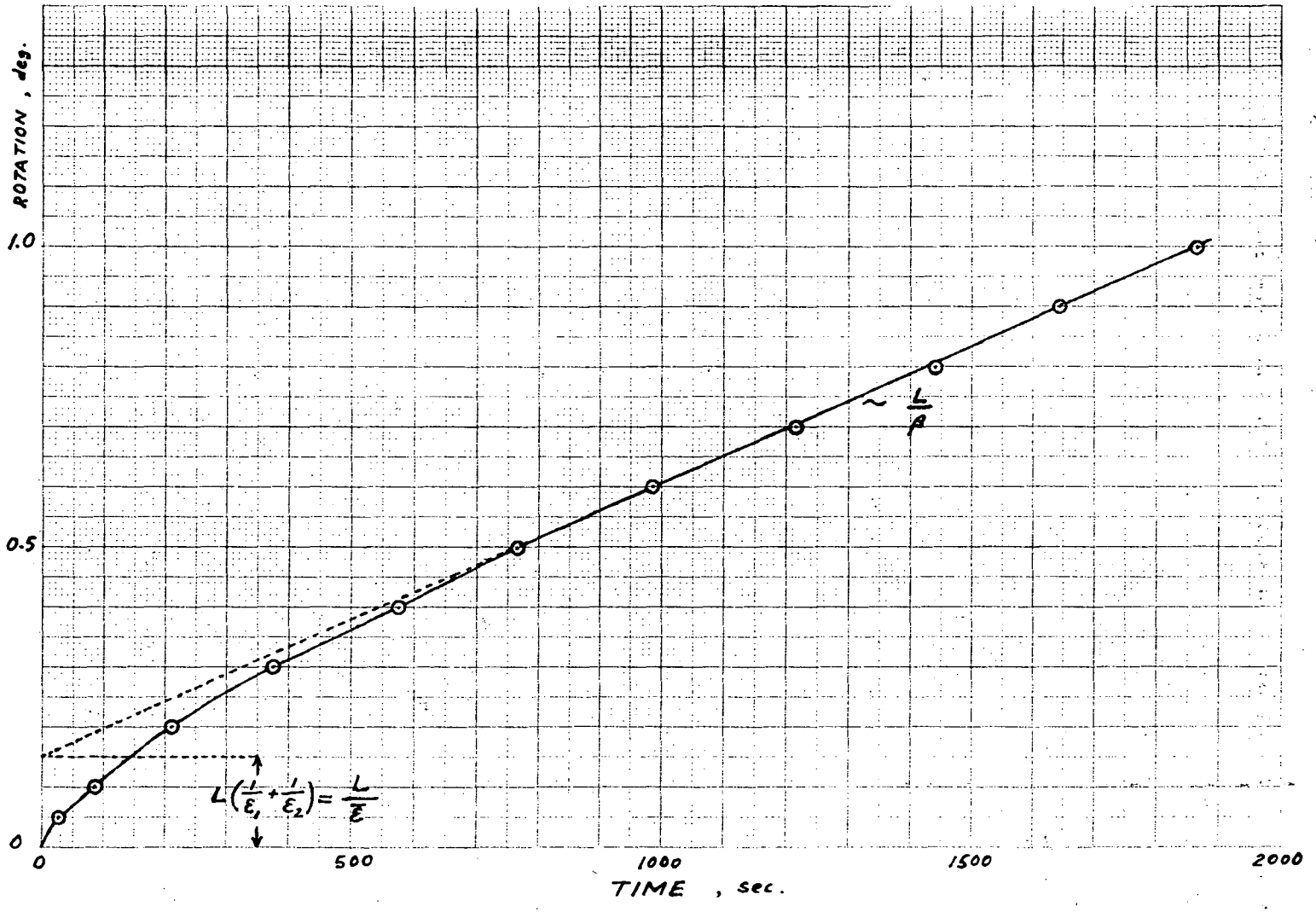

Figure 4. Viscometer rotation plotted vs. time (Sample: J05-01-0 at +5°C, after cooling from +25°C for 65 hrs; L = 100 g; cone constant = 1215 p. deg/g/sec).

Three of the samples (J05-01-0, SC-S, and WR-S) were also investigated similarly after quenching them from room temperature to -30°C for one hour and rewarming to +5°C at a rate of 0.7 degrees/min. This conditioning was an attempt to simulate the occasional severe winter conditions.

2.2.2. High performance liquid chromatography (HPLC): HPLC, specifically high pressure gel permeation chromatography (HP-GPC) is a technique by which the molecular size distribution of asphalt is determined by means of gels of selected pore sizes as in sieve analysis. Recent reports from a Montana asphalt quality study using this technique have shown considerable promise and have led the Montana State Department of Highways to institute special provisions based on requirements based on HP-GPC (Jennings et al., 1982, 1985, 1988). While there were unresolved exceptions, it has been concluded that large molecular size asphaltic constituents contribute to low temperature cracking of asphalt pavements. Other studies (Zenewitz and Tran, 1987; and Button et al., 1983) have related the amounts of small molecular size fractions to rutting and tender mixtures.

Even though the purchase request for HPLC equipment was initiated in early February 1987, shortly after the start of the research project, the equipment was not complete and operational until late August 1987. While we were able to complete the analyses of all the asphalt samples following the Montana protocol, because of time limitations we were not able to explore other experimental techniques and data analysis approaches. Recognizing the potential of the HP-GPC technique and the weakness of the Montana procedure and interpretation, it is planned that a more vigorous investigation for alternative procedures and data interpretations of HP-GPC work will be pursued in Task 2.

A high performance gel permeation chromatography system (Waters) was used during this study. This system consisted of a solvent reservoir; a high pressure pump (Waters model 510); an injector (Waters model U6K); three

"Ultrastyragel" columns (Waters), one 1000 Å followed by two 500 Å units; a UV absorbance detector set at 340 nm. (Waters model 481); and a data module (Waters model 745). The assembly of these units are seen in Fig. 5.

The solvent reservoir was a one liter bottle of tetrahydrofuran (THF) with a stopper that had been modified so that three tubes entered the solvent reservoir.

HPLC grade THF is packaged under nitrogen to preserve spectral integrity and is not inhibited for full UV transparency. To preserve these conditions and isolate the THF from atmosphere, helium gas was slowly bubbled into the solvent via the tubing connected to the helium gas cylinder.

The second tube in the stopper contained desiccant chips to prevent moisture from entering the solvent.

The third tube in the stopper was the draw-off line through which solvent was drawn from the reservoir to the pump.

The dual head design of the Waters Model 510 pump allowed one head to fill with solvent while the other was delivering solvent at increased pressure to the system and vice versa. This alternating action minimized flow fluctuations and improved flow rate.

Asphalt samples of 0.02 to 0.05 grams were accurately weighed into a 20 ml. glass Scintillation vial. THF (drawn from the solvent reservoir) was pipetted into the vial to prepare a 0.5% (w/v) solution. The sample solution was then transferred to a 15 ml. centrifuge tube, capped, and centrifuged for 10 minutes to remove foreign particles capable of plugging columns. Samples were weighed ahead of time but dilution and centrifugation were done just before injection. The delay time between sample dissolution and injection was kept constant from sample to sample (approximately 30 minutes +5 minutes).

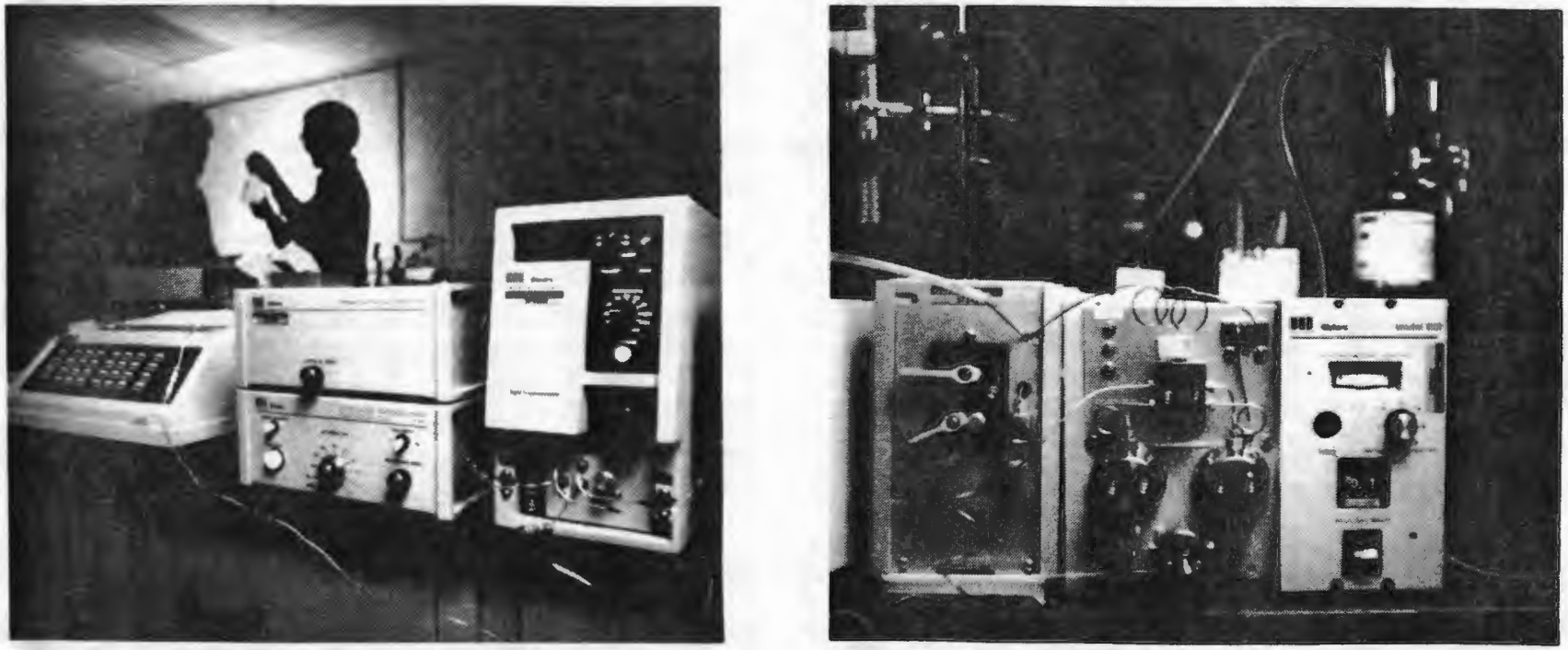

Figure 5. HP-GPC units.

The Model U6K Universal Liquid Chromatograph Injector allowed samples to be loaded at atmospheric pressure while THF was simultaneously being delivered to the system at increased pressure. This was accomplished by isolating the sample loading channel from the main stream while injecting a sample. The sample channel, opened to atmosphere, made it possible to displace solvent with sample as the sample was delivered from a syringe. After sample injection, the channel was closed to atmosphere and pressurized. The solvent preferentially passed through the sample channel (since it followed the path of least resistance) and carried the sample to the columns. Flow rate was set at 0.9 ml./min. Sample size was 100 ul.

The gel permeable columns separated the sample by molecular size. The total solvent volume in the columns was distributed between interstitial volume and pore volume. Each column contained six milliliters of interstitial and six milliliters of pore volume for a total of twelve milliliters per column. Thus, the system with three columns had a total of 36 milliliters of solvent volume. Therefore, large molecules that didn't penetrate the pores (referred to as total exclusion), passed directly through the columns and exited (or eluted) after 18 milliliters of interstitial solvent.

However, small molecules that penetrated all pores (total inclusion of both interstitial and pore volumes) eluted after 36 milliliters of solvent. Intermediate size molecules eluted between 18 and 36 milliliters. During the method's development, columns of appropriate pore size were selected so that the sample was neither totally excluded nor included, but distributed in the range between 18 and 36 milliliters. A 1000 Å and two 500 Å columns in series effectively separated the components in asphalt samples. To determine the actual exclusion and inclusion pore sizes of the columns, prior to the present studies a series of monodisperse polystyrene standards of known molecular

weight were analyzed using the uv detector at 254 nm. The following retention times were determined from these standards:

Molecular Weight	Retention Time (minutes)
470,000	17.20
240,000	17.34
110,000	17.58
35,000	18.32
8,500	20.61
1,800	23.79
Phenolphtalein (320)	28.50
Xylene (106)	34.98

These retention times will vary depending on the individual columns, the precise flow rate, the amount of dead volume in the system and possible other factors such as temperature and dilution time. Note that at molecular weights greater than 110,000 there was little change in retention time, this indicated total exclusion. The lower limit was not determined.

Gel particles within the columns are compressible and may be damaged at high pressures so the maximum pump flow rate was set at 1.2 ml./min. (or 2000 psi backpressure). Additionally, column temperature fluctuations cause particles to swell or shrink, thus changing pore size. To alleviate this problem, a constant temperature water bath at 27 °C isolated the columns from room temperature fluctuations and maintained columns at a constant temperature.

The sample eluted from columns passed through the sample side of the flow cell of the Lambda-Max Model 481 LC Spectrophotometer where a beam of UV light passed through the sample. The amount of absorbed light is assumed to be directly proportional to the concentration of asphaltic components. Absorption units detected by spectrophotometer were converted to volts and transferred to the Waters 745 Data Module where the signal was amplified and plotted versus

time. The resulting chromatograph depicted the molecular size distribution of the sample. Chromatographs were automatically divided into slices of specified time intervals and the area, molecular weight per slice, and cumulative percent of area were calculated from dialog input and printed at the end of the analysis. To standardize procedures, samples were analyzed using the same dialog settings.

Twelve virgin asphalt (O) samples and their TFOT residues (R samples), as well as six recovered core samples were analyzed by this method to determine their large molecular size (LMS) ratings. This rating has been proposed by the Montana State University research group as an index of low temperature susceptibility of an asphalt sample (Jennings et al., 1980; 1982; and 1985). It has been defined as the percent of the area under the chromatographic (340 μm) UV absorbance vs. elution time curve as far as to a retention time (ca. 22 minutes) at which a standard asphalt sample exhibits its second inflexion point, relative to the total surface area under the whole curve. Therefore, prior or subsequent to each run, the standard asphalt supplied by the Montana State University was also run to determine the correct cut-off time for that sample. This way it was possible to make the estimations independent of possible day-to-day drifts in the performance of the GPLC equipment. The absorbance printouts of the data module were used for these computations.

Needless to add that between the runs, the "Ultrastyragel" columns were routinely flushed with pure solvent for a sufficient length of time. The columns were also flushed with pyridine once approximately in every two months.

2.2.3. Thermal analyses: Thermal analysis techniques have been used extensively by chemists to identify and characterize polymers. Breen and Stephens (1967) recommended the use of glass transition temperature from thermal analysis data for predicting low temperature cracking of asphalt pavements and also point out the possibility of using it for predicting cracks due to aging.

Following the methodologies initiated by Ferry et al. (Ferry, 1961) for polymers, Schmidt et al. (1966) determined glass transition temperatures of asphalts volumetrically and used them to predict their low temperature viscosities. The predicted viscosities were not in good agreement with the measured viscosities, in general. However, although based on a single comparison, Schmidt (1966) correlates a high glass transition point, rather than a high viscosity, to low temperature cracking of pavements.

The glass transition point is known to depend on the rate of temperature change during scanning. Schmidt et al. recommend a rate of 2 degrees/min. to obtain meaningful data. They tested 52 reference samples supplied by the Bureau of Public Roads. In the present study we ran DSC tests in sealed aluminium sample holders with one of these samples (B 2975, an AC-10 asphalt) at various heating rates, using a DuPont 1090 instrument. The results are shown in Figs. 6a, b, and c. The glass transition point of this sample reported by Schmidt et al. is tg = +5.4 C. Glass transitions traceable on the curves by the method of inflexion point (Wendlandt, 1984) in the vicinity of this value are indicated on these figures. It appears from those values that the higher the heating rate, the higher the estimated transition point, and that the tg estimated at a rate of 5°C/min. is the closest to the reported value. We, therefore, used this rate throughout the present work, scanning between -80 and +80° C. The precooling rate was 10°C/min.

However, whether the apparent inflexion point in the vicinity of +5 observed with the sample B2975 indicates a glass transition or a transformation of another kind is an open question. Indeed these DSC thermograms are very similar to those reported by Noel and Corbett (1970) and Albert et al. (1985). The apparent inflexion point just mentioned happens to be in a region which is interpreted by these authors as the region of an endothermic transformation such as fusion or dissolution of crystallized asphaltic components, as will be

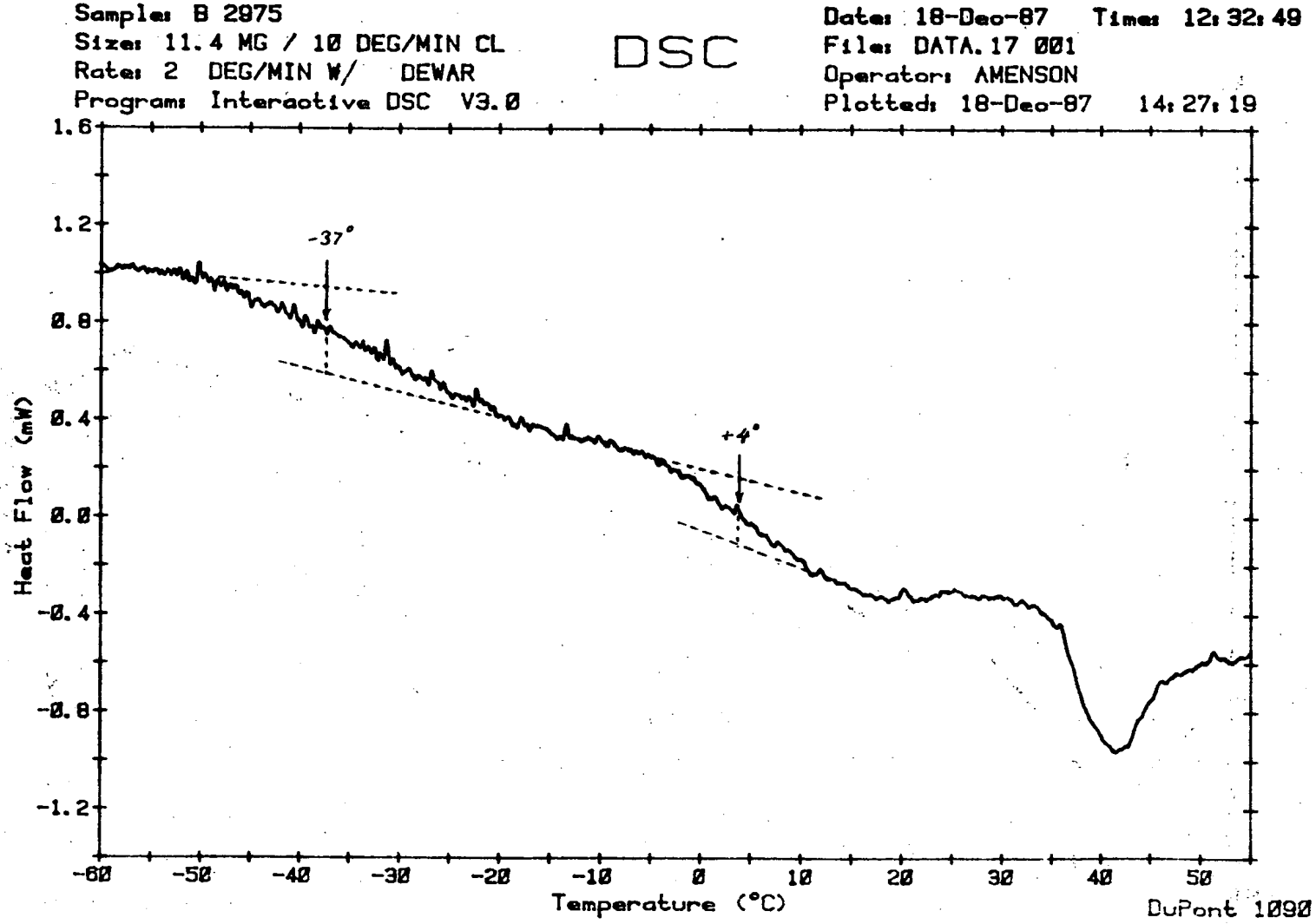

Figure 6(a). DSC thermogram of B2975 at 2 deg/min scanning rate.

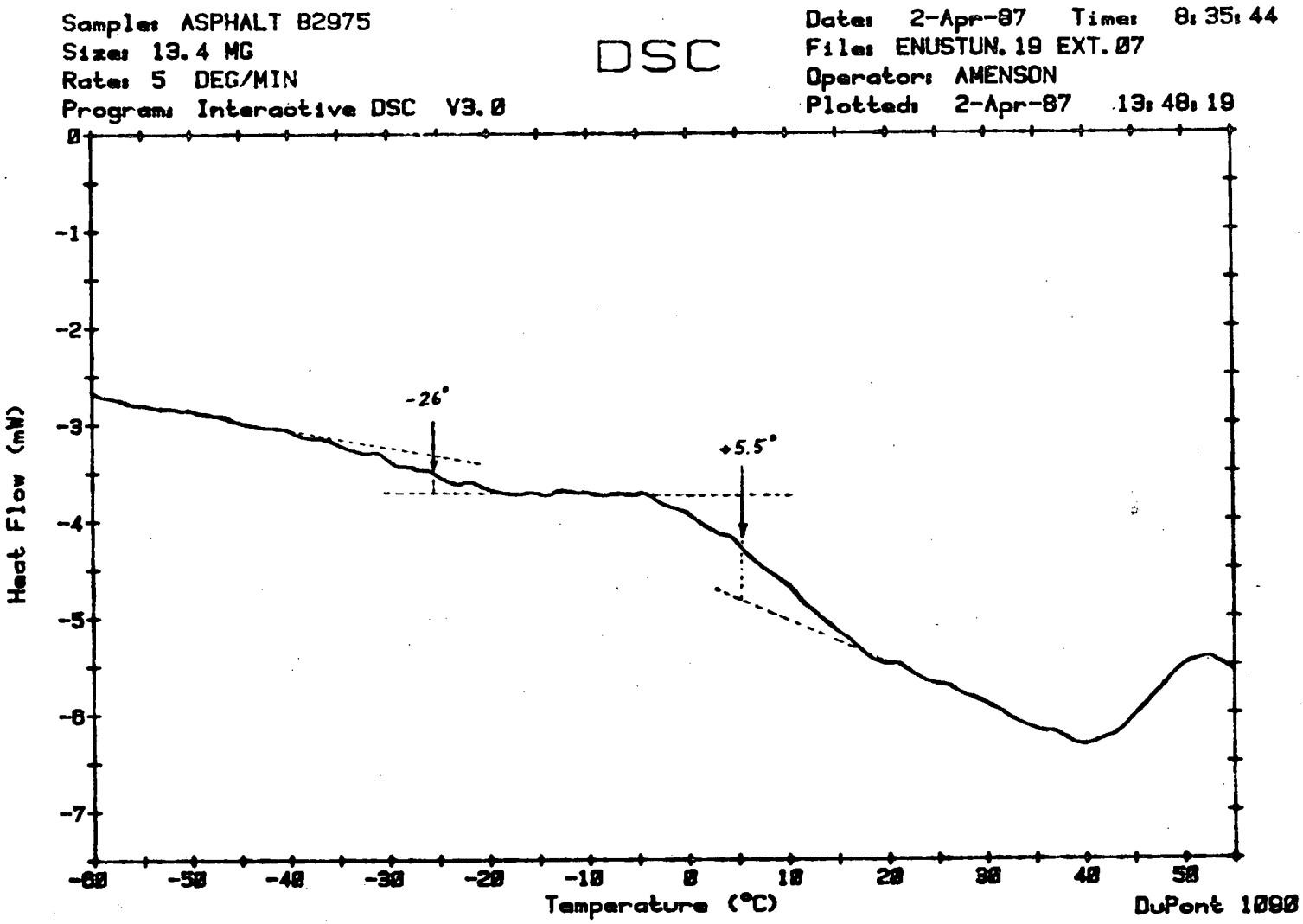

Figure 6(b). DSC thermogram of B2975 at 5 deg/min scanning rate.

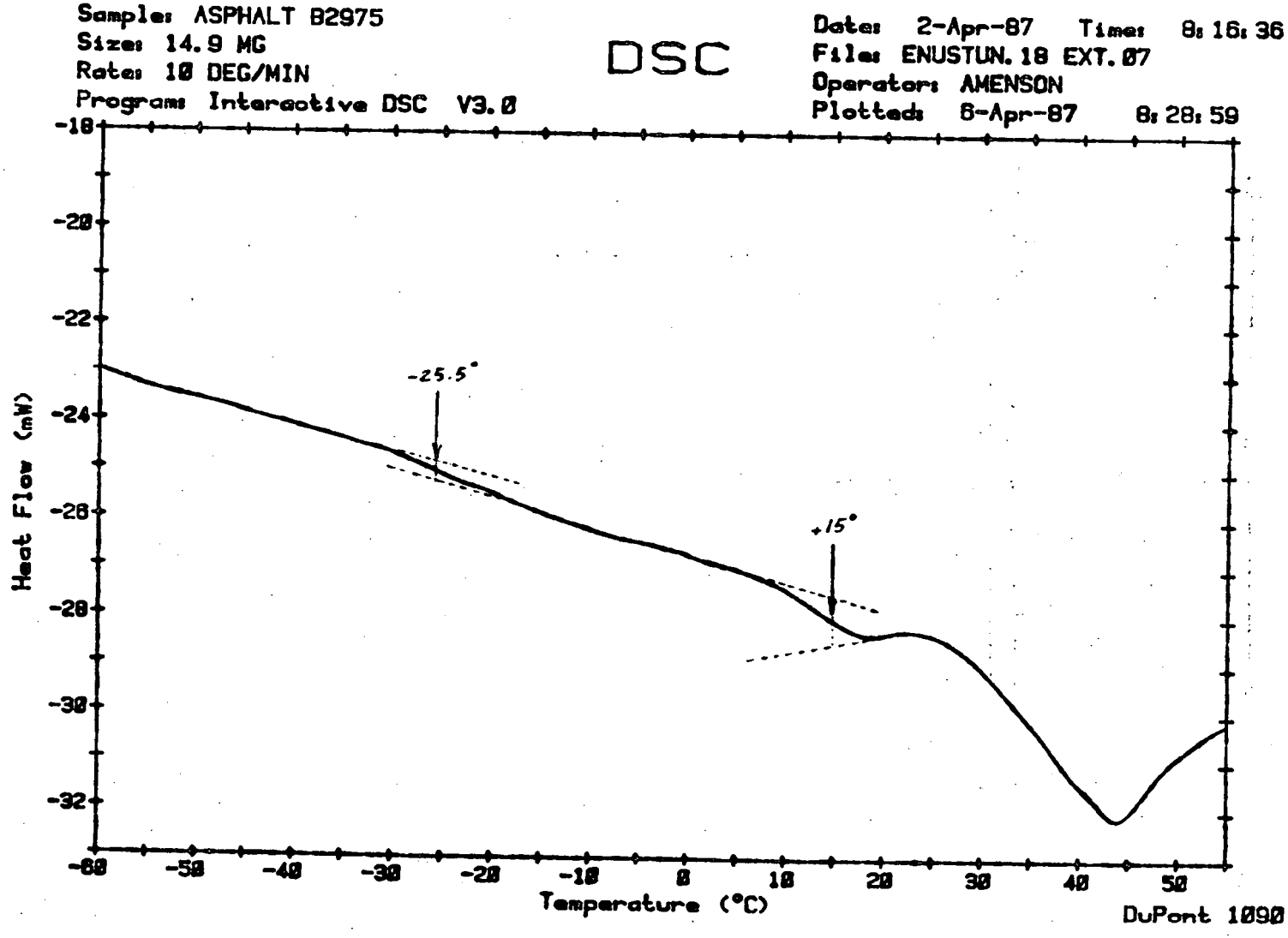

Figure 6(c). DSC thermogram of B2975 at 10 deg/min scanning rate.

discussed later. Also, there exists another inflexion point in the present thermograms at a much lower temperature which corresponds to what these authors consider as the glass transition point.

It appears that there is no correspondence between calorimetrically and volumetrically determined transition points. It is possible that the transition reported by Schmidt et al. (1966) as glass transition in the vicinity of $+5^{\circ}C$ is a volumetric manifestation of the above mentioned endothermic transformation. Our previous experience is also such that glass transition points of an asphalt sample determined by DSC do not correlate with thermomechanical results (*).

This state of affairs casts a shadow of doubt on the significance of the glass transition points of asphalts, whether determined by calorimetric or by volumetric measurements. Similar views were also expressed by Sisko et al. (1968) and Jongepier et al. (1969) to the effect that the glass transition point is an unsuitable parameter to describe the temperature dependence of rheological properties of asphalts. In spite of this criticism, we consider that DSC of asphalts may prove to be useful in indicating transformations of other kinds related to their low-temperature susceptibility, as will be discussed later.

2.2.4. X-ray diffraction: X-ray diffraction spectra of asphalts have been used for their structural characterization in relation to their quality (Williford, 1943; and Lee and Demirel, 1987).

All 12 original asphalt samples and their TFOT residues were subjected to X-ray diffraction analysis by $\theta - 2\theta$ scanning, using monochromatized CuK_{α} beam with 1.54 Å wavelength. The samples were molded in circular Plexiglas holders exactly flush with their brim. The cross section of a sample holder is seen in Fig. 7.

(*) Private communication with E. I. DePont de Nemours & Company, Wilmington, Delaware, 1971.

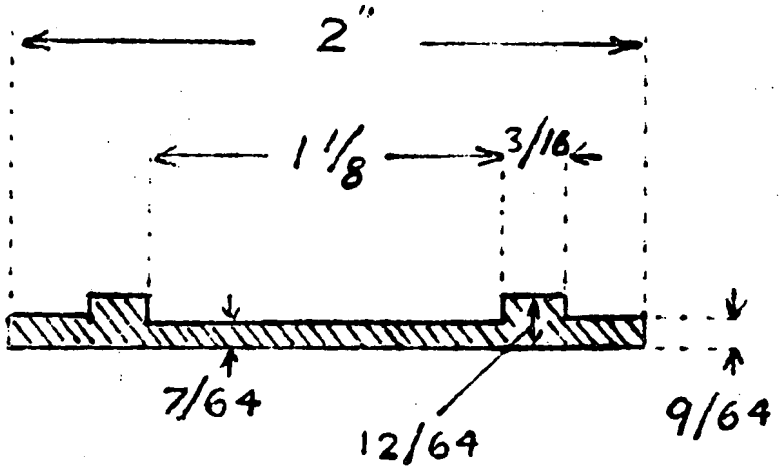

Figure 7. Cross section of x-ray analysis sample holder.

3. RESULTS

3.1. Rheological Properties

Penetrations at 5 and 25°C (41 and 77°F), viscosities at 60 and 135°C and softening points of the 12 original asphalt (O) samples as well as their thin film oven test residues (R) are given in Table 1. While all 12 samples generally met AASHTO M226-2 specifications, variations between samples and between suppliers within given viscosity grades existed. The variability in penetrations are shown in Fig. 8; the variability in viscosities are shown in Figs. 9 and 10. By far the most uniform results were observed in softening points (Fig. 11).

Table 1. Rheological properties.

Sample ID	Sp.Gr. @ 25/25	P25	P5	VIS 60 poise	VIS 135 c.s	S.P C
J05-01-O	1.024	162	16	654.0	232.8	41.5
J05-01-R	1.027	98	15	1369.6	309.3	48.0
J05-02-O	1.019	160	15	493.3	213.0	41.5
J05-02-R	1.032	79	11	1528.1	336.7	50.0
K05-01-O	1.023	193	22	556.0	225.0	40.5
K05-01-R	1.026	103	13	1272.7	334.7	49.0
K05-02-O	1.023	182	17	483.7	211.8	40.0
K05-02-R	1.026	95	13	1159.5	321.5	48.0
J10-01-O	1.031	91	11	1466.6	329.5	48.0
J10-01-R	1.034	60	8	2640.4	453.9	54.0
J10-02-O	1.019	92	11	1091.2	312.1	45.5
J10-02-R	1.031	59	10	2639.9	469.5	53.0
K10-01-O	1.028	123	15	1024.3	307.1	45.5
K10-01-R	1.030	72	9	2540.7	457.4	51.5
K10-02-O	1.028	102	11	1078.9	311.2	46.0
K10-02-R	1.031	61	10	2734.9	461.9	53.5
J20-01-O	1.028	78	12	2444.6	448.7	50.0
J20-01-R	1.029	57	10	5062.5	660.7	56.0
J20-02-O	1.018	66	8	1828.8	450.8	49.5
J20-02-R	1.029	50	8	3929.3	592.8	54.0
K20-01-O	1.031	75	10	1893.3	430.3	49.0
K20-01-R	1.034	49	8	4647.6	618.2	55.5
K20-02-O	1.031	67	7	2010.0	428.3	50.0
K20-02-R	1.034	43	6	5000.9	581.4	55.5

P25 : penetration @ 25 C, 100 g, 5 sec.
P5 : penetration @ 5 C, 100 g, 5 sec.
VIS 60 : viscosity @ 60 C.
VIS 135 : viscosity @ 135 C.
S.P : R & B softening point.
O : original.
R : thin film oven test residue.

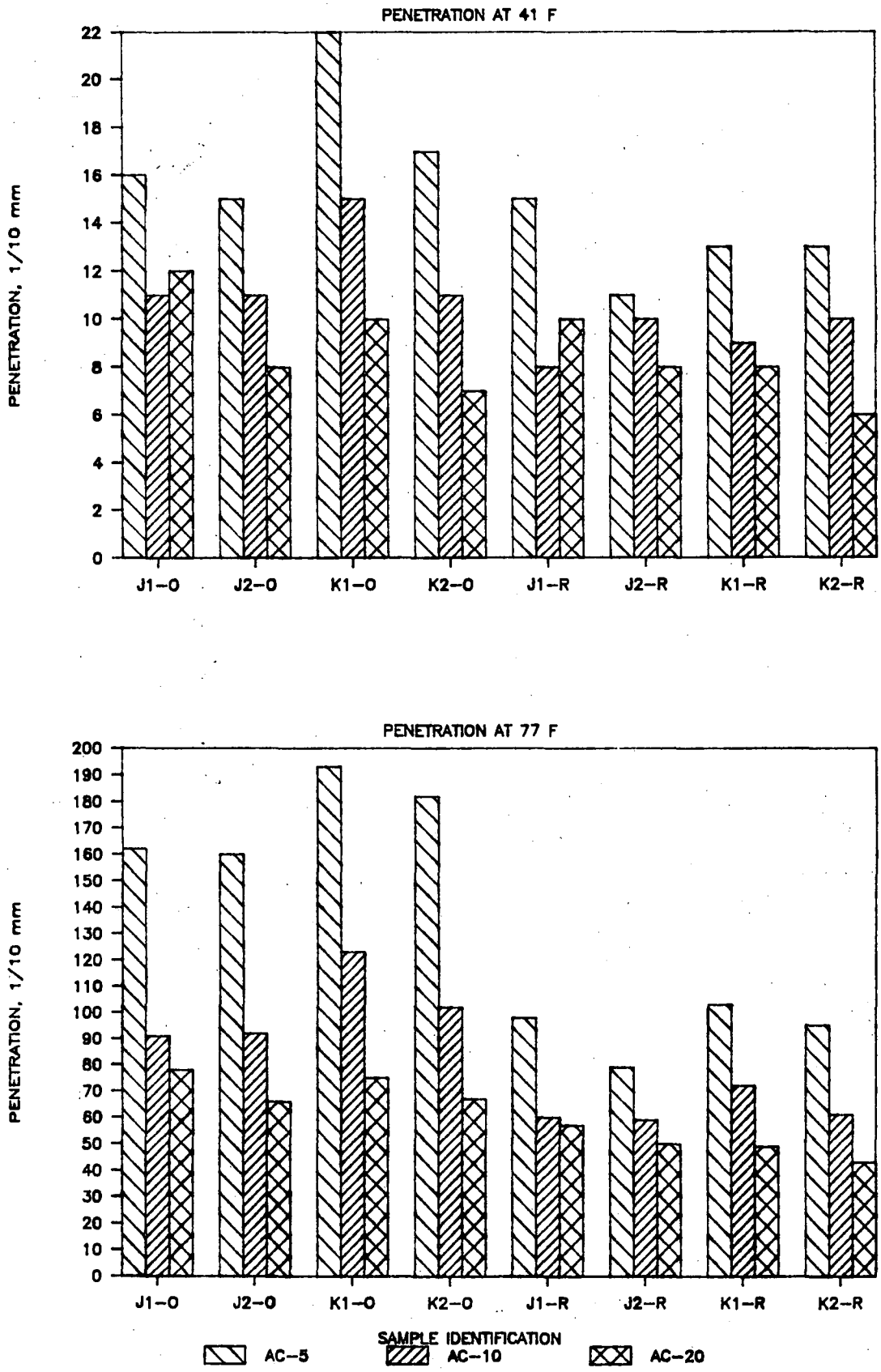

Figure 8. Penetration at 25°C (77°F) and at 5°C (41°F).

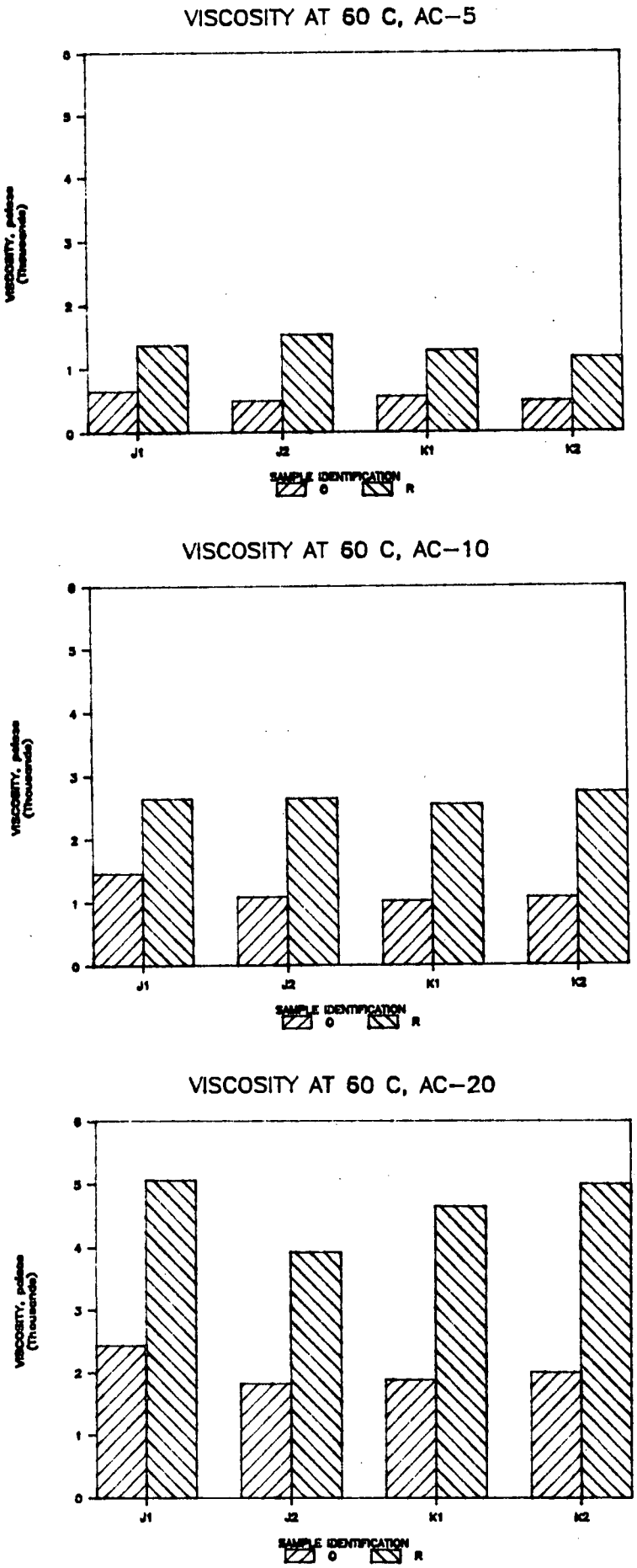

Figure 9. Viscosity at 60°C (140°F).

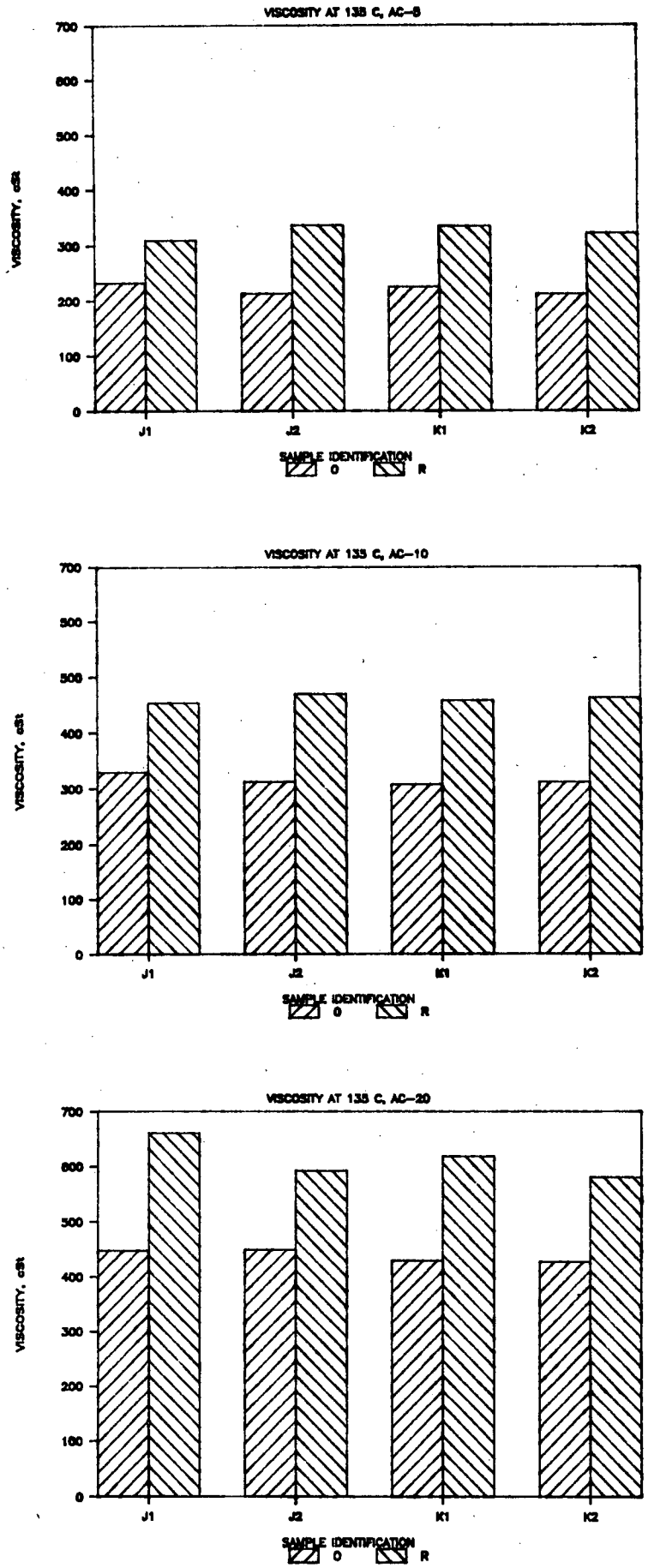

Figure 10. Viscosity at 135°C (275°F).

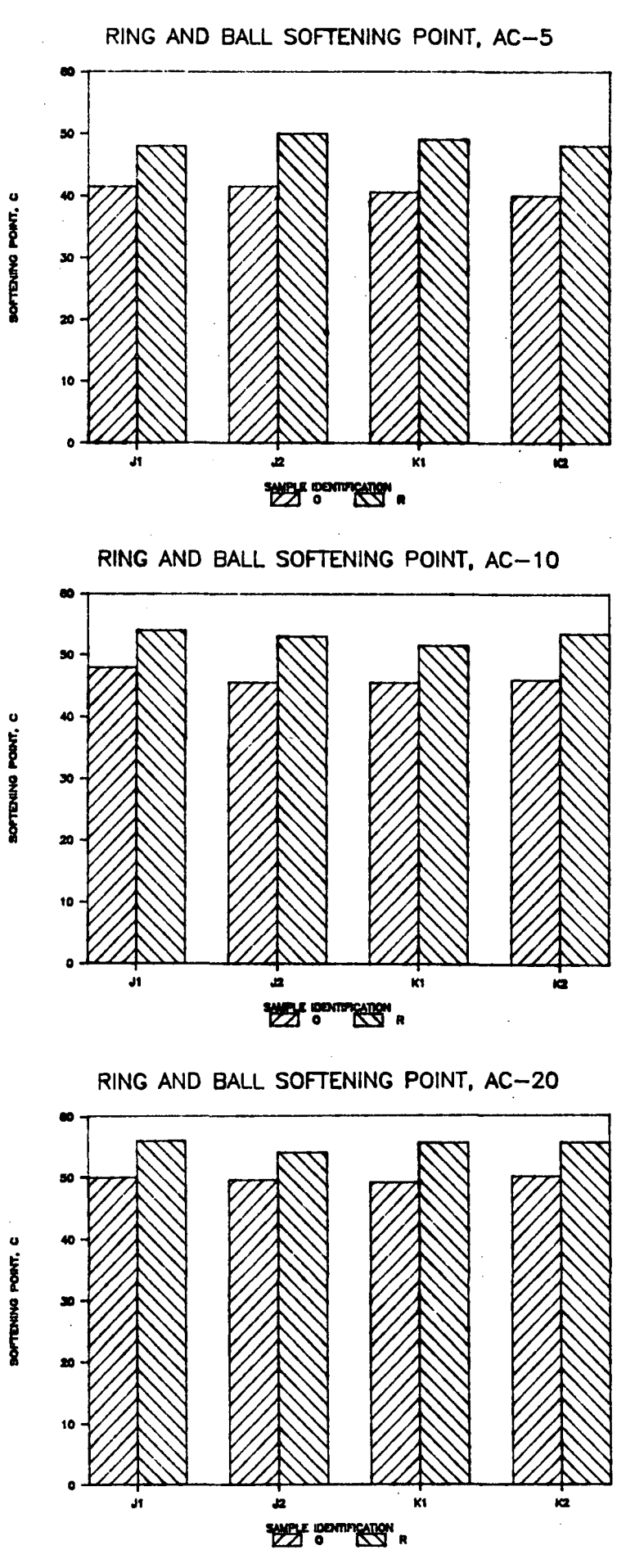

Figure 11. Ring and ball softening point.

Asphalt cements of high temperature-susceptibility may contribute to rutting at high pavement temperatures and cracking at low pavement temperatures. Temperature susceptibility of an asphalt can be evaluated by using the Shell Bitumen Test Data Chart (BTDC), the Penetration Index (PI), the Pen-Vis Number (PVN) based on viscosity at 60°C or viscosity at 135°C, the viscosity-temperature susceptibility (VTS), and the Asphalt Class Number (CN). The basic rheological data as plotted on BTDC are shown in Figs. 12 and 13; and the derived PI, PVN, VTS and CN of the asphalt cement samples studied are given in Table 2.

The CN shows the difference between measured and predicted penetration at 25°C. A small negative or positive CN value indicates a Class S (straight run with a straight line, temperature-viscosity-penetration plot) asphalt. High positive CN values indicate Class W (waxy) asphalts, and high negative CN values indicate Class B (blown) asphalts. Either case reflects substantially high and low temperature-susceptibility. While a few of the samples showed somewhat higher (e.g. J2 samples) or lower (e.g. K1 samples) temperature susceptibility, the results on temperature susceptibility, especially measured by VTS and PVN, were remarkably uniform. These are shown in Figs. 14-17.

Low-temperature asphalt stiffness has been correlated with pavement cracking associated with nonload conditions. The low-temperature behavior of asphalts can be evaluated either by estimating the temperature at which asphalt reaches a certain critical or limiting stiffness or by comparing the stiffness of asphalts at low temperatures (long loading times).

Table 3 presents the results of estimated low-temperature cracking properties of the 12 asphalts. The properties include cracking temperature (CT), temperature corresponding to asphalt thermal cracking stress of 72.5 psi (5×10^5 Pa), based on penetrations at 5°C and 25°C, temperature of equivalent

Table 2. Temperature susceptibility.

Sample ID	CN	PIm	VTS	PVN,60	PVN,135
J05-01-O	5.17	-0.327	3.538	-0.432	-0.510
J05-01-R	2.44	0.060	3.601	-0.462	-0.639
J05-02-O	11.00	-0.378	3.497	-0.784	-0.675
J05-02-R	6.38	-0.036	3.569	-0.689	-0.742
K05-01-O	5.09	0.028	3.497	-0.306	-0.344
K05-01-R	4.76	0.510	3.503	-0.459	-0.462
K05-02-O	8.73	-0.455	3.490	-0.580	-0.526
K05-02-R	8.30	-0.038	3.498	-0.691	-0.614
J10-01-O	3.67	-0.171	3.571	-0.509	-0.624
J10-01-R	4.67	0.206	3.540	-0.552	-0.595
J10-02-O	9.98	-0.884	3.504	-0.807	-0.694
J10-02-R	5.75	-0.072	3.515	-0.577	-0.565
K10-01-O	4.82	0.056	3.483	-0.400	-0.390
K10-01-R	1.28	0.091	3.522	-0.309	-0.393
K10-02-O	7.94	-0.414	3.494	-0.654	-0.586
K10-02-R	3.60	0.132	3.542	-0.492	-0.554
J20-01-O	-0.01	-0.072	3.524	-0.221	-0.333
J20-01-R	-3.67	0.526	3.499	0.016	-0.125
J20-02-O	11.75	-0.658	3.411	-0.778	-0.507
J20-02-R	4.10	-0.247	3.487	-0.433	-0.411
K20-01-O	6.84	-0.451	3.453	-0.548	-0.438
K20-01-R	1.08	0.039	3.514	-0.300	-0.375
K20-02-O	7.98	-0.488	3.481	-0.660	-0.564
K20-02-R	1.24	-0.264	3.589	-0.422	-0.586

CN : class number.
PIm : measured penetration index.
VTS : Viscosity-temperature susceptibility.
PVN,60 : Penetration-viscosity number @ 60 C.
PVN,135 : Penetration-viscosity number @ 135 C.
O : original.
R : thin film oven test residue.

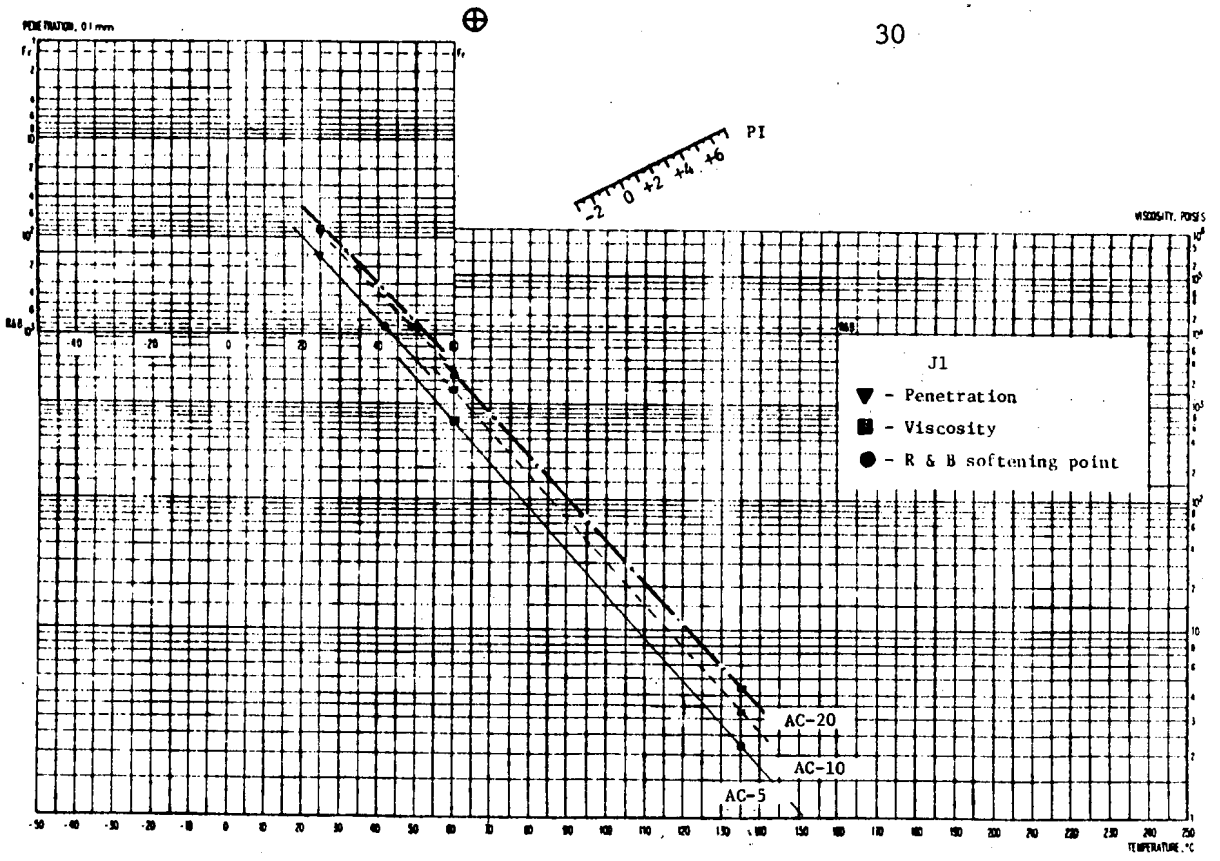

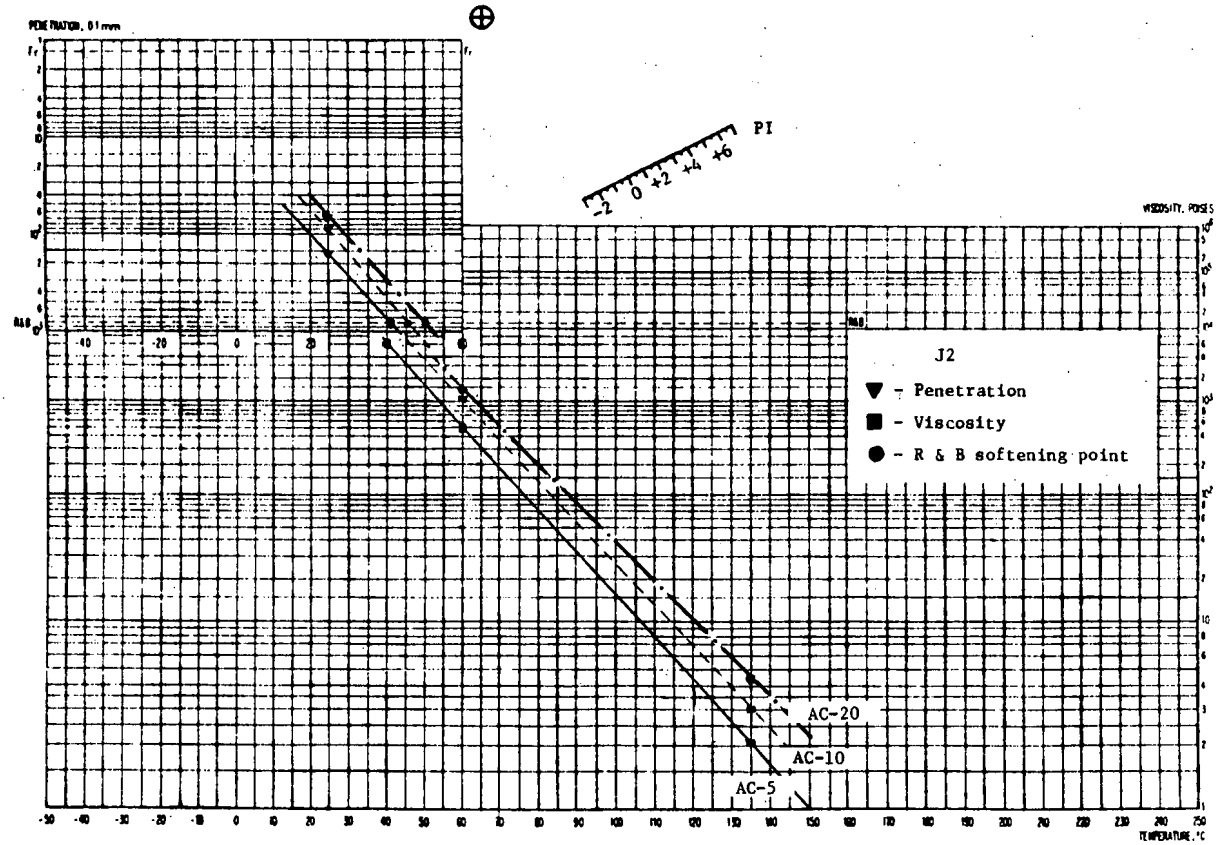

Figure 12. BTDC of original (0) Jebro asphalts.

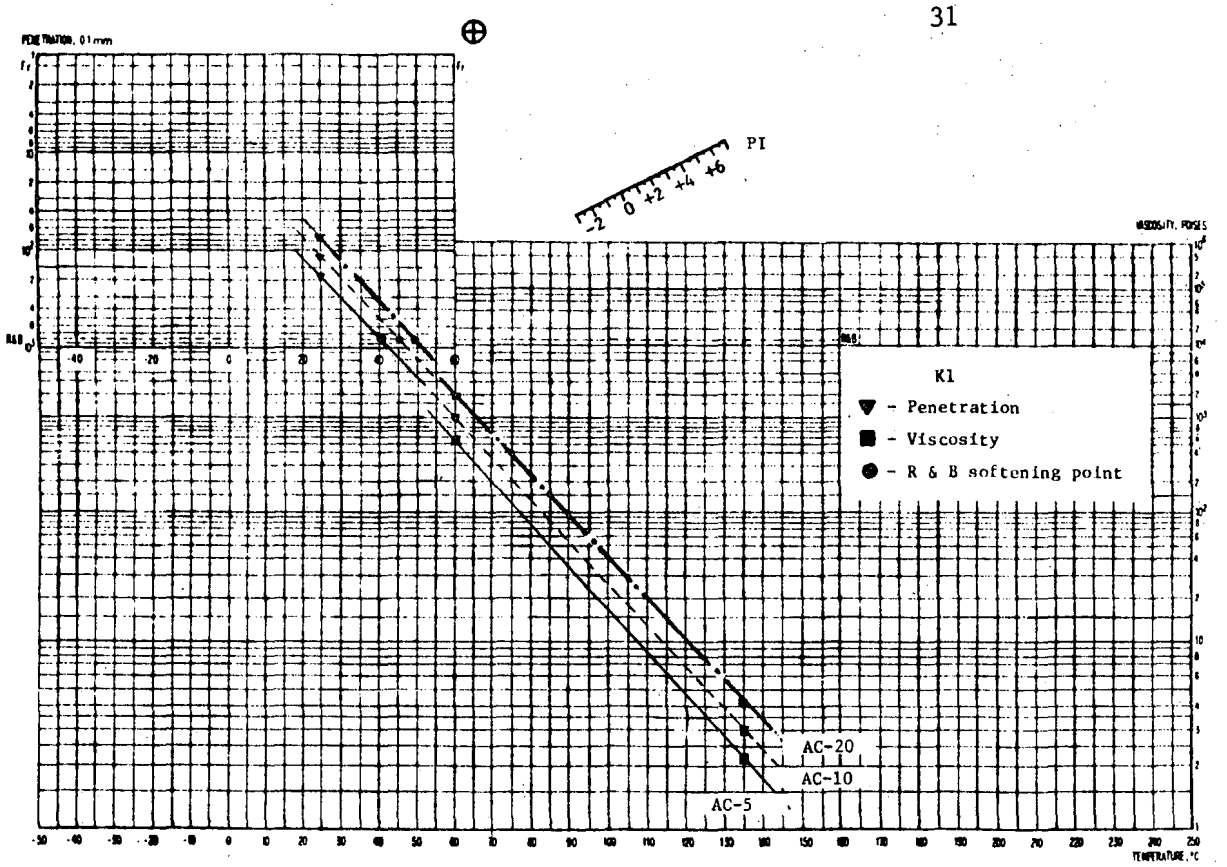

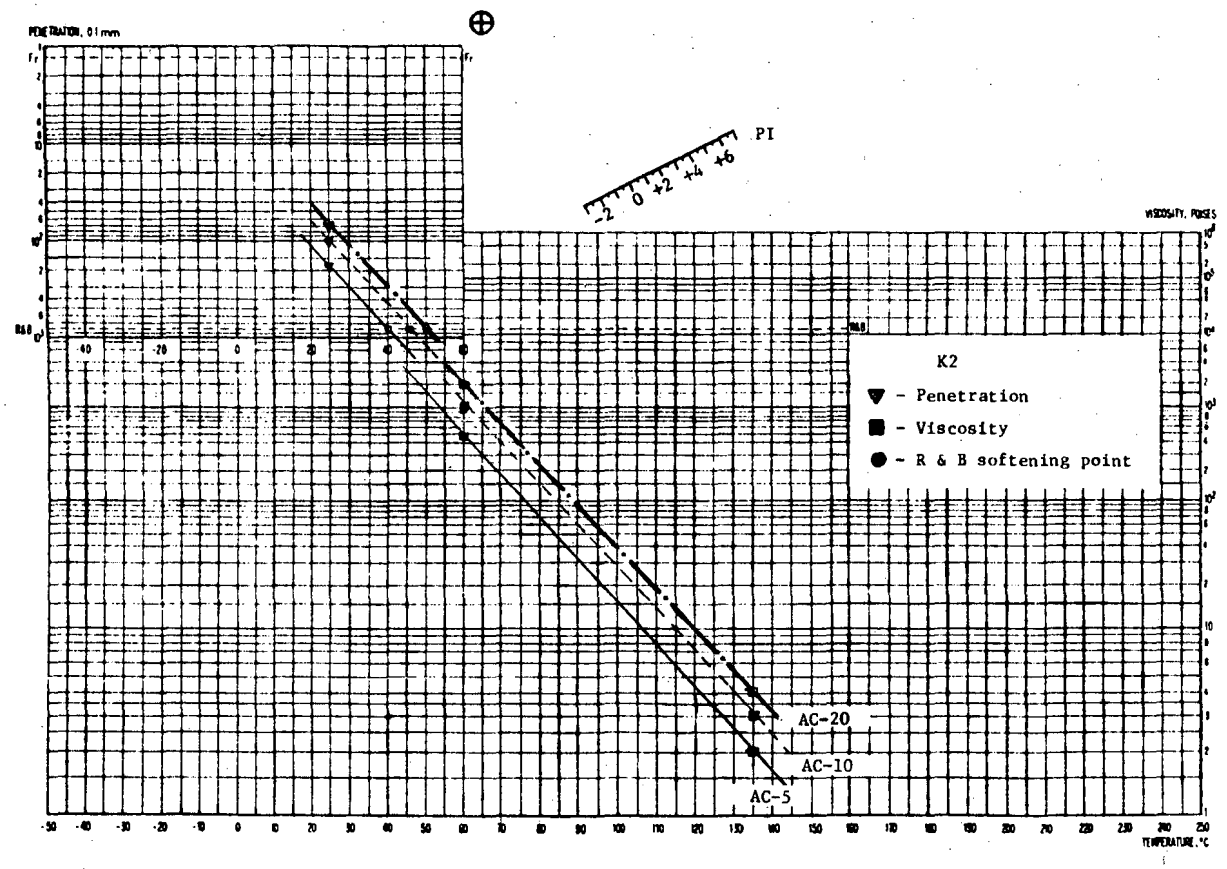

Figure 13. BTDC of original (O) Koch asphalts.

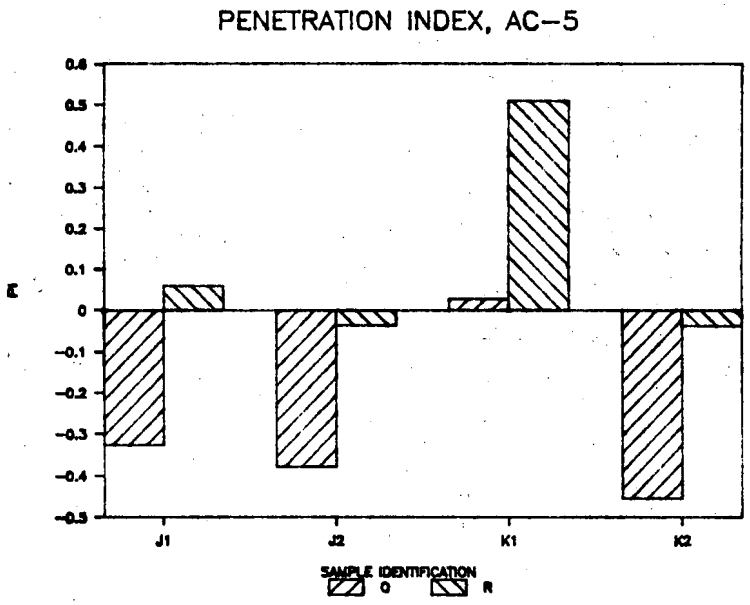

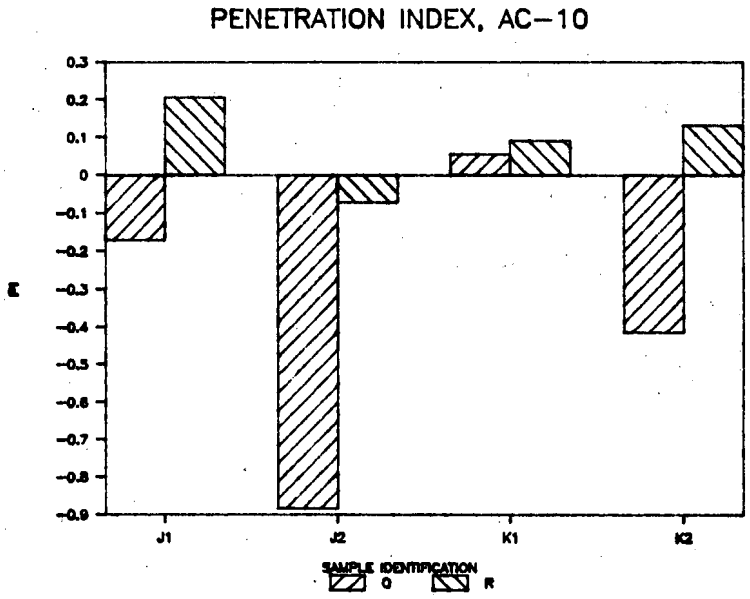

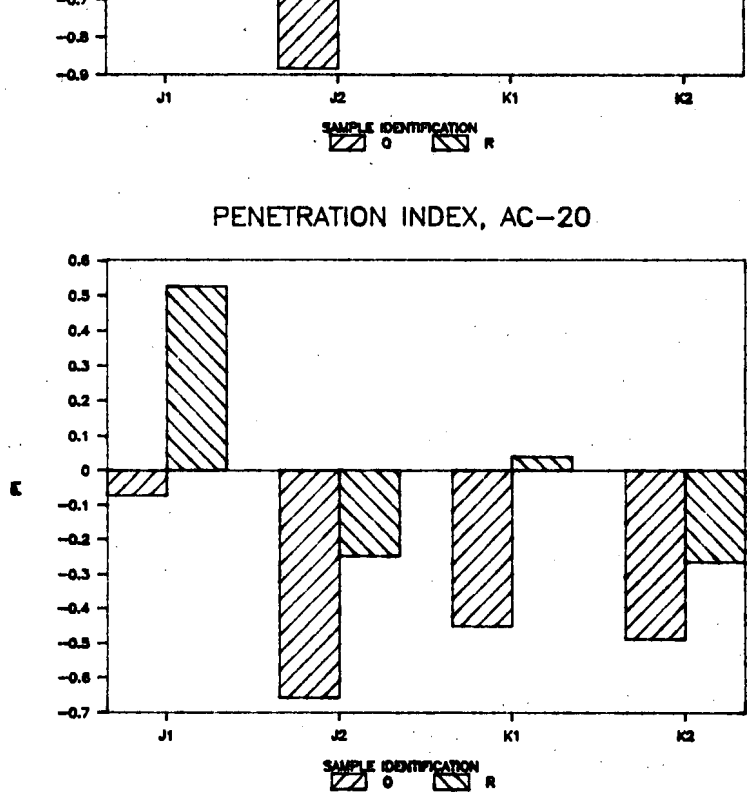

Figure 14. Penetration index.

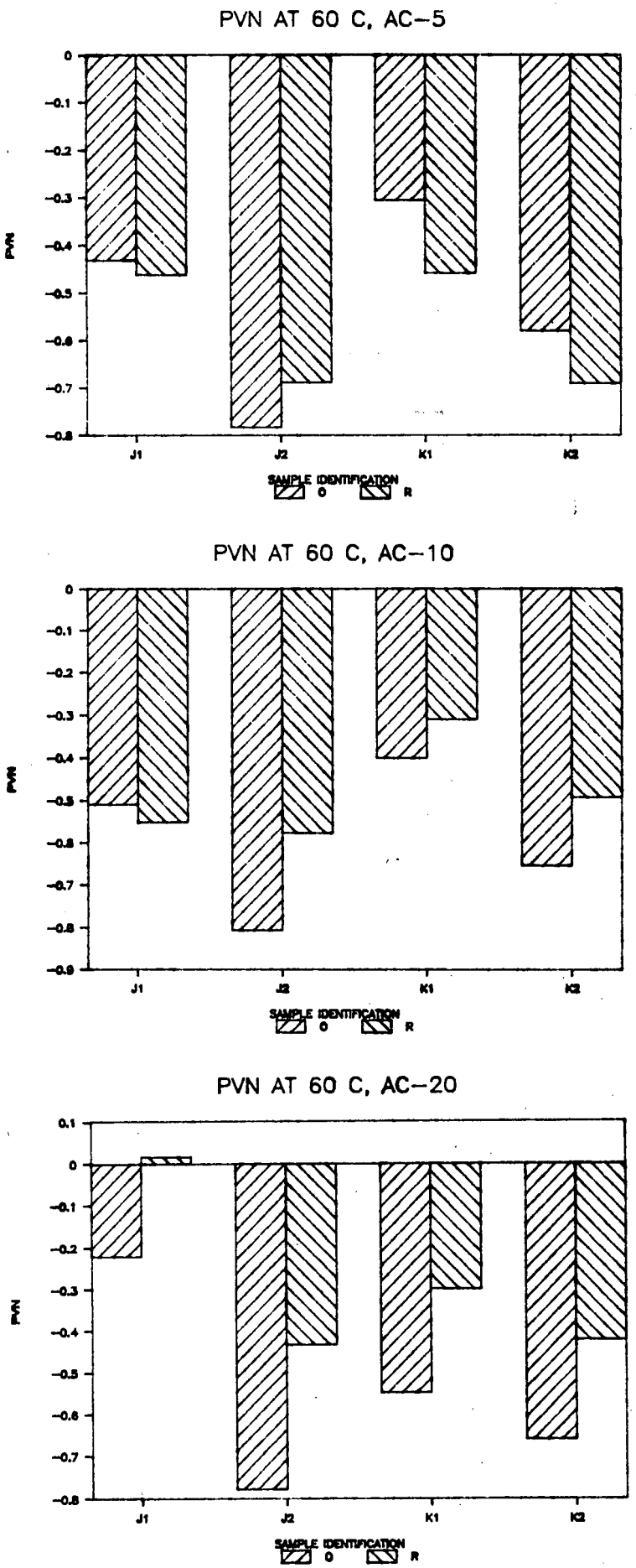

Figure 15. PVN at 60°C (140°F).

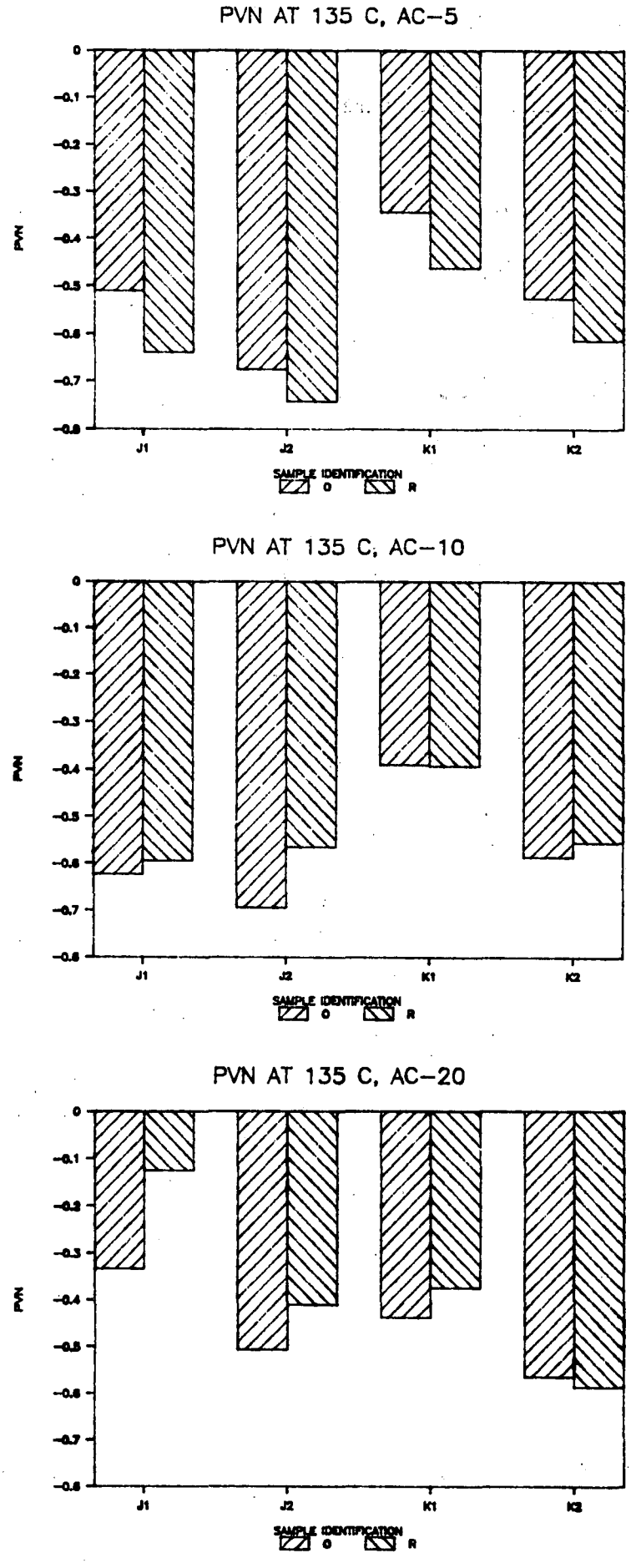

Figure 16. PVN at 135°C (275°F).

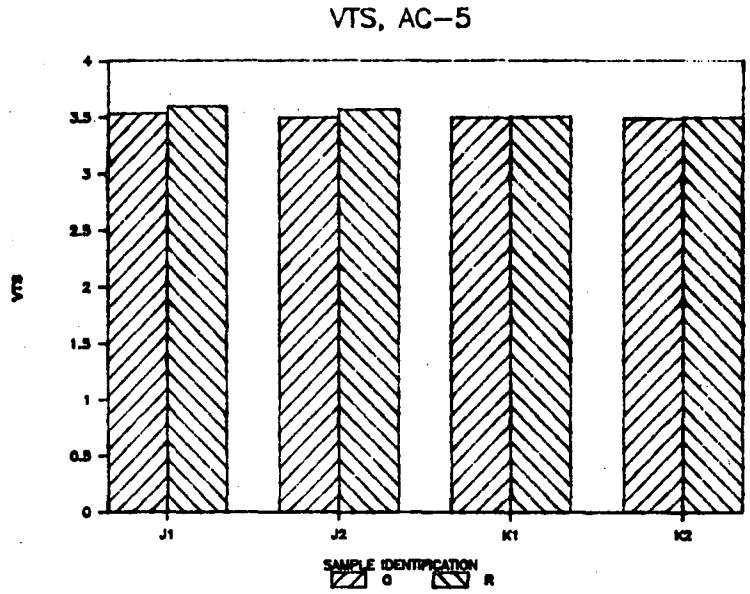

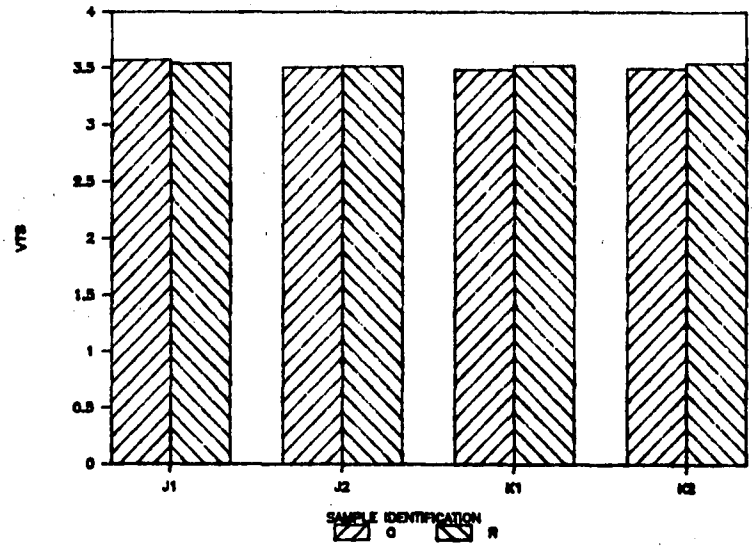

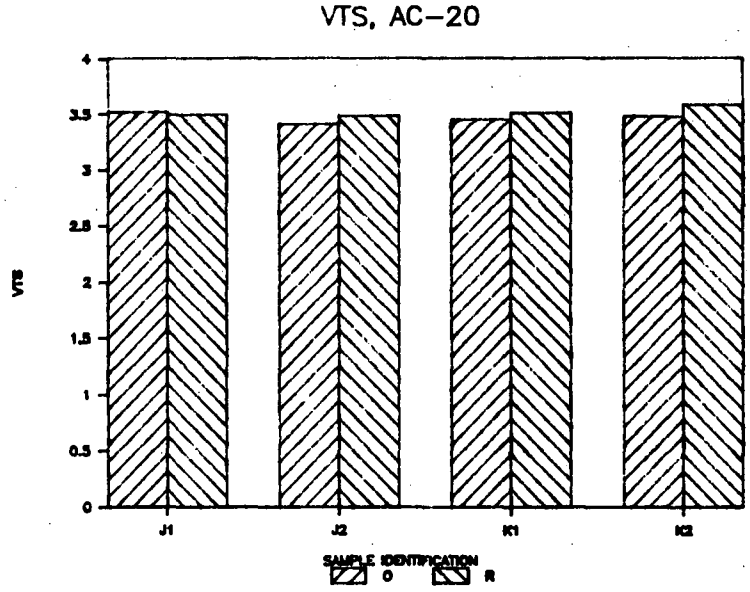

Figure 17. Viscosity temperature susceptibility.

Table 3. Low-temperature cracking properties.

Sample ID	CT C	TES C	S,-23 ksi	S,-29 ksi
J05-01-O	-40.5	-46.5	0.406	1.160
J05-01-R	-45.0	-47.0	1.305	2.610
J05-02-O	-40.0	-46.5	0.348	1.595
J05-02-R	-40.0	-40.0	1.740	4.350
K05-01-O	-45.0	-49.5	0.218	0.725
K05-01-R	-42.0	-43.0	1.015	1.740
K05-02-O	-40.0	-45.0	0.290	0.725
K05-02-R	-43.0	-42.0	1.015	3.625
J10-01-O	-38.0	-40.5	1.450	2.900
J10-01-R	-37.5	-37.0	2.900	4.350
J10-02-O	-38.5	-34.5	2.755	5.800
J10-02-R	-42.0	-36.0	3.335	7.250
K10-01-O	-42.5	-44.5	0.580	1.450
K10-01-R	-37.5	-38.5	1.740	5.800
K10-02-O	-38.0	-42.0	1.305	3.045
K10-02-R	-41.5	-36.5	2.030	5.800
J20-01-O	-42.5	-39.0	1.740	3.480
J20-01-R	-42.5	-36.0	2.175	4.350
J20-02-O	-36.5	-32.5	3.625	10.150
J20-02-R	-39.0	-34.5	4.350	8.700
K20-01-O	-39.5	-36.0	2.900	7.250
K20-01-R	-39.0	-34.5	4.350	8.700
K20-02-O	-34.0	-35.0	2.900	7.250
K20-02-R	-35.0	-32.5	7.250	14.500

CT : cracking temperature.
TES : temperature of equivalent stiffness at 20 ksi, 10,000 sec.
S,-23 : stiffness at -23 C, 10,000 sec.
S,-29 : stiffness at -29 C, 20,000 sec.
O : original sample.
R : thin film oven test residue.

asphalt stiffness of 20,000 psi at 10,000 sec loading time (TES), estimated stiffness at -23°C and 10,000 sec loading time, and stiffness at -29°C and 20,000 sec loading time. The following can be observed:

- Softer grade AC-5 had a lower cracking temperature and reached a critical stiffness of 20,000 psi at a lower temperature than harder asphalt AC-20.
- Within a given viscosity grade, cracking temperatures of asphalts could vary by as much as 5°C.
- Low temperature stiffness values for asphalts of a given viscosity grade could differ by a factor of 4.

The effect of heat, as determined by viscosity at 60°C (140°F) and penetration at 25°C (77°F), on the thin film oven test residues, are given in Table 4 and shown in Fig. 18. Viscosity ratios were uniform at between 1.8 to 3.1 (all meeting AASHTO M226, Table 2, maximum ratio of 5); penetration ratios varied between 0.49 and 0.76.

The resistance of asphalts to hardening during hot-mixing and their temperature susceptibilities are indirectly specified in AASHTO M226, Table 2. These important properties are plotted in Fig. 19 in terms of PVN and viscosity ratio at 60°C (140°F). Except for the second set of samples from Jebro, asphalts supplied in Iowa appeared to be rather uniform. Relationships between viscosity at 60°C (140°F), penetration at 25°C (77°F) and PVN of the 12 asphalts are presented in Fig. 20 with reference to AASHTO M226.

The properties of recovered asphalt samples from Research Project HR-217, 80 months after construction, are given in Table 5. While aging has increased the viscosities, the average PVN of -0.64 for Wood River asphalts and -0.97 for Sugar Creek asphalts, changed little from those reported by Marks and Huisman

Table 4. Thin film oven test hardening.

sample ID	Viscosity ratio @ 60 C	Penetration ratio @ 25 C
J05-01	2.09	0.60
02	3.10	0.49
J10-01	1.80	0.66
02	2.42	0.64
J20-01	2.07	0.73
02	2.15	0.76
K05-01	2.29	0.53
02	2.40	0.52
K10-01	2.48	0.59
02	2.53	0.60
K20-01	2.45	0.65
02	2.49	0.64

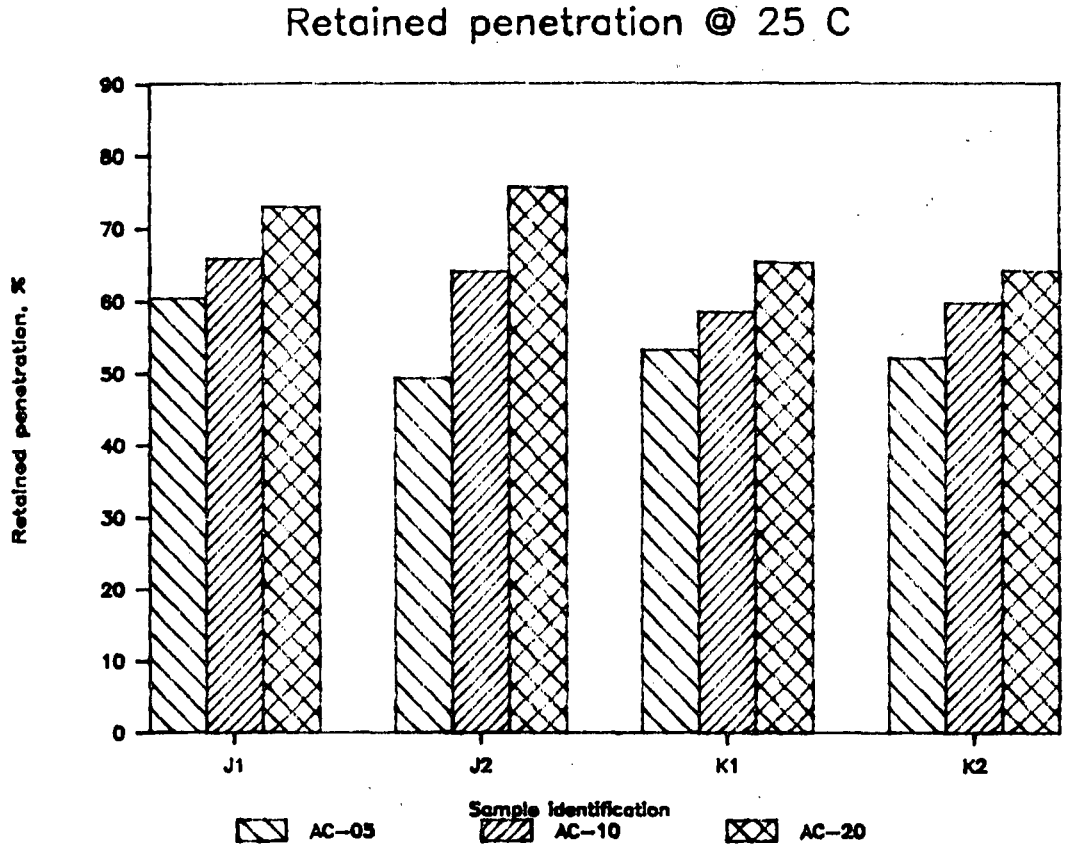

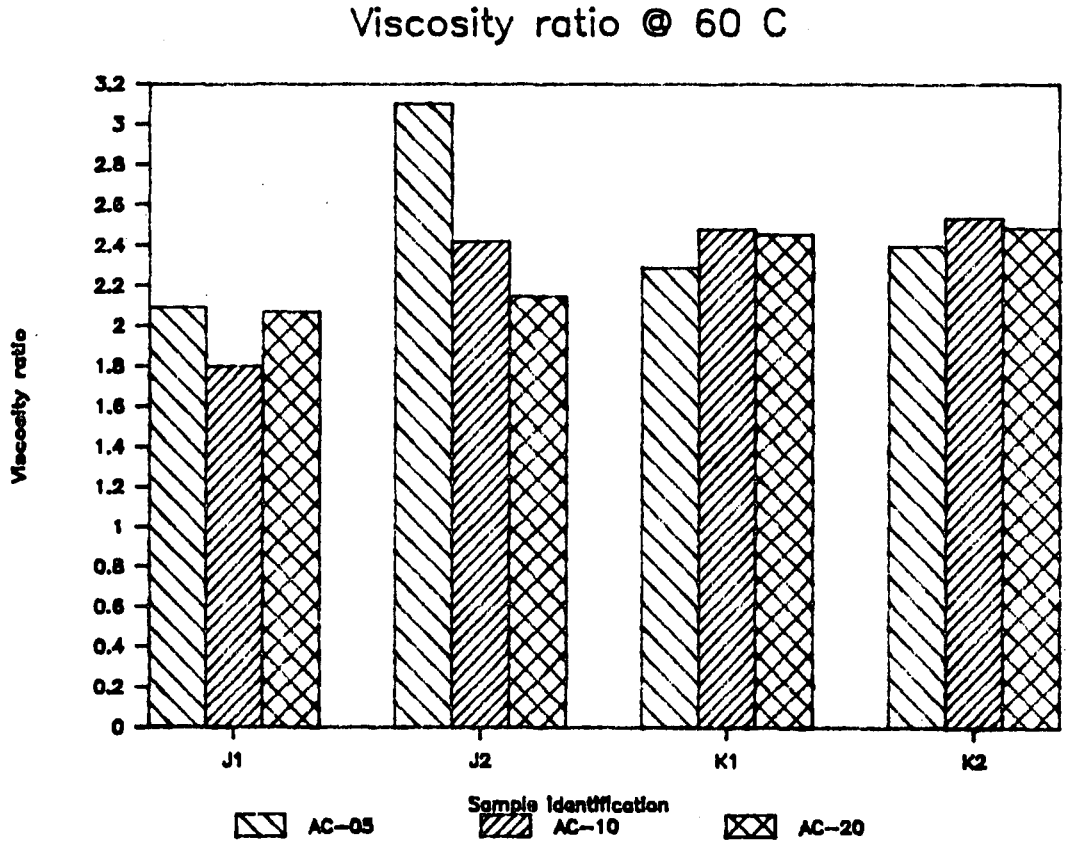

Figure 18. Retained penetration and viscosity ratio, thin film oven test.

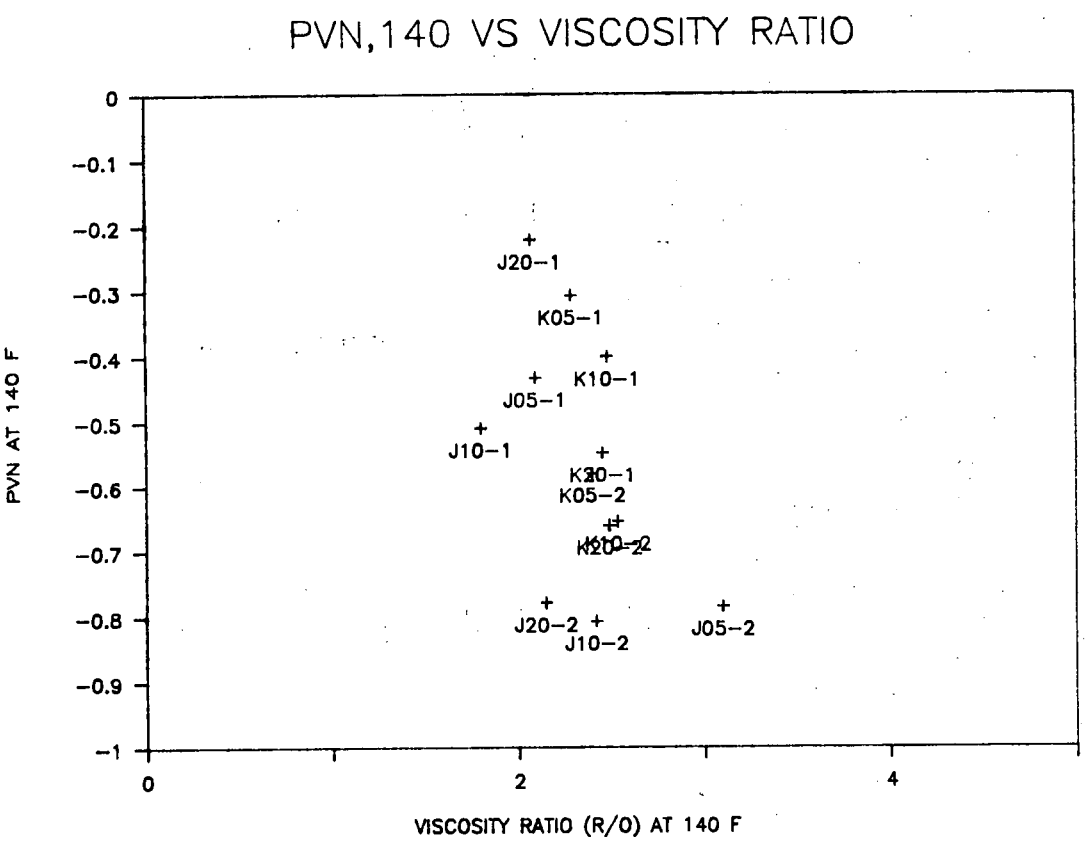

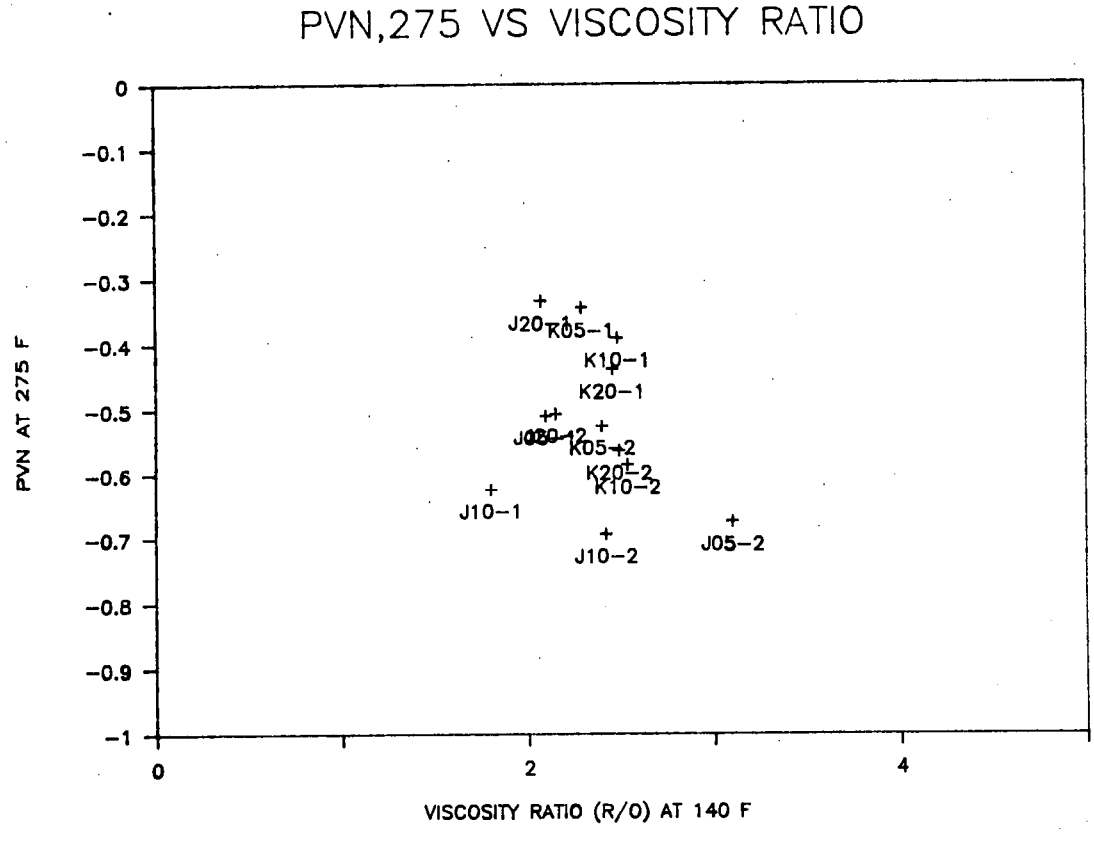

Figure 19. PVN vs viscosity ratio.

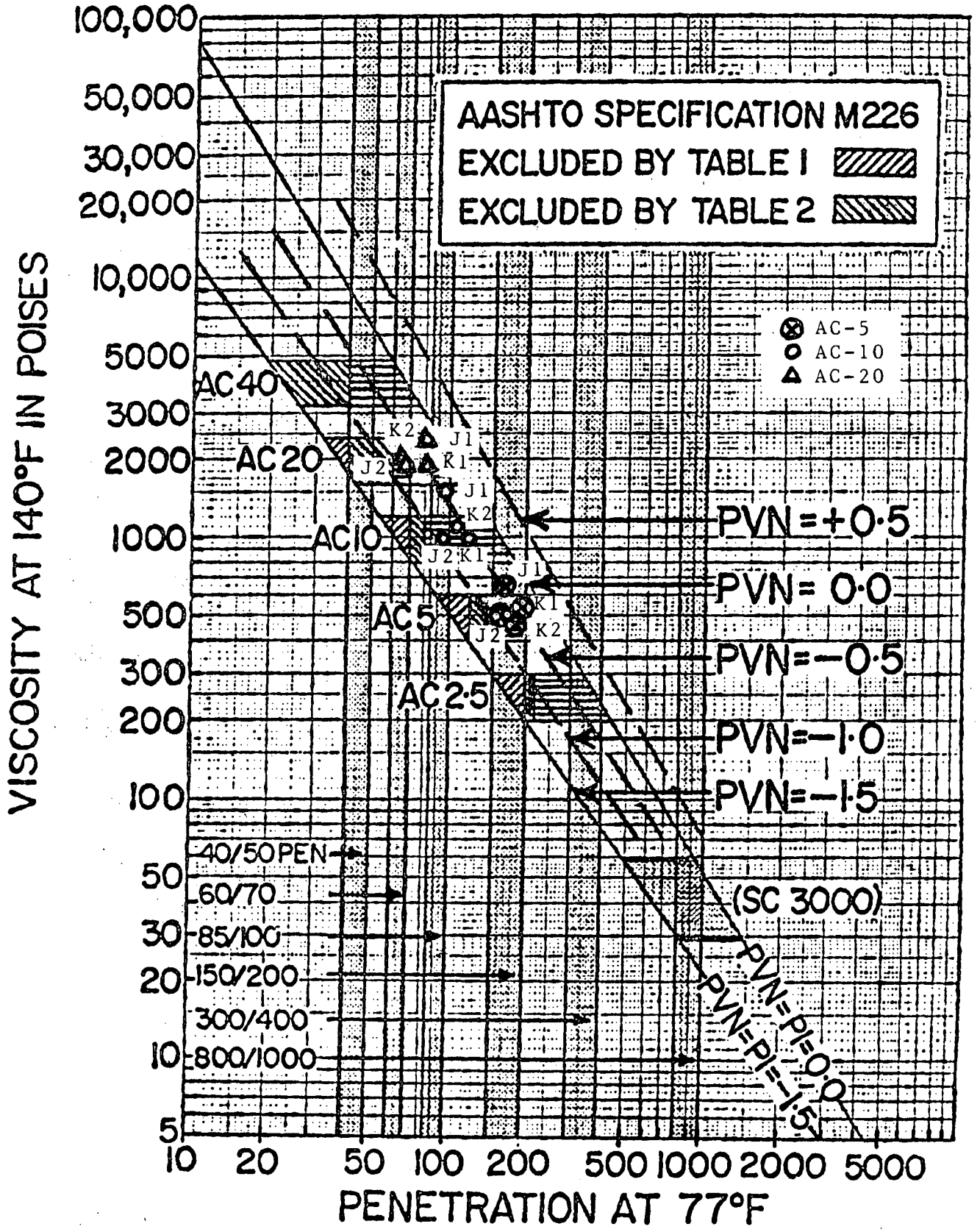

Figure 20. **Relationships Between Viscosity at 140°F in Poises, Penetration At 77°F, and Temperature Susceptibility.**

Table 5. Properties of recovered asphalts

Sample	P25	VIS60 poise	PVN60
WOOD RIVER			
Surface	43	4806.0	-0.460
Binder	71	1701.3	-0.742
Base	56	2471.2	-0.720
SUGAR CREEK			
Surface	24	8268.3	-0.763
Binder	35	3624.3	-1.010
Base	26	4817.1	-1.137

P25 : penetration @ 25 C, 100 g, 5 sec.
VIS60 : viscosity @ 60 C.
PVN60 : Penetration-viscosity number @ 60 C.

(1985). The significance of these data will be analyzed during Tasks 3 to 6 of the study in relation to chemical changes and performance data.

The results of viscoelastic measurements at +5°C described in 2.2.1 are given in Figs. 21 and 22, plotting viscosity and elasticity indices against time. It will be clear from the description of these measurements that the viscosity data presented pertain to Newtonian viscosity, i.e. viscosity at zero shear rate.

Reviewing the viscoelastic data, one can observe that the rheological properties of these samples exhibit strikingly different dependence on their thermal history and time. Some properties do not stabilize even after seven days. The estimated viscoelastic properties of these samples and their trends are summarized in Table 6.

3.2. Gel Permeation Liquid Chromatrography (GPLC)

The results of GPLC runs with 12 virgin asphalt samples, their TFOT residues and six recovered core samples as described in 2.2.2 are given in the form of chromatograms in Appendix I. The estimated large molecular size (LMS) ratings of these samples as defined by the Montana State University research group (Jennings et al., 1980; 1982; and 1985) are tabulated in Table 7. In the third column of this table tabulated are the fractional change of LMS upon TFOT, except the last two values. The latter are the fractional change of LMS, going from the base course to the surface course sample of the Sugar Creek and Wood River projects, respectively.

3.3 Thermal Analysis

The results of DSC tests described in 2.2.3 are presented in Appendix II as thermograms. The low temperature inflexion points on these thermograms, as interpreted by Noel et al. (1970) and Albert et al. (1984) as glass transition points, tg, are tabulated in Table 8. The rest of the thermograms, which have

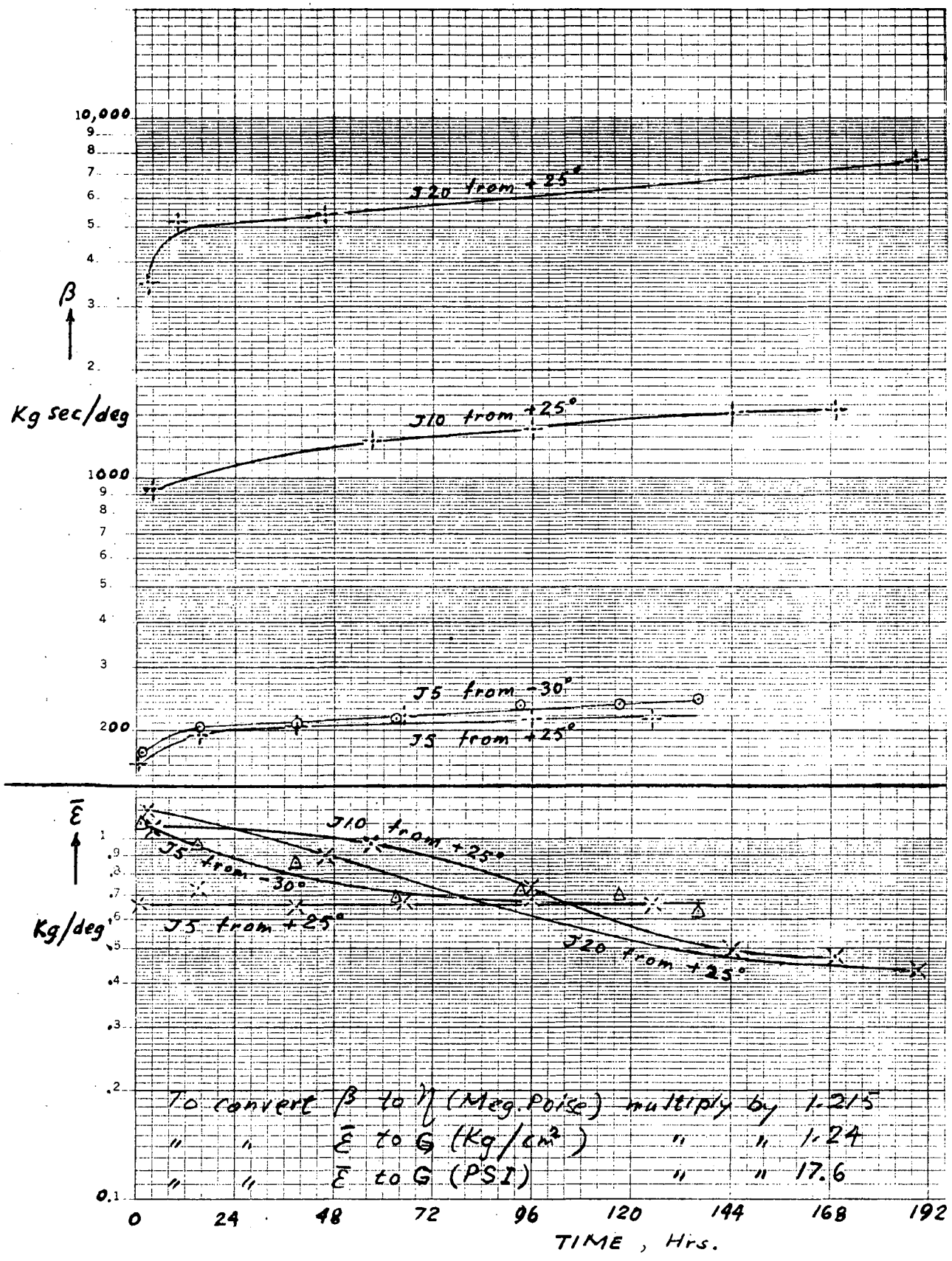

Figure 21. Viscoelastic properties of J05-01-0, J10-01-0 and J20-01-0 at +5°C.

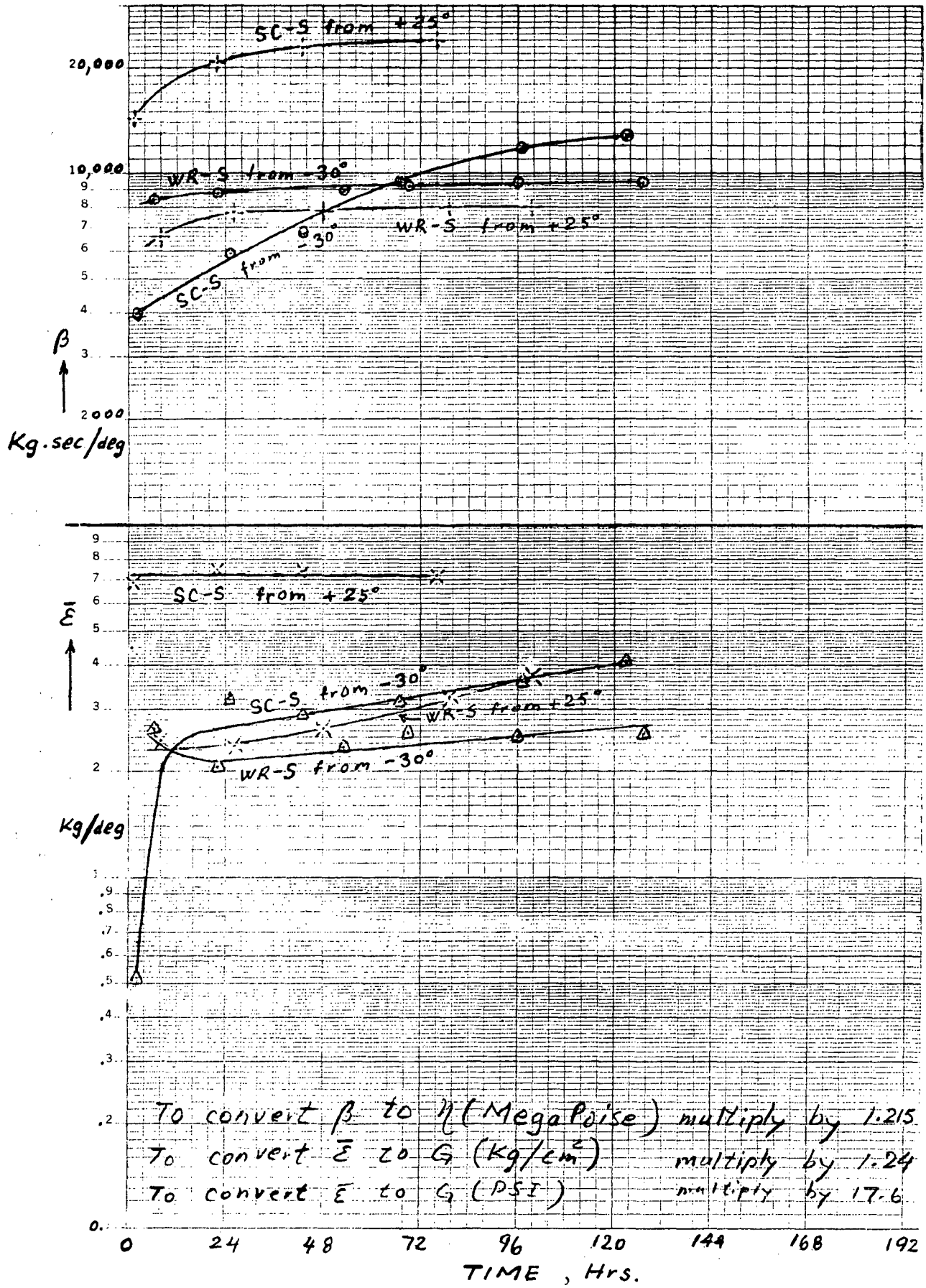

Figure 22. Viscoelastic properties of SC-SU and WR-SU at +5°C.

Table 6. Viscoelastic properties of thermal cycled samples at +5 C.
n : Viscosity, MP
G : Elastic shear modulus, psi

Sample	3rd day value after cooling from +25 C		% variation in the first 3 days after				% change*	
			cooling from +25 C		warming from -30 C			
	n	G	n	G	n	G	n	G
J05-01-0	225	12	31	0	29	-38	6	67
J10-01-0	1580	16	44	-18	--	--	--	--
J20-01-0	6990	13	93	-38	--	--	--	--
SC-S	29200	130	71	0	160	650	-72	-94
WR-S	9720	54	43	20	16	-14	43	16

* : % fractional change in initial value observed after warming from -30 C relative to that after cooling from +25 C.

Table 7. Results of HP-GPC analyses.

Sample	LMS, %	change, %	$LMS_{18.125}$, %	change, %
J05-01-O	22.5		0.70	
J05-01-R	26.2	+16	1.28	+83
J05-02-O	20.6		0.35	
J05-02-R	24.0	+16	0.66	+89
K05-01-O	30.2		2.26	
K05-01-R	31.4	+4	2.42	+71
K05-02-O	27.2		2.12	
K05-02-R	30.7	+13	3.25	+53
J10-01-O	21.8		0.64	
J10-01-R	24.9	+14	1.06	+66
J10-02-O	24.9		0.64	
J10-02-R	27.4	+10	1.02	+59
K10-01-O	30.8		2.26	
K10-01-R	32.8	+7	2.78	+23
K10-02-O	28.3		1.76	
K10-02-R	31.2	+10	2.57	+46
J20-01-O	30.9		1.46	
J20-01-R	33.0	+7	2.02	+38
J20-02-O	23.5		0.36	
J20-02-R	27.3	+16	0.74	+105
K20-01-O	28.8		1.85	
K20-01-R	32.3	+12	2.92	+58
K20-02-O	27.3		1.68	
K20-02-R	30.0	+10	2.37	+41
SC-Ba	23.4		0.88	
SC-Bi	26.7	+19	1.50	+102
SC-S	27.9		1.78	
WR-Ba	29.5		1.68	
WR-Bi	34.9	+2	3.34	+13
WR-S	30.1		1.89	

the same general appearance as reported by the latter authors, consist of two shallow endothermic peaks. The peak temperatures t_1, t_2 and their mean t_m are also tabulated in Table 8. These regions were analyzed in the manner described by Albert et al. to determine the enthalpies of transformation ΔH given in the last column of this table.

3.4. X-ray Analyses

The X-ray diffraction spectra obtained by $\theta - 2\theta$ scanning of the original samples and the TFOT residues, as described in 2.2.4, as well as of an empty sample holder to represent the background, are presented in Appendix III.

According to Williford (1943) the height of the shoulder of the spectral curve at low angles is a measure of the quality of the asphalt. This height above the background (at $2\theta = 4.83$ degrees) for various samples and their TFOT residues are tabulated in Table 9.

Also indicated are the qualitative changes in the shoulder height and the peak height upon TFOT for each sample.

3.5 Correlations

Poor field performance of asphalts under extreme climate conditions are attributed mainly to low-temperature susceptibility of their rheological properties (Schmidt, 1966; Breen et al., 1967; and Albert et al., 1985).

It has long been attempted to correlate some low temperature transitions in asphalts, which are believed to effect their low-temperature rheology, such as glass transition (Schmidt, 1966; Breen et al., 1967) and phase transformations (Noel et al., 1970; and Albert et al., 1985) to their field performance.

One of the most fundamental, direct and conclusive approaches to correlate rheological properties with another physicochemical property was made in the Central Laboratory of Highways and Bridges in France (Brule et al., 1987). The researchers of this organization, starting from the experimental fact that

Table 8. DSC test results.

Sample	t_g	t_1	t_2	t_m	Enthalpy change J/g
J05-01-O	-31	17.0	47.5	32.0	12.0
J05-01-R	-29	16.0	48.0	32.0	10.1
J05-02-O	-29	17.0	41.0	29.0	10.3
J05-02-R	-30	17.0	39.5	28.0	15.0
K05-01-O	-26	17.5	53.0	35.0	8.2
K05-01-R	-26	17.0	47.0	32.0	8.8
K05-02-O	-30	16.0	47.0	31.5	8.8
K05-02-R	-29	17.0	53.0	35.0	8.4
J10-01-O	-30	16.5	47.5	32.0	11.2
J10-01-R	-31	16.0	45.0	30.5	13.9
J10-02-O	-32	16.5	48.0	32.0	9.3
J10-02-R	-30	16.5	48.5	32.5	10.5
K10-01-O	-31	17.0	41.0	29.0	6.9
K10-01-R	-30	17.5	48.0	33.0	7.5
K10-02-O	-29	17.0	48.0	32.5	6.8
K10-02-R	-30	17.0	46.0	31.5	6.7
J20-01-O	-35	16.0	44.5	30.0	11.4
J20-01-R	-35	17.0	47.5	32.0	9.7
J20-02-O	-30	16.5	47.5	32.0	9.7
J20-02-R	-29	16.0	53.0	34.5	10.6
K20-01-O	-25	17.5	47.5	32.5	5.7
K20-01-R	-22	19.5	47.5	33.5	4.8
K20-02-O	-26	22.0	50.5	36.0	6.0
K20-02-R	-30	29.5	53.0	41.0	7.8
SC-Ba	-26	17.0	50.5	34.0	9.6
SC-Bi	-31	16.0	44.0	30.0	11.2
SC-S	-30	16.5	48.0	32.0	10.6
WR-Ba	-37	15.0	44.5	30.0	10.8
WR-Bi	-35	14.0	44.0	29.0	13.3
WR-S	-35	16.0	43.5	30.0	10.7

Table 9. Shoulder height of X-ray diffraction spectrum at two theta = 4.83 degree.

Sample	Shoulder height counts x 10	change in shoulder height	change in peak height
J05-01-O	33		
J05-01-R	37	+	O
J05-02-O	26		
J05-02-R	40	+	+
K05-01-O	26		
K05-01-R	37	+	-
K05-02-O	36		
K05-02-R	36	O	O
J10-01-O	43		
J10-01-R	37	-	-
J10-02-O	44		
J10-02-R	32	-	+
K10-01-O	34		
K10-01-R	26	-	+
K10-02-O	25		
K10-02-R	25	O	+
J20-01-O	25		
J20-01-R	41	+	-
J20-02-O	48		
J20-02-R	13	-	-
K20-01-O	36		
K20-01-R	18	-	+
K20-02-O	25		
K20-02-R	39	+	-

non-Newtonian behavior of asphalts is enhanced at lower temperatures, and considering the associative interactions between asphaltene micelles leading to sizeable colloidal agglomerates, were able to correlate the GPLC profiles and the asphaltene contents to rheological properties.

For this correlation they made use of the intensity of a sharp GPLC peak at a molecular weight of greater than 100,000 obtained by a fast elution (3.5 ml/min.) using two 30 cm long Styragel columns of 1000 and 10,000 Å pore sizes. The purpose of this fast method was preventing the breaking up of asphaltene agglomerates in the presence of the THF solvent. They also showed that TFOT increases this agglomeration significantly.

The message in the results of the French research group is that the gel $\rightleftarrows$ sol equilibrium in asphalts has an important bearing on their rheological properties. Since agglomeration (gel formation) is exothermic, at low temperatures the gel form, at higher temperatures the sol form is predominant at equilibrium. The DTA studies of this group, as well as the DSC studies of Noel et al. (1970) and Albert et al. (1985) in the absence of oxygen clearly shows endothermic transformations as temperature is raised in the range of $-5^{\circ}C$ through $+80^{\circ}C$.

Although this transformation is referred to as melting of the crystallized asphaltic components by Noel et al., as dissolution of these components in the matrix by Albert et al., and vaguely as melting by Brule et al.; it may solely or partly be gel to sol transformation following a sol to gel transformation taken place at lower temperatures.

It appears, therefore, that the following factors may effect the asphalt rheology at low temperatures:

(a) Predominance of agglomerates of asphaltene micelles,

(b) Presence of crystallizable components.

The LMS fraction defined and estimated by the Montana research group using a GPLC method as described in 2.2.2 includes the agglomerated asphaltene molecules in addition to other asphaltic components. If the concentration of these agglomerates happens, for some reason, to be proportional to or be a monotonic function of the LMS content in general, and further if they are responsible for low temperature susceptibility of the asphalt (factor a), then the LMS rating of a sample is expected to measure its poor low-temperature performance. This is exactly what has been put forward by the Montana research group on grounds of their experimental findings.

Whatever the nature of the endothermic transformation observed in thermal analysis (factors a and/or b) is, it follows from the DTA results and the ideas put forward by Brule et al. (1987) and the DSC results of Noel et al. (1970) and Albert et al. (1985) that the location of the endothermic transformations on the temperature scale described above may also characterize the low-temperature susceptibility of the asphalt. For instance, the larger the endothermicity of this transformation and higher the temperature range in which it occurs, the more susceptible may be the sample.

As associative interaction between asphaltene molecules promotes a structural order in the system, such an interaction is also expected to reflect on x-ray diffraction spectra of the sample.

The experimental data presented in Section 3.1 through 3.4 will be reviewed below, in relation to these expectations. Since no engineering service information is available at this stage of the present project, except in the case of samples labelled as SC and WR, this review will be confined to parallel comparisons of various properties between samples, and between artificially aged and unaged samples.

3.5.1 Rheological properties: An inspection of viscoelastic data presented in Figs. 21 and 22, and in Table 6 reveals that:

(a) All samples studied exhibit an increase in viscosity at +5°C after cooling from +25°C in various extents. This trend appears to be more pronounced in more viscous asphalts.

(b) With the virgin asphalts of high viscosity this increase is accompanied by a decrease in elastic modulus. Some parallelism is observed between this drift and their LMS rating, as well as the peak-height of their X-ray diffraction spectra.

(c) Among the samples conditioned at -30°C, the effect of low temperature on viscoelastic properties of SC-SU is dramatic and in the opposite direction of those of the other two samples. A drastic fall followed by a fast rise, especially in its elastic modulus, deserves attention. Before low temperature conditioning, the viscosity and elastic modulus of this sample are also incomparably greater than those of the others. Comparing the two core samples (SC-SU and WR-SU) one observes that the low-temperature (-30 C) susceptibility of SC-SU is far greater. It is significant that the effect of natural aging in the pavement as reflected on their LMS ratings (Table 7, column 3) is also much greater in the case of the Sugar Creek sample.

(d) From the viewpoint of its time dependence after a cold shock, the elastic modulus appears to be more characteristic and discriminating than viscosity.

3.5.2 GPLC: The results on %LMS defined by MSU method as given in Table 7 showed the following:

1. The %LMS of original asphalts studied ranged from 20.6 to 30.9, all higher than the maximum allowable %LMS of 16-17% for the Montana climate (Jennings and Pribanic, 1988).

2. The %LMS of asphalts in a given viscosity grade varied up to 7.4% between samples from the same supplier; this difference was as high as 9.6% between samples of different suppliers.

3. While %LMS increased with viscosity at 140 F for asphalts from Jebro, this was not the case for Koch asphalts which had relatively higher %LMS but in a narrow range between 27.2 to 30.8.

4. Thin film oven treatment increased %LMS by an average of 2.87% (1.2 to 3.8%) to a low of 24% for J0502 and a high of 33% for J2001.

The last observation means that the GPLC technique can be used as a reliable test to monitor aging, as concluded also by Brule et al. (1987) who used a different and accelerated modification of the Montana method as described earlier.

A comparative analysis of the GPLC size distribution curves shows that the fractional increase in the largest detectable molecular size region (earliest elution) as a result of TFOT, is the largest among the other regions of the LMS fraction as defined by the Montana research group. Although this version of the GPLC method differs from that used by Brule et al. in that the former is unable to detect all asphaltene agglomerates in the 100,000 molecular weight range due to their peptization during testing as mentioned earlier, we believe that the early-eluted fraction is made up by the remnants of undissociated agglomerates, and that the observation just mentioned is the result of formation of extra agglomerates induced by TFOT.

Then, the early-eluted fraction content of a sample is expected to be approximately proportional to the original agglomerate concentration, and thus is a more sensitive index than LMS to characterize aging, as well as the low-temperature susceptibility of the sample.

With this consideration, in Table 7 we also tabulate (LMS) 18.125, the percentage of the fraction eluted within 18.125 minutes taken from the

printouts, and the fractional change of this fraction upon TFOT. It will be noted that the fractional change of (LMS) 18.125 due to aging is much larger than that of LMS defined by the Montana group.

In Fig. 23 (LMS) 18.125 is plotted against LMS for all the samples studied. The trend shown in this plot is an evidence of approximately linear dependence of the agglomerate concentration on the LMS rating, as hypothetically postulated earlier in Section 3.5.

Repeated tests on a sample appear to yield (LMS) 18.125 values in close agreement with each other. However, to take care of day-to-day drifts in the performance of the GPLC equipment, the adoption of a comparative procedure using an external standard (such as the sample J05-01-0) to determine the correct cutoff time, is recommended for future work.

No correlation is observed between GPLC results and X-ray diffraction results.

A quick search for correlations between the standard rheological indices tabulated in Tables 1 through 5 and the LMS ratings shows that neither VTS nor CT correlates with LMS, whereas there is a weak correlation between PVN and LMS ($r = -0.59$) meaning that the samples of higher LMS content tend to behave less temperature susceptible.

Glover et al. (1988) at Texas A&M University, using two columns and RI detector, and defining LMS and SMS by retention times of 25 and 30 minutes (the chromatograms were divided into three equal-time sections between 20 and 35 minutes), found relationships between viscosity temperature susceptibility (VTS) and the molecular size distribution by HP-GPC: the lower the %LMS and the higher the %SMS, the higher the temperature susceptibility. They also found correlations between asphalt tenderness, percent asphaltenes and %LMS: high %LMS was related to high asphaltene contents and non-tender asphalts. Based on this

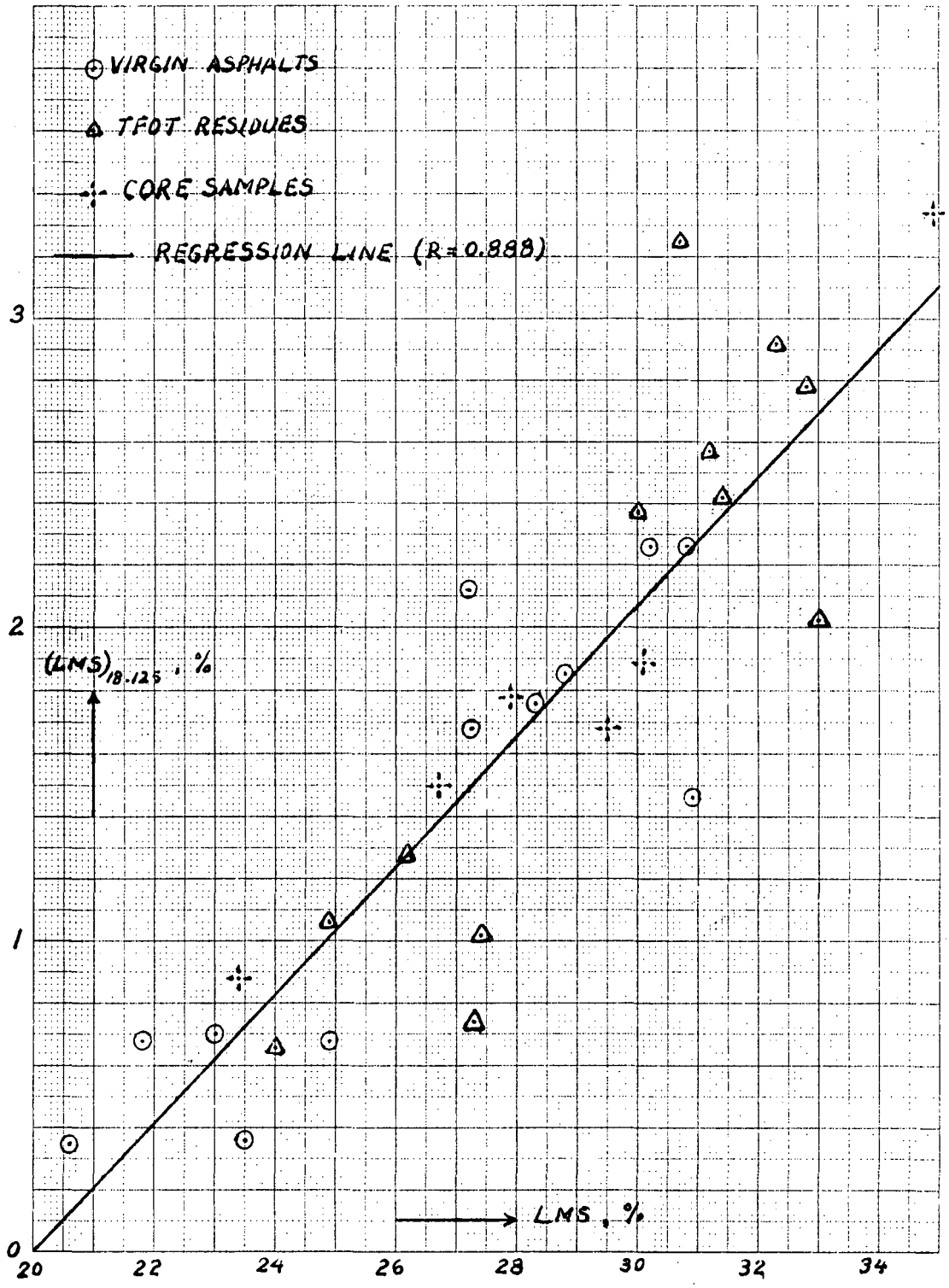

Figure 23. $(LMS)_{18.125}$ plotted vs LMS.

study, there appeared to be desired lower limits of %LMS in asphalts to reduce asphalt problems associated with tenderness. In view of the considerable data by Jennings and his co-workers on the relationships between cracking, %LMS and climate, it is likely that, for a given climatic zone, there is an optimum range of %LMS (or %SMS) for the best pavement performance: too high LMS percentage causes low-temperature cracking: too low %LMS causes high temperature rutting and setting (tenderness) problems.

More extensive and systematic correlation tests will be conducted, during the second phase of this project, between these indices and LMS ratings, as well as the results of thermal and x-ray analyses.

3.5.3 Thermal analyses: A comparison of the DSC data summarized in Table 8 with each other and the results of other tests shows that the only correlation that can be pointed out concerns ΔH and the source of the sample: ΔH values for original J samples are on the average 24% higher than those for K samples.

The effect of aging on tg and other transformation points, as well as on ΔH appears to be in random directions. Considering that this effect on GPLC results is unidirectional (see Section 3.5.2), it can be argued that the thermal effect of the gel to sol transition is overshadowed in thermal analysis by the larger thermal effect of dissolution of the crystallized components as treated by Albert et al. (1985).

3.5.4 X-ray analyses: It appears from the X-ray diffraction spectra and the Table 9 summarizing these spectra that no regular trend exists in these spectra regarding the penetration grade or the sample source, nor regarding the effect of aging. In contrast to what is observed in GPLC, the X-ray spectra are effected by TFOT in quite a random fashion and direction. The significance and implications of data in Table 9 will be investigated in Tasks 3-6 when in-service pavement samples of known performance information are studied.

4. SUMMARY AND CONCLUSIONS

Twelve samples from local asphalt suppliers and their TFOT residues, as well as six core samples were studied by standard and some specific rheological tests (at +5°C), GPLC, DSC and X-ray diffraction analysis. The following conclusions can be drawn from the results of these studies:

(1) Within each viscosity grade of asphalt cements available in Iowa and meeting AASHTO Specification M226, there were differences in temperature susceptibility between suppliers and between samples from the same supplier over time.

(2) Distinctively different GPLC chromatograms were obtained among asphalts of the same grades, same suppliers and samples supplied at different times.

(3) Distinctively different thermal analysis results and x-ray diffraction patterns were obtained from asphalts of the same viscosity grades, same suppliers and samples from the same suppliers but at different times.

(4) Whether and how these differences in physicochemical parameters among asphalts available in Iowa reflect in mixture properties when they are mixed with aggregates and in pavement performance under Iowa climatic conditions will be investigated in Tasks 2 through 6 of this research.

(5) Large differences are observed between samples regarding the time-dependence of their rheological properties at a low temperature when brought from a higher or a lower temperature. Especially the strikingly different and dramatic effect of a cold shock (-30°C) on the properties of the sample SC-SU (core sample from the surface course of the Sugar Creek project) might have an important bearing on its poor field performance.

(6) The said dependence appears to be proportionate to their viscosity and LMS rating, in the case of virgin asphalts.

(7) The elastic modulus may be at least as important as the viscosity to determine the performance-related low temperature rheology.

(8) No decisive correlation is observed between GPLC, DSC and X-ray results.

(9) In contrast to thermal analytic behavior and X-ray diffraction spectra, LMS rating is found to be unidirectionally sensitive to aging. Hence, it can be used to monitor or predict aging.

(10) The endothermic peaks on DSC thermograms indicate the presence of crystallizable components, while the LMS rating measures the presence or tendency of formation of gels. Therefore, the extent of these peaks (ΔH) may be used to evaluate the low temperature susceptibility of asphalts, together with their LMS rating. These peaks are on the whole more pronounced in original J samples than in K samples.

(11) The early-eluted fraction (e.g. (LMS)18.125) in GPLC is found to be a better measure than the LMS defined by the Montana research group.

(12) Although it is based on a single comparison (Sugar Creek versus Wood River), the "ageability", i.e. the increase in LMS rating by aging, rather than the initial LMS rating, appears to be a performance predictor.

5. RESEARCH PLAN IN TASK 2 (YEAR 2)

Research in the second year will concentrate on changes in physicochemical properties of asphalts tested in Task 1 when they are mixed with aggregates in asphalt concrete mixtures. Asphalt concrete mixtures will be prepared in a laboratory pugmill mixer using representative Iowa aggregates and asphalts tested in Task 1. These mixes, both before and after artificially aged in chambers under accelerated environmental conditions, will be tested for Marshall properties (density, voids, stability and flow), resilient modulus, tensile strength, stiffness, moisture susceptibility and fatigue life. Asphalts from these mixes will be extracted and tested as in Task 1.

The number, type and sources of aggregates as well as the gradation of the aggregates and levels of asphalt contents, will be selected in consultation with the Iowa DOT and county engineers.

In addition, more vigorous investigation for alternative procedures and data interpretation techniques for HP-GPC work will be undertaken for Task 1 asphalt samples.

6. ACKNOWLEDGMENTS

This research was sponsored by the Highway Division of the Iowa Department of Transportation (DOT) under Research Project HR-298. This study, under the same title, was also supported by and designated as Project 1942 of the Engineering Research Institute, Iowa State University.

The support of this research by the Iowa Highway Research Board and the Iowa DOT is gratefully acknowledged. The authors wish to extend sincere appreciation to the engineers of the Iowa DOT, especially Bernie Brown, Vernon Marks, and Rod Monroe, for their support, cooperation, and counsel. The authors would also like to thank Gerald Reinke, Koch Asphalt Co.; Alden Bailey, Jebro, Inc.; Brian Chollar, FHWA; and Joan Pribanic, Montana State University, for supplying the asphalt samples tested in the study.

The following individuals contributed, in various capacities, to this investigation: Jerry Amenson, Barbara Hanson, Sang Soo Kim, and Shelley Melcher.

We are indebted to Turgut Demirel for the unselfish giving of his time and consultation.

7. REFERENCES

1. Albert, M., F. Bosselet, P. Claudy, J. M. Letoffe, E. Lopez, B. Damin, and B. Neff. 1985. Comportement Thermique des BitumesRoutiers. Determination Du Taux De Fractions Cristallisees Par Analyse Calorimetrique Differentielle. Thermochimica Acta. 84:101-110.

2. Anderson, D. A. and E. L. Dukatz. 1985. Fingerprinting versus field performance of paving grade asphalts. Report No. FHWA/RD-84/095.

3. The Asphalt Institute. 1981. Design techniques to minimize low temperature asphalt pavement transverse cracking. Research Report No. 81-1. College Park, Md.

4. Breen, J. J. and J. E. Stephens. 1967. The glass transition temperature and mechanical properties of asphalts. Proc. Canadian Technical Asphalt Association 12: 137-144.

5. Brodnyan, J. G. et al. 1960. The rheology of asphalt III. Trans. Soc. Rheology, IV:274-296.

6. Brule, B. et al. 1987. Relationships between the composition, structure and properties of roadmaking bitumens: the progress of research at LCPC (in French). Bulletin, LCPC 148:69-81.

7. Button, J. W. et al. 1983. Influence of asphalt temperature susceptibility on pavement construction and performance. NCHRP Report 268.

8. Dobson, G. R. 1969. The dynamic mechanical properties of bitumen. Proceedings of the Association of Asphalt Paving Technologists. None:1-10.

9. Ferry, J. D. 1961. Dependence of viscoelastic behavior on temperature. Viscoelastic Properties of Polymers, 201-247.

10. Glover, C. J. et al. 1988. Asphalt cement chemical characterization and performance related properties. Paper presented at the Annual Meeting of the Transportation Research Board.

11. Goodrich, J. L. et al. 1985. Asphalt composition tests: their application and relation to field performance. Chevron Research Co., Richmond, California. Also: TRR 1096:146 (1986).

12. Hodgson, Roy S. 1984. Changes in Asphalt. Transportation Research Record 999:10.

13. Jennings, P. W. et al. 1980. High pressure liquid chromatography as a method of measuring asphalt composition. Research Report FHWA-MT-7930.

14. Jennings, P. W. et al. 1982. Use of high pressure liquid chromatography to determine the effects of additives and fillers on the characteristics of asphalt. Research Report FHWA/MT-82/001.

15. Jennings, P. W. et al. 1985. The expanded Montana asphalt quality study using high pressure liquid chromatography. Research Report FHWA/MT-85-001.

16. Jennings, P. W. and J. A. S. Pribanic. 1988. Predicting the performance of the Montana test sections by physical and chemical testing. Paper presented at the Annual Meeting of the Transportation Research Board.

17. Jongepier, R. and B. Kuilman. 1969. Characteristics of the rheology of bitumens. Proceedings of the Association of Asphalt Paving Technologists, 38:98-122.

18. Lee, D. Y. and T. Demirel. 1987. Beneficial effects of selected additives on asphalt cement mixes. Final Report for the Iowa Department of Transportation Project HR-278, Ames, IA.

19. Marks, V. J. and C. L. Huisman. 1985. Reducing the adverse effects of transverse cracking. Transportation Research Record 1034:80.

20. Noel, F. and L. W. Corbett. 1970. A study of the crystalline phases in asphalt. Journal of the Institute of Petroleum, 56:261-268.

21. Pagen, Charles A. 1964. Rheological response of bituminous concrete. Highway Research Record, No. 67:1-26.

22. Petersen, J. C. 1984. Chemical composition of asphalt as related to asphalt durability: state of the art. Transportation Research Record 999:13.

23. Schmidt, R. J. 1966. The relationship of the low-temperature properties of asphalt to the cracking of pavements. Proceedings Association of Asphalt Paving Technologists 35, 263-269.

24. Schmidt, R. J. and L. E. Santucci. 1966. A practical method for determining the glass transition temperature of asphalts and calculation of their low-temperature viscosities. Proceedings of the Association of Asphalt Paving Technologists, 35:61-90.

25. Sisko, A. W. and L. C. Brunstrum. 1968. The rheological properties of asphalts in relation to durability and pavement performance. Proceedings of the Association of Asphalt Paving Technologists, 37:448-473.

26. Wendlandt, W. Wm. 1986. Thermal Analysis, Wiley., 439-440.

27. Williford, C. L. 1943. X-ray studies of paving asphalts. Texas Engr. Exp. Station Bulletin 73. A & M College of Texas, College Station, Texas.

28. Zakar, P. 1971. Asphalt. Chemical Publishing Co., Inc., New York.

29. Zenewitz, J. A. and Tran, K. T. 1987. A further statistical treatment of the expanded Montana asphalt quality study. Public Roads, 51(3):72-81.

APPENDIX I

HP-GP CROMATOGRAMS

Jebro AC-5, Sample 1
Original
(J-05-01-0)

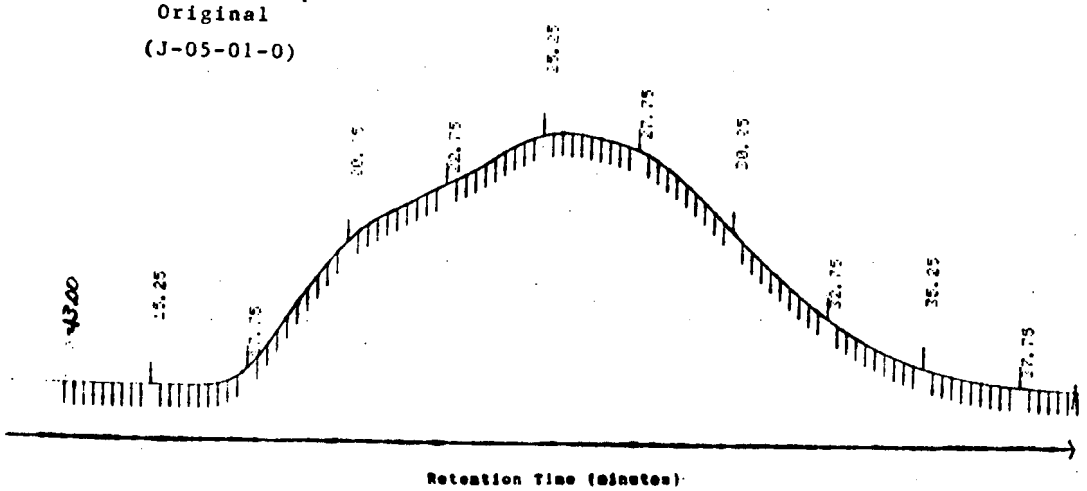

Jebro AC-5, Sample 1
Oven Treated
(J-05-01-R)

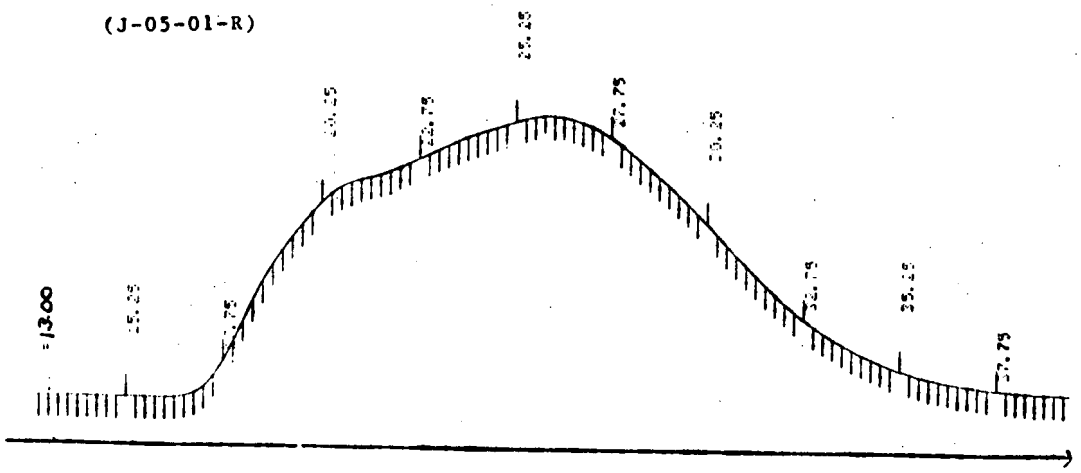

Jebro AC-5, Sample 2
Original
(J-05-02-0)

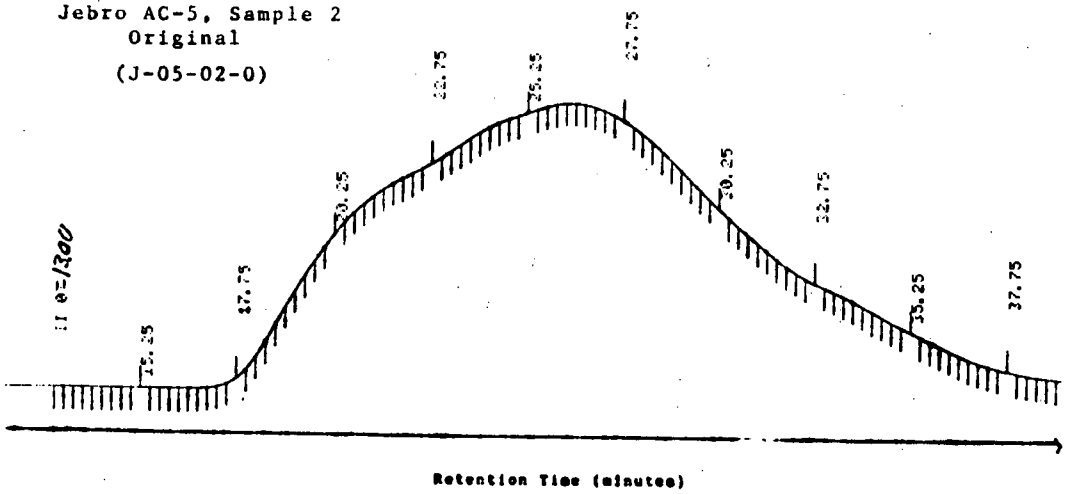

Jebro AC-5, Sample 2
Oven Treated
(J-05-02-R)

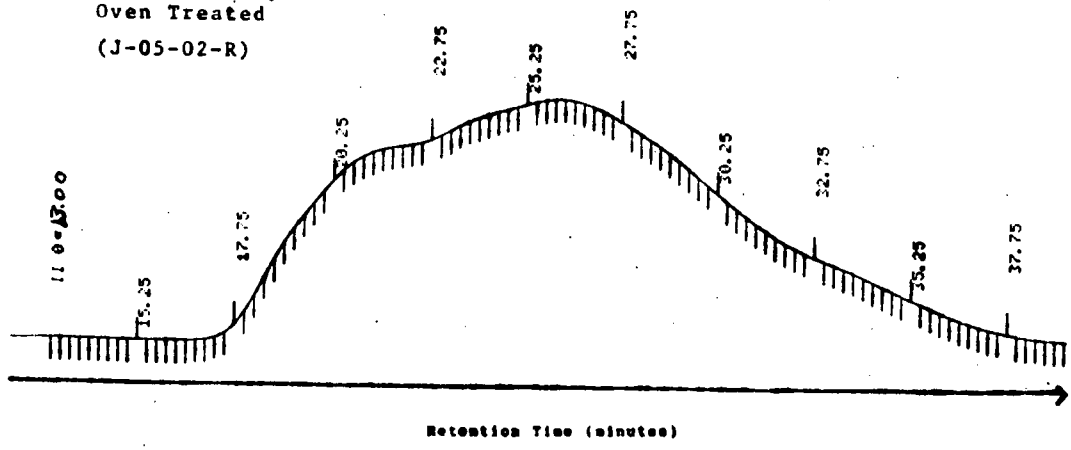

Koch AC-5, Sample 1
Original
(K-05-01-0)

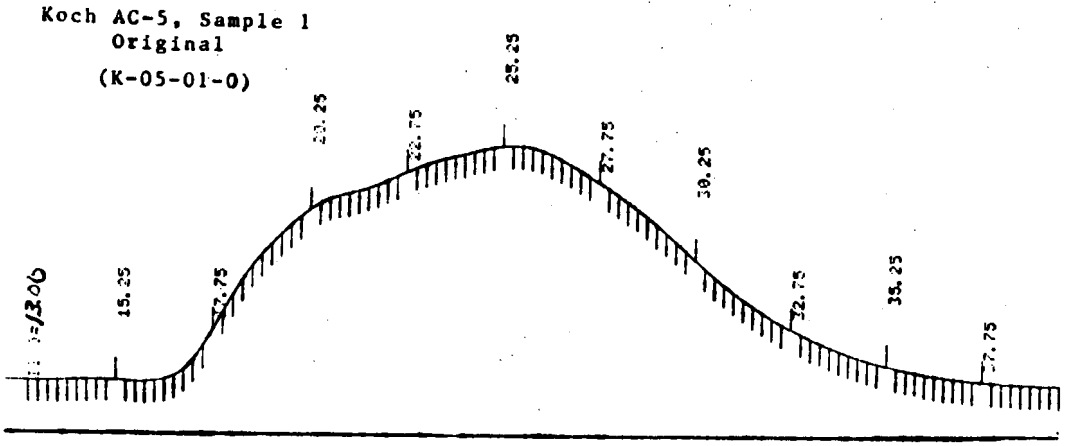

Retention Time (minutes)

Koch AC-5, Sample 1
Oven Treated
(K-05-01-R)

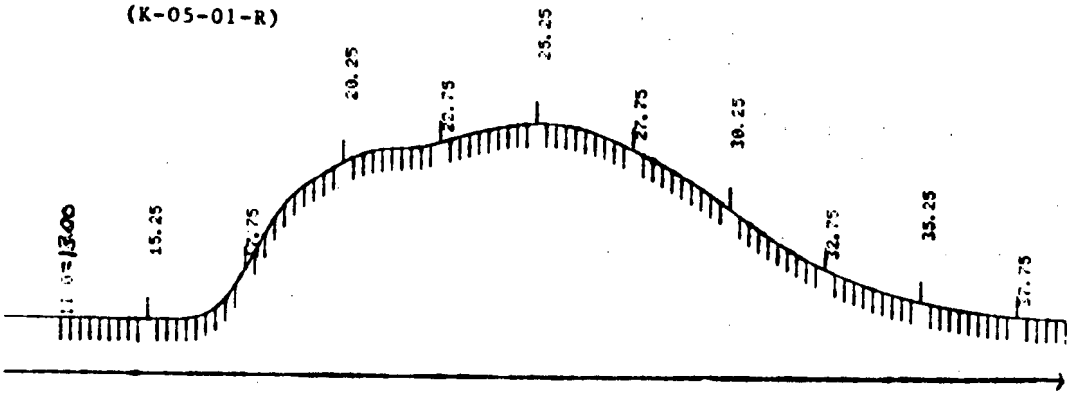

Retention Time (minutes)

Koch AC-5, Sample 2
Original
(K-05-02-0)

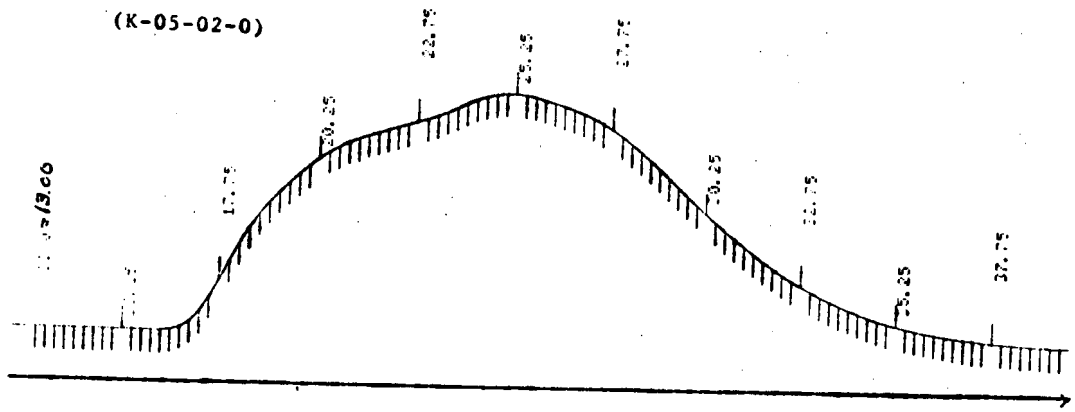

Retention Time (minutes)

Koch AC-5, Sample 2
Oven Treated
(K-05-02-R)

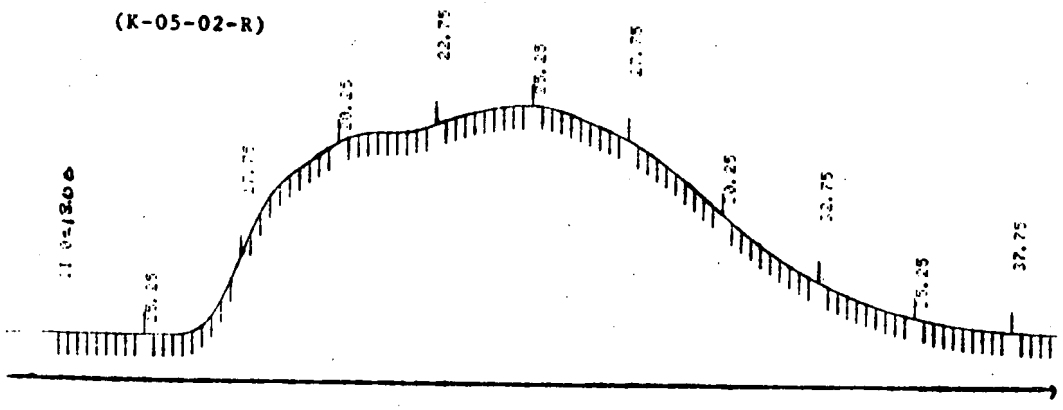

Retention Time (minutes)

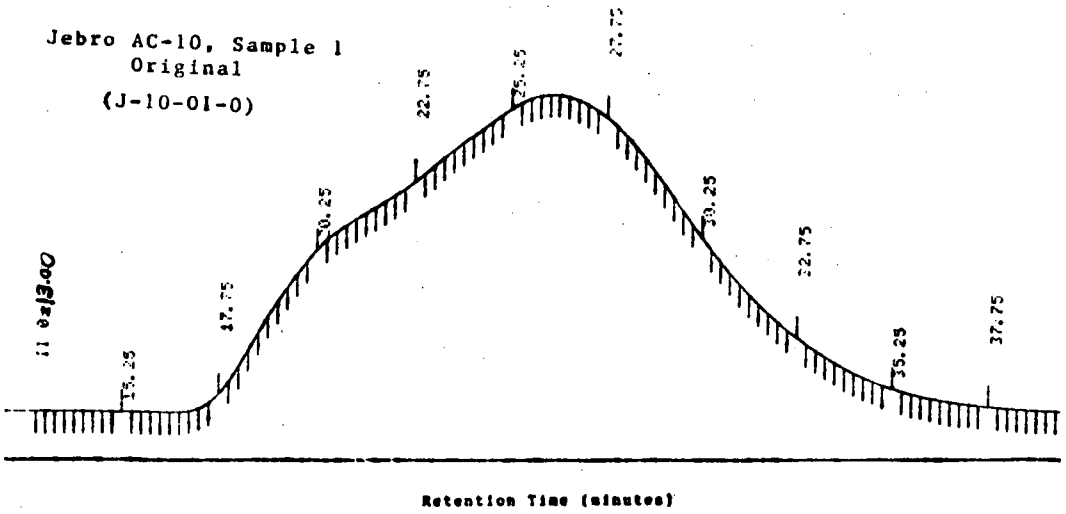
Jebro AC-10, Sample 1
Original
(J-10-01-0)
17.75
22.75
27.75
30.25
32.75
35.25
37.75
Retention Time (minutes)

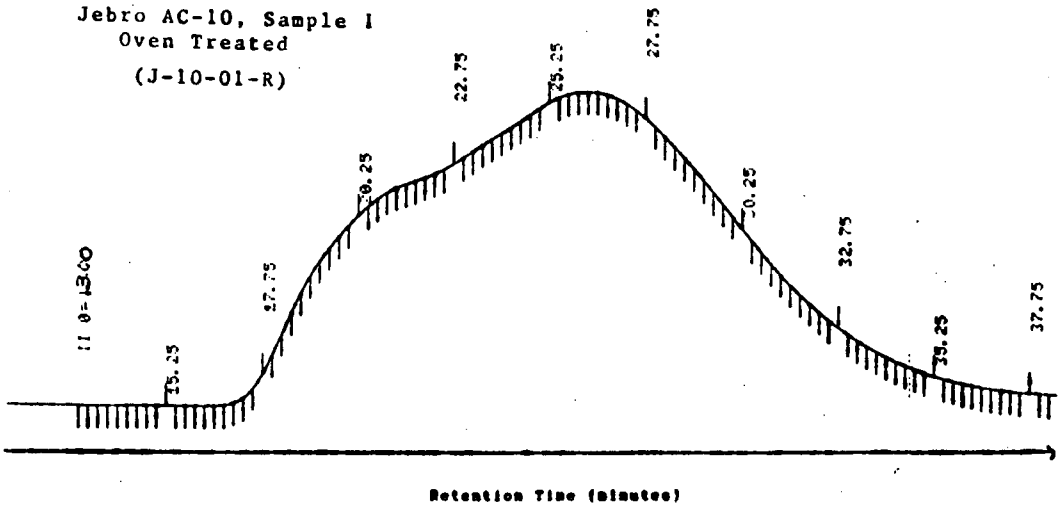
Jebro AC-10, Sample 1
Oven Treated
(J-10-01-R)
17.75
22.75
27.75
30.25
32.75
35.25
37.75
Retention Time (minutes)

Jebro AC-10, Sample 2
Original
(J-10-02-0)

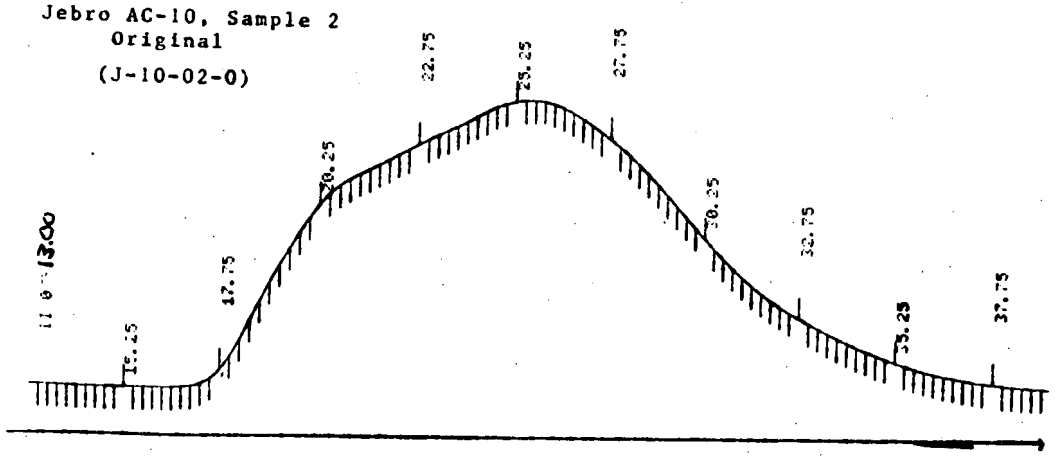

Retention Time (minutes)

Jebro AC-10, Sample 2
Oven Treated
(J-10-02-R)

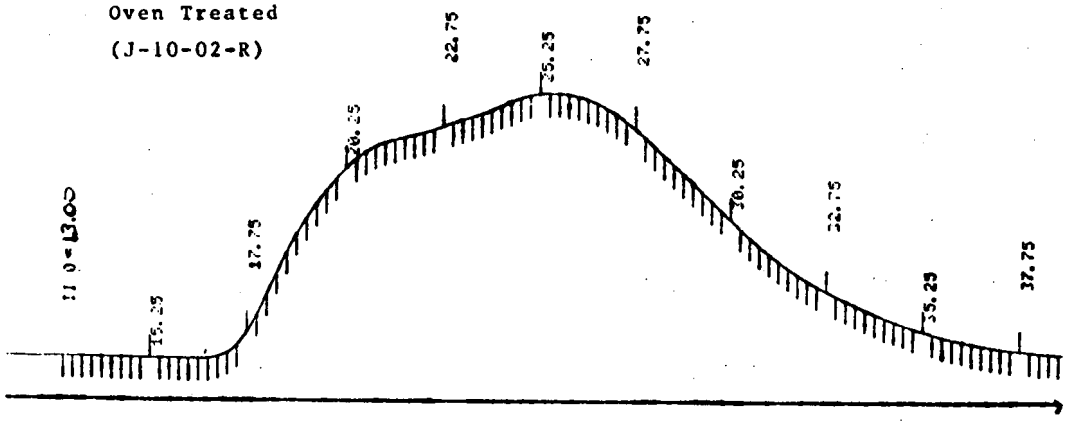

Retention Time (minutes)

Koch AC-10, Sample 1
Original

(K-10-01-0)

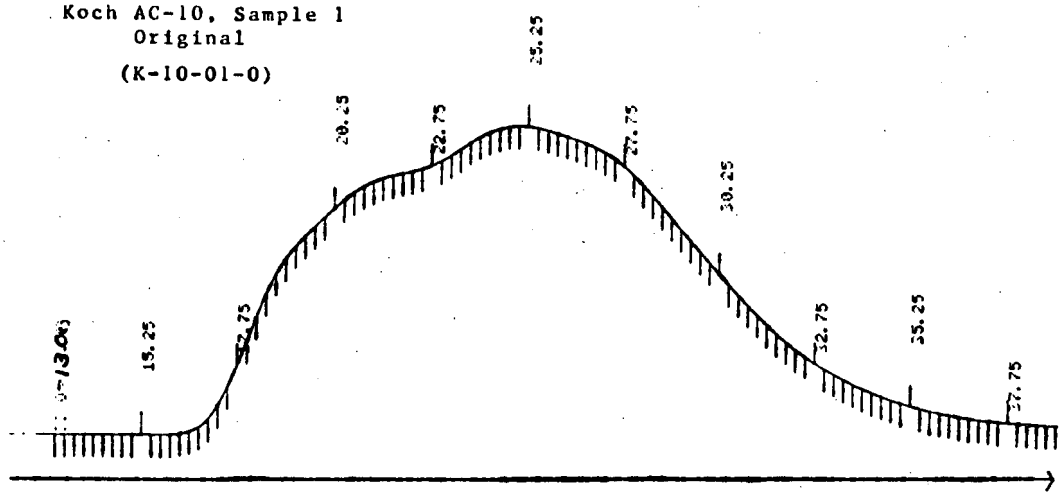

Koch AC-10, Sample 1
Oven Treated

(K-10-01-R)

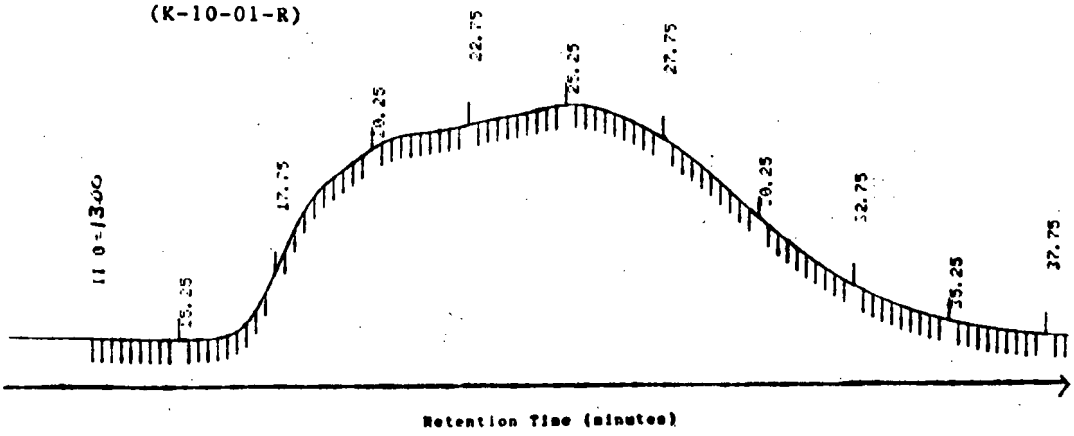

Koch AC-10, Sample 2
Original
(K-10-02-0)

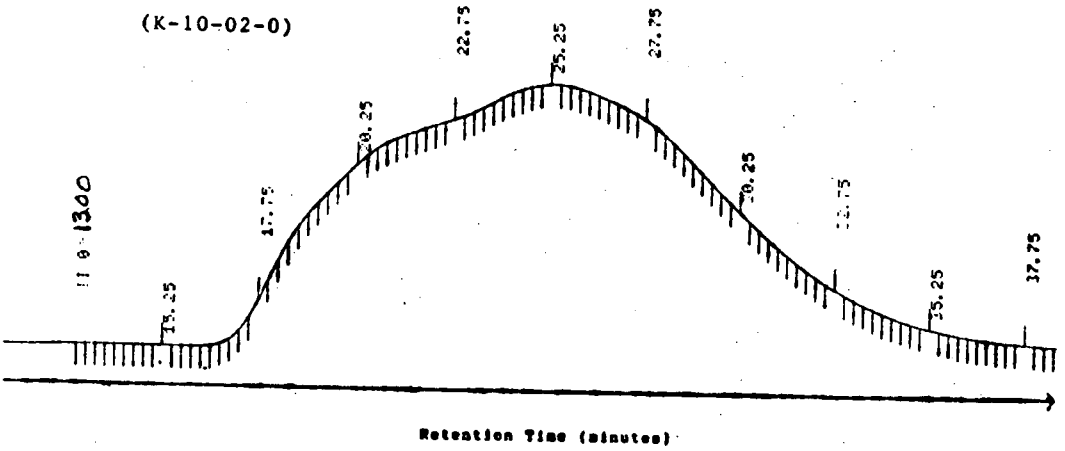

Koch AC-10, Sample 2
Oven Treated
(K-10-02-R)

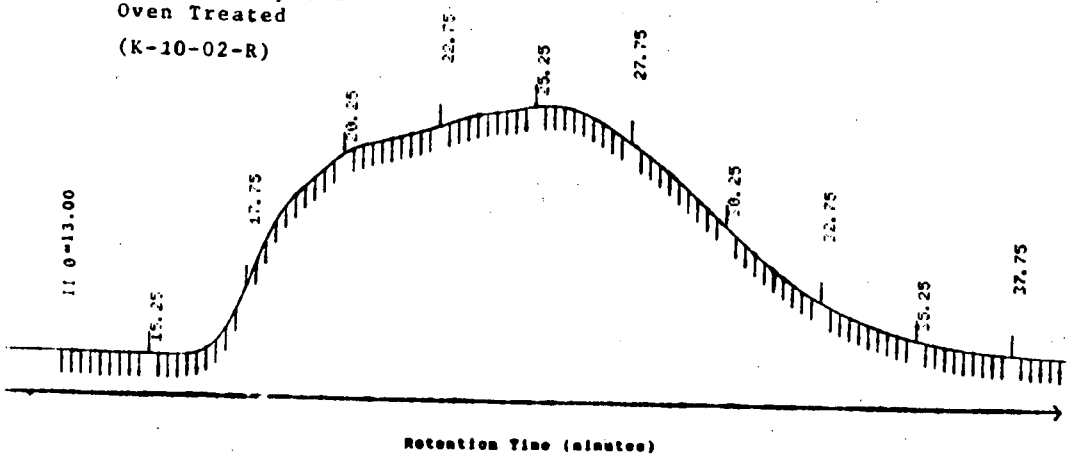

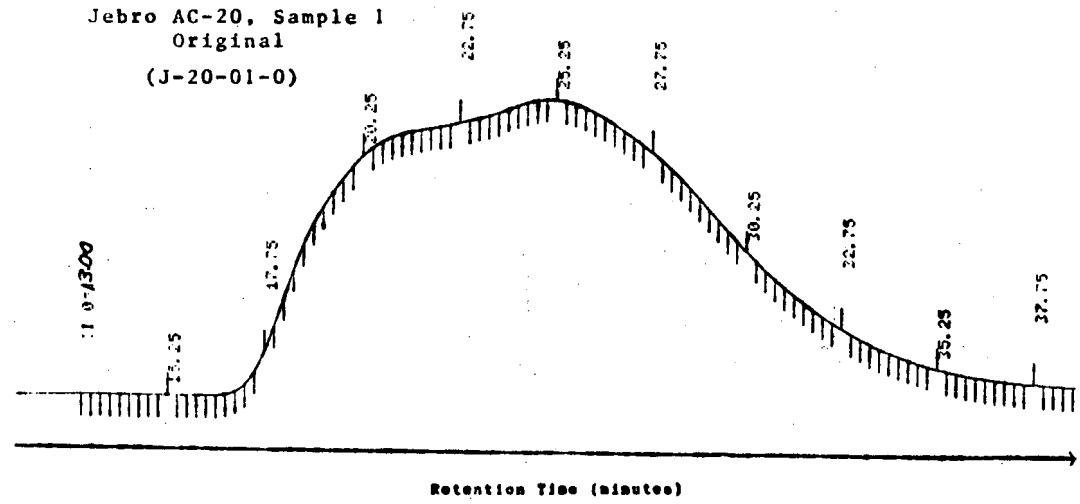
Jebro AC-20, Sample 1
Original
(J-20-01-0)
Retention Time (minutes)

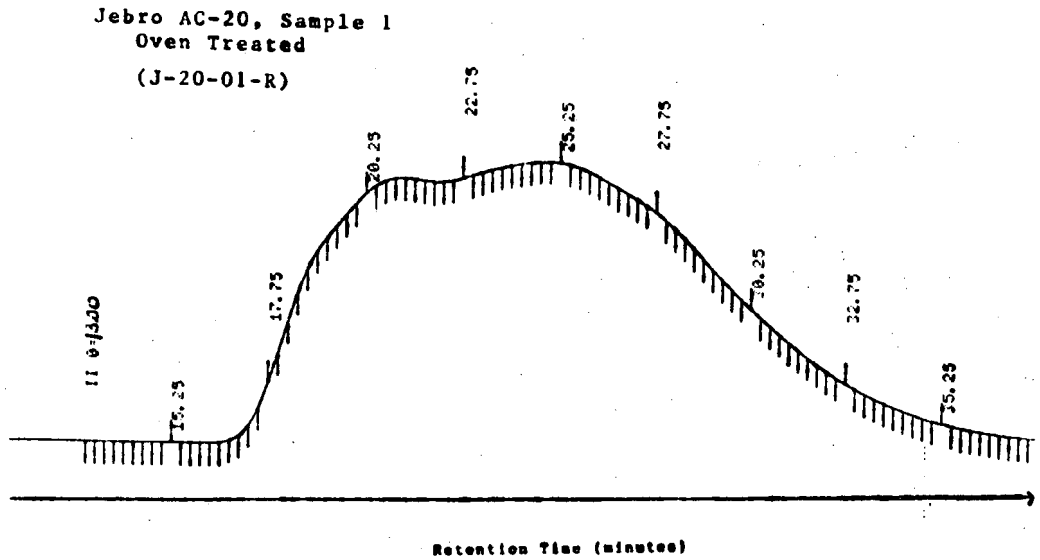
Jebro AC-20, Sample 1
Oven Treated
(J-20-01-R)
Retention Time (minutes)

Jebro AC-20, Sample 2
Original

(J-20-02-0)

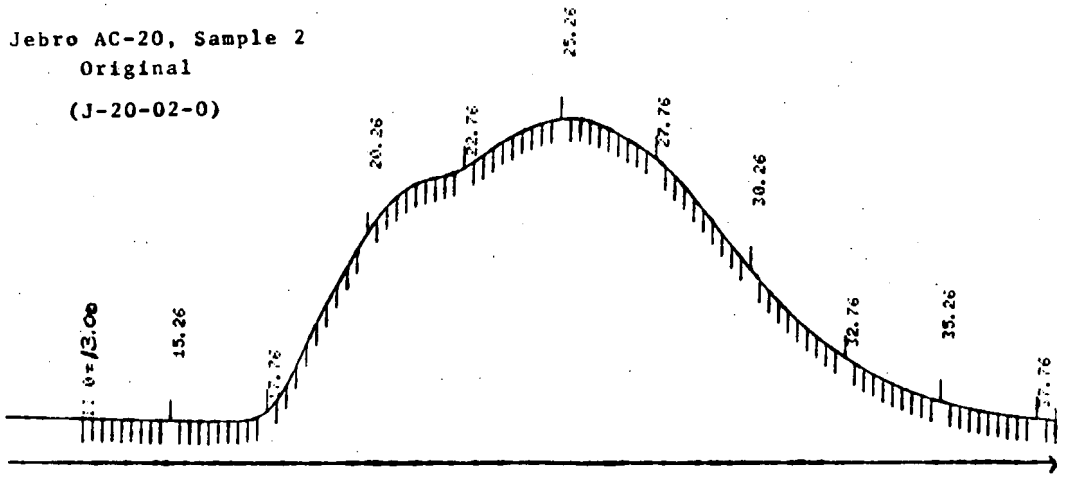

Retention Time (minutes)

Jebro AC-20, Sample 2
Oven Treated

(J-20-02-R)

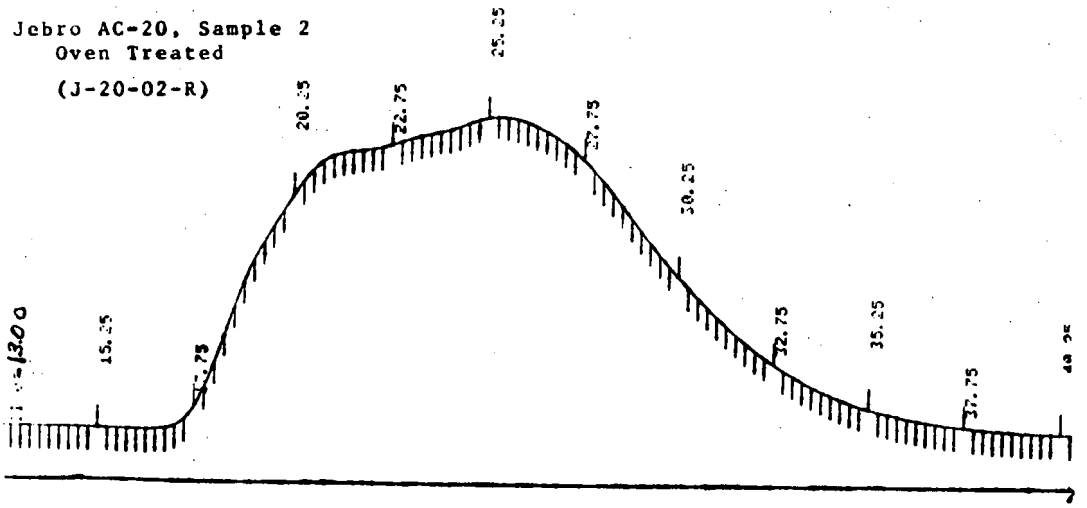

Retention Time (minutes)

Koch AC-20, Sample 1
Original
(K-20-01-0)

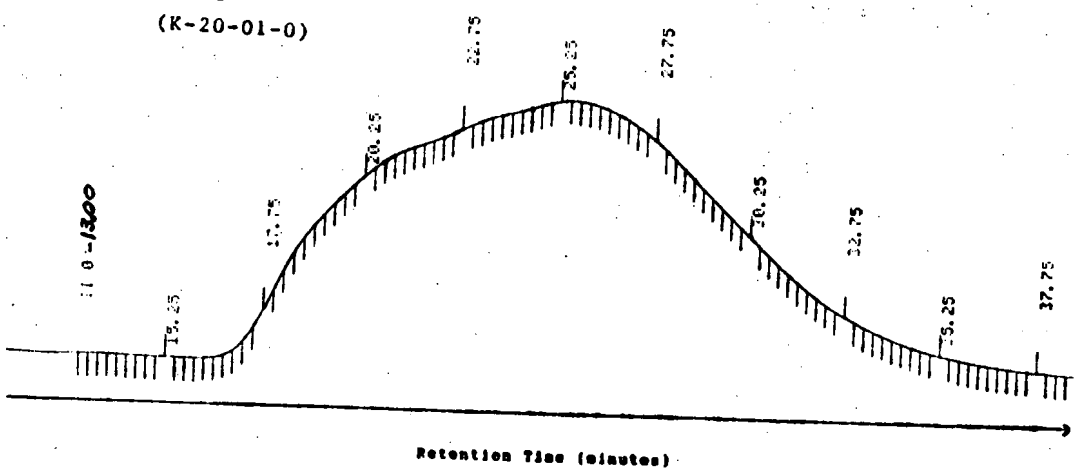

Koch AC-20, Sample 1
Oven Treated
(K-20-01-R)

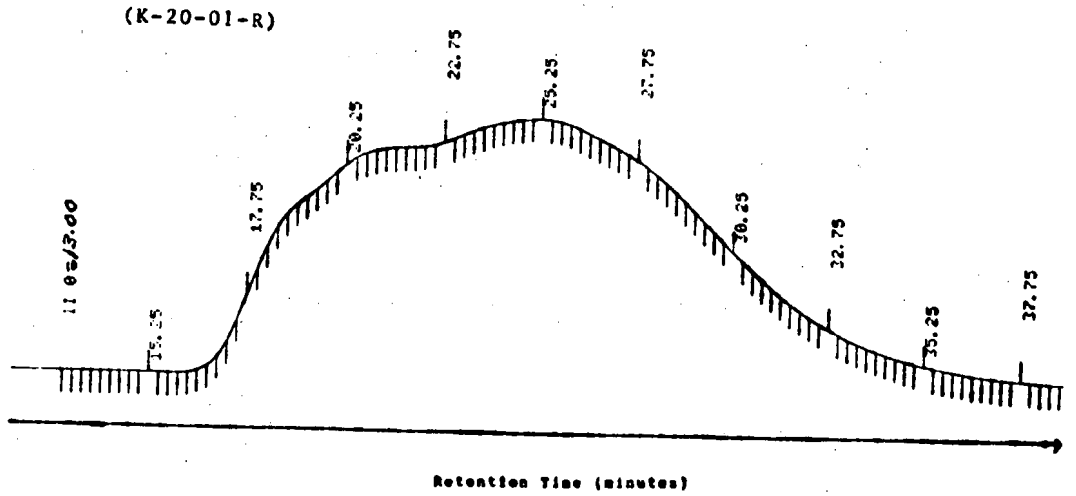

Koch AC-20, Sample 2
Original
(K-20-02-0)

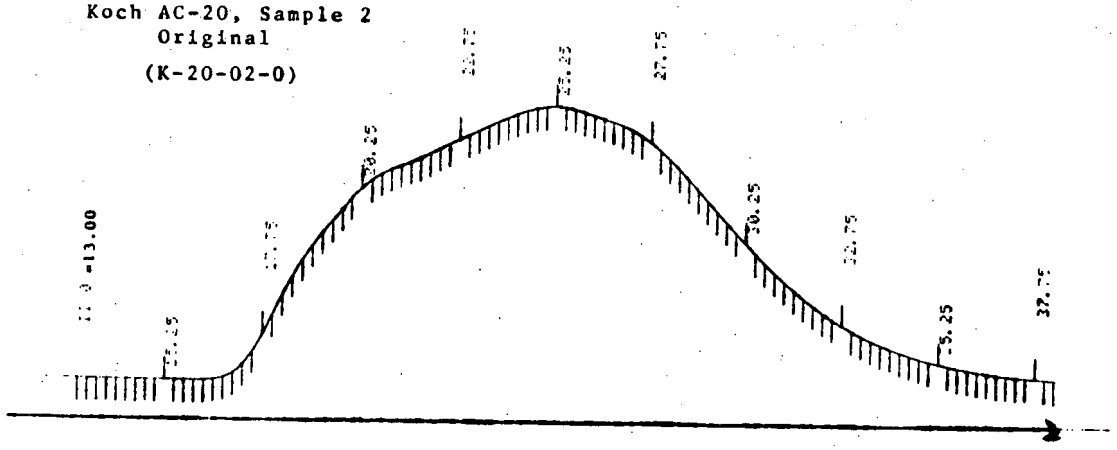

Koch AC-20, Sample 2
Oven Treated
(K-20-02-R)

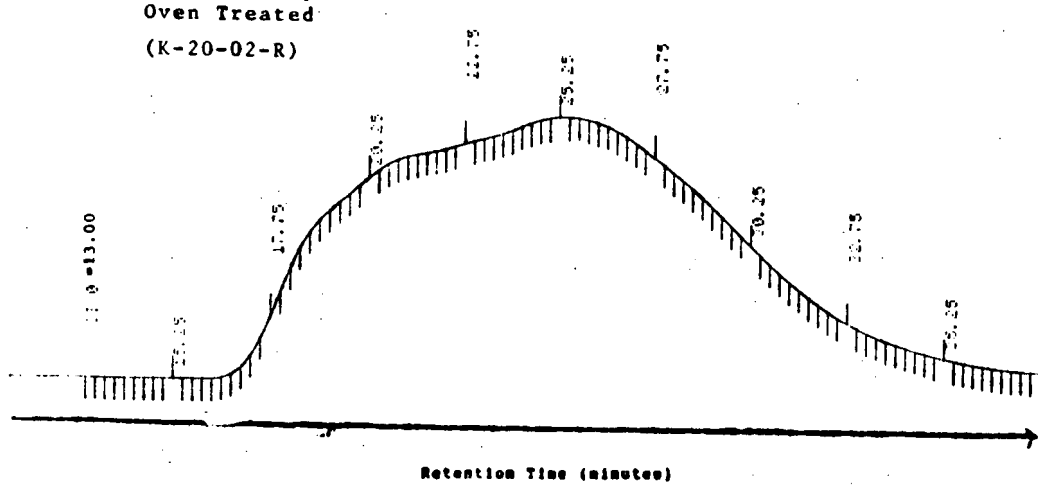

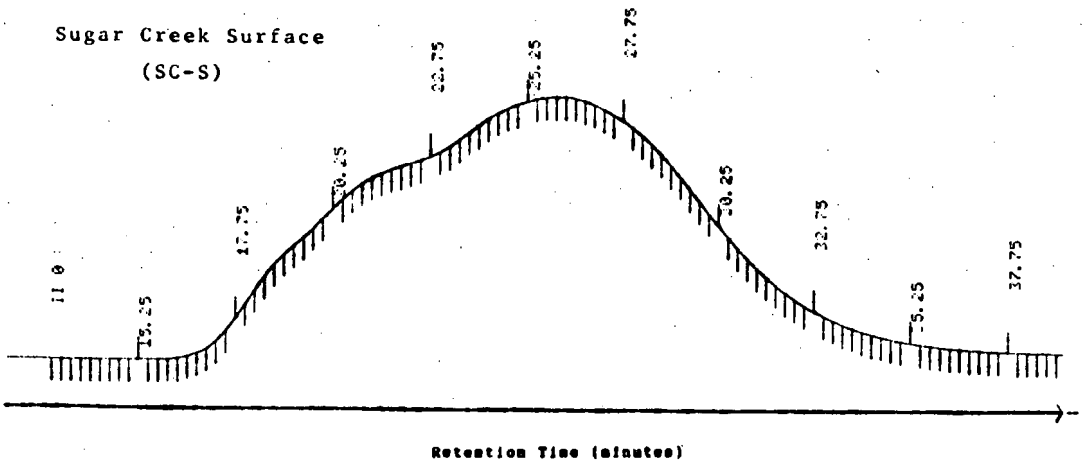
Sugar Creek Surface
(SC-S)
15.25
17.75
20.25
22.75
25.25
27.75
30.25
32.75
35.25
37.75
Retention Time (minutes)

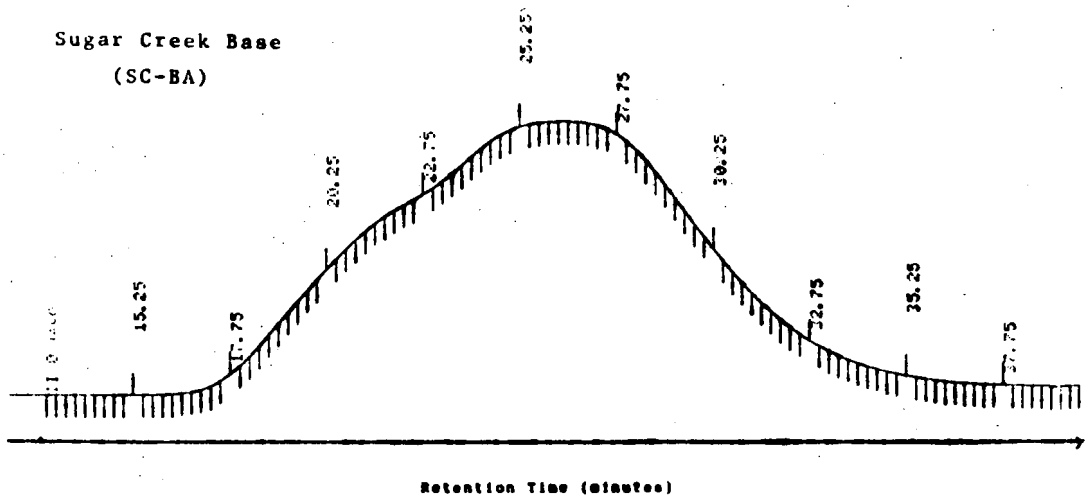
Sugar Creek Base
(SC-BA)
15.25
17.75
20.25
22.75
25.25
27.75
30.25
32.75
35.25
Retention Time (minutes)

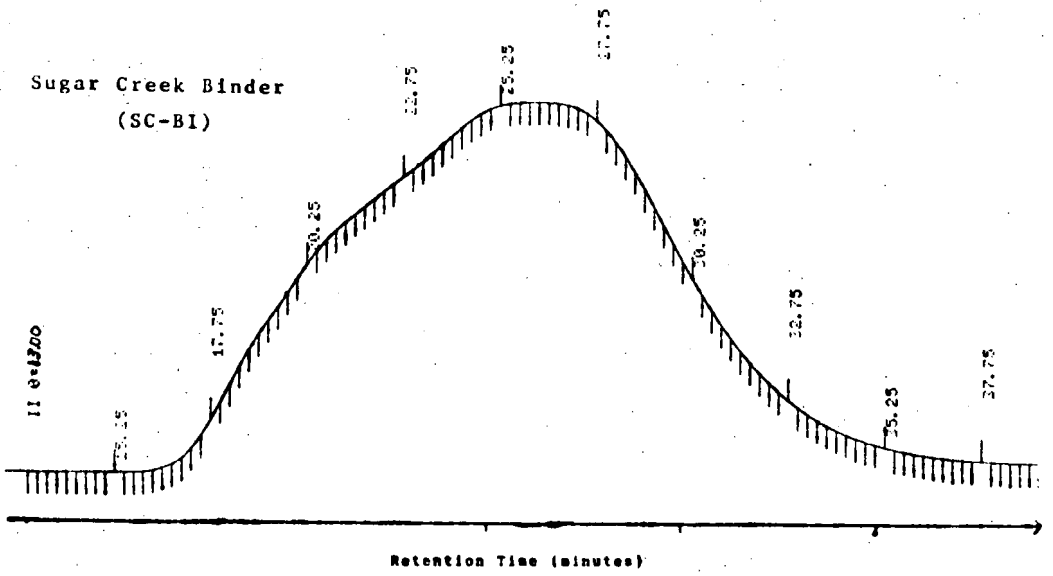
Sugar Creek Binder
(SC-BI)
Retention Time (minutes)

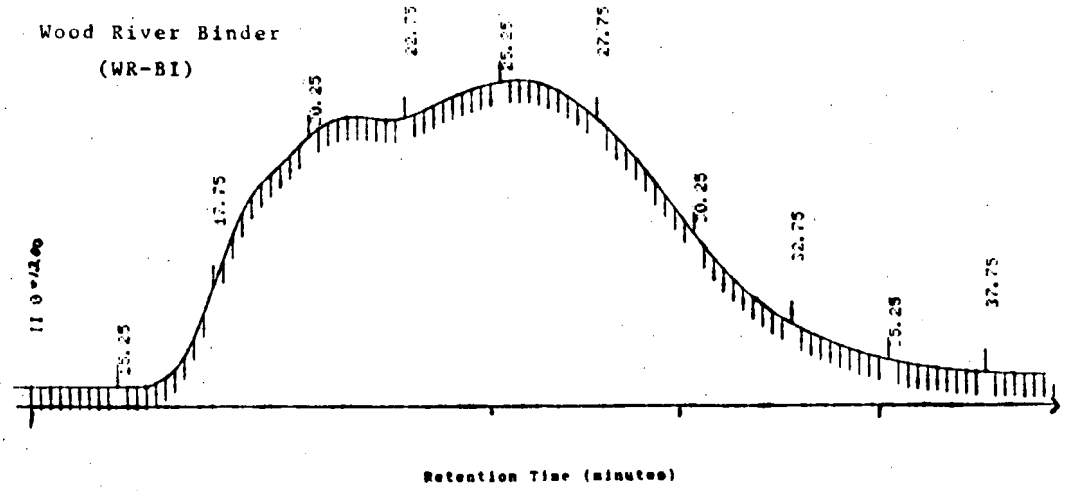
Wood River Binder
(WR-BI)
Retention Time (minutes)

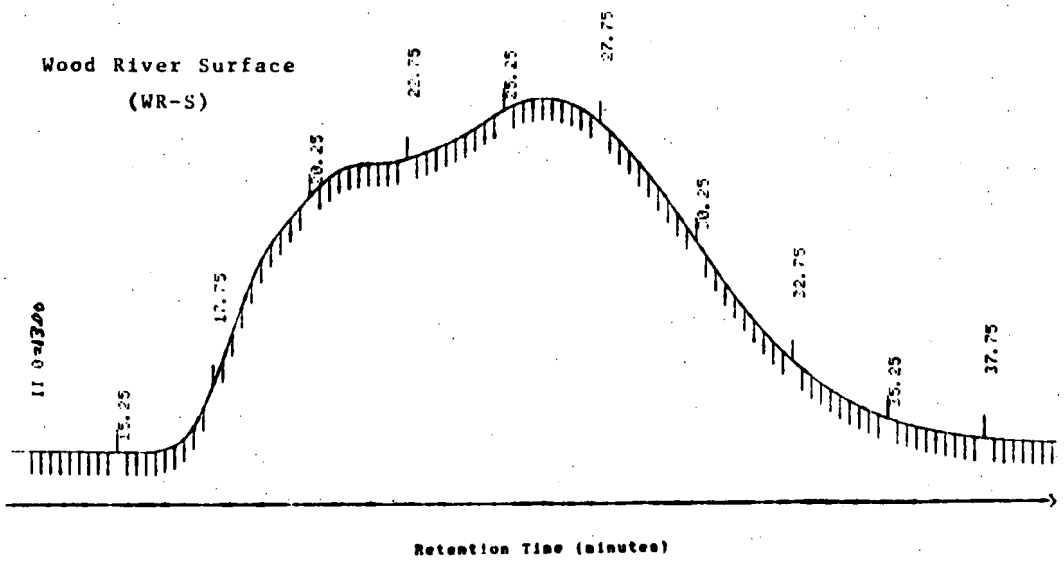
Wood River Surface
(WR-S)
Retention Time (minutes)

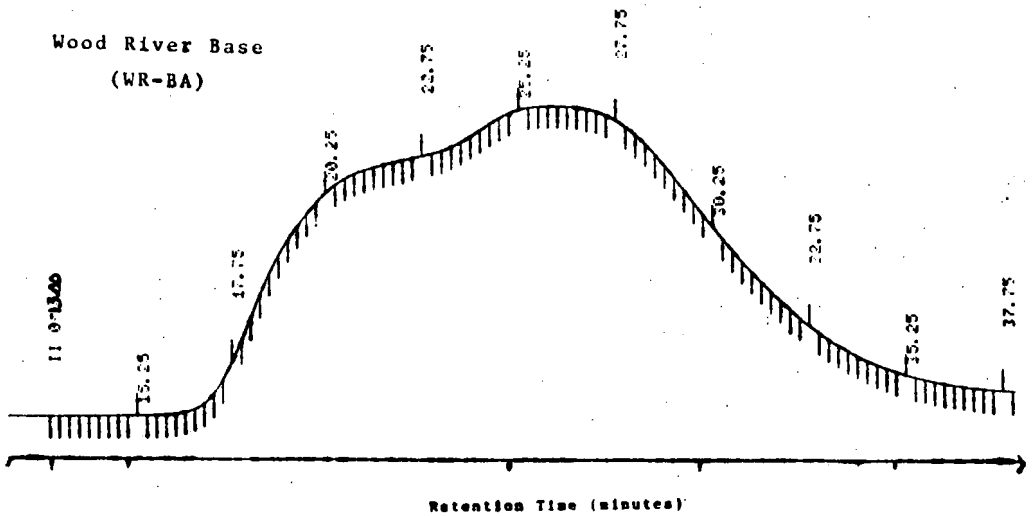
Wood River Base
(WR-BA)
Retention Time (minutes)

APPENDIX II

DSC THERMOGRAMS

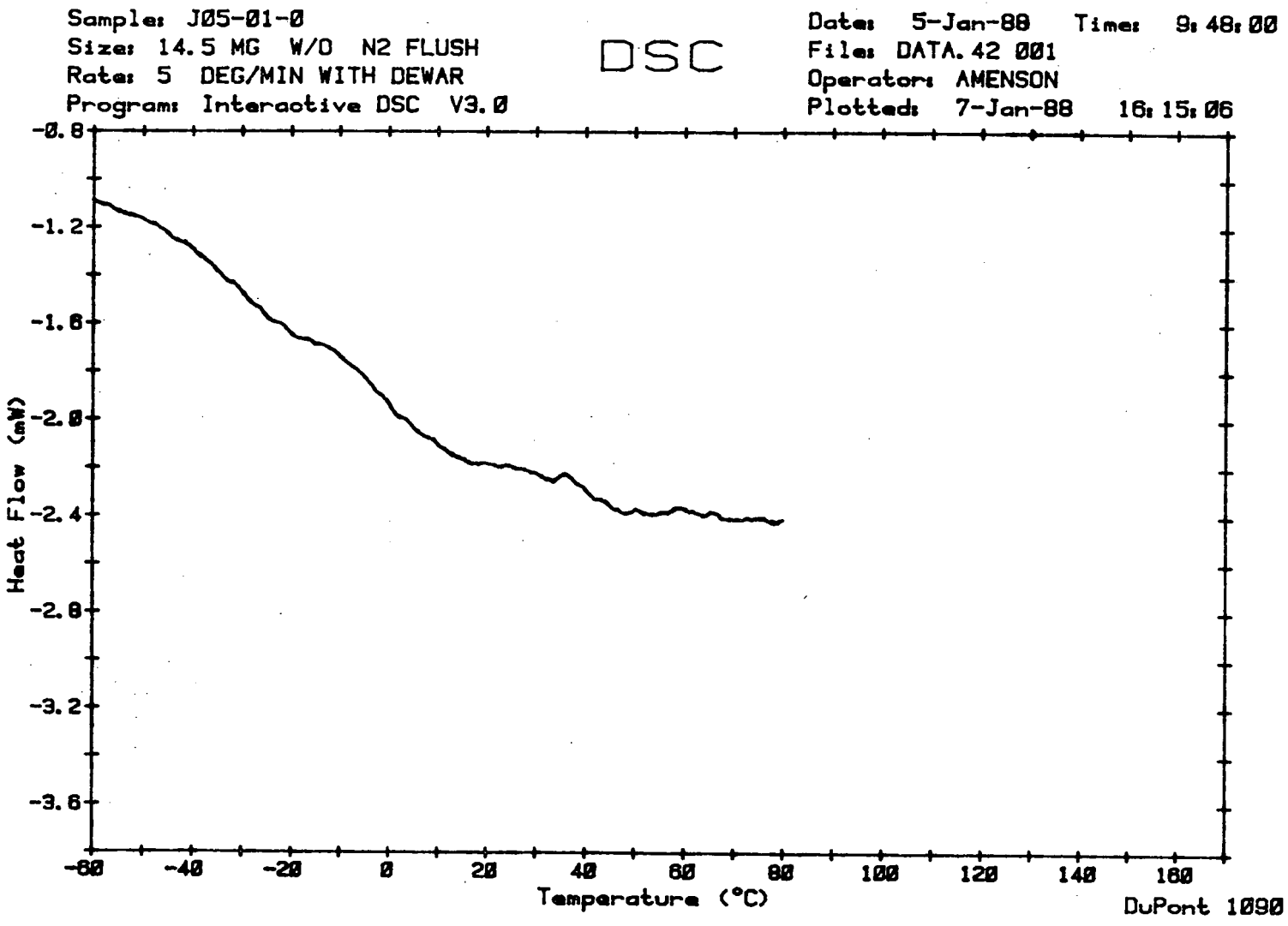

Appendix II-1

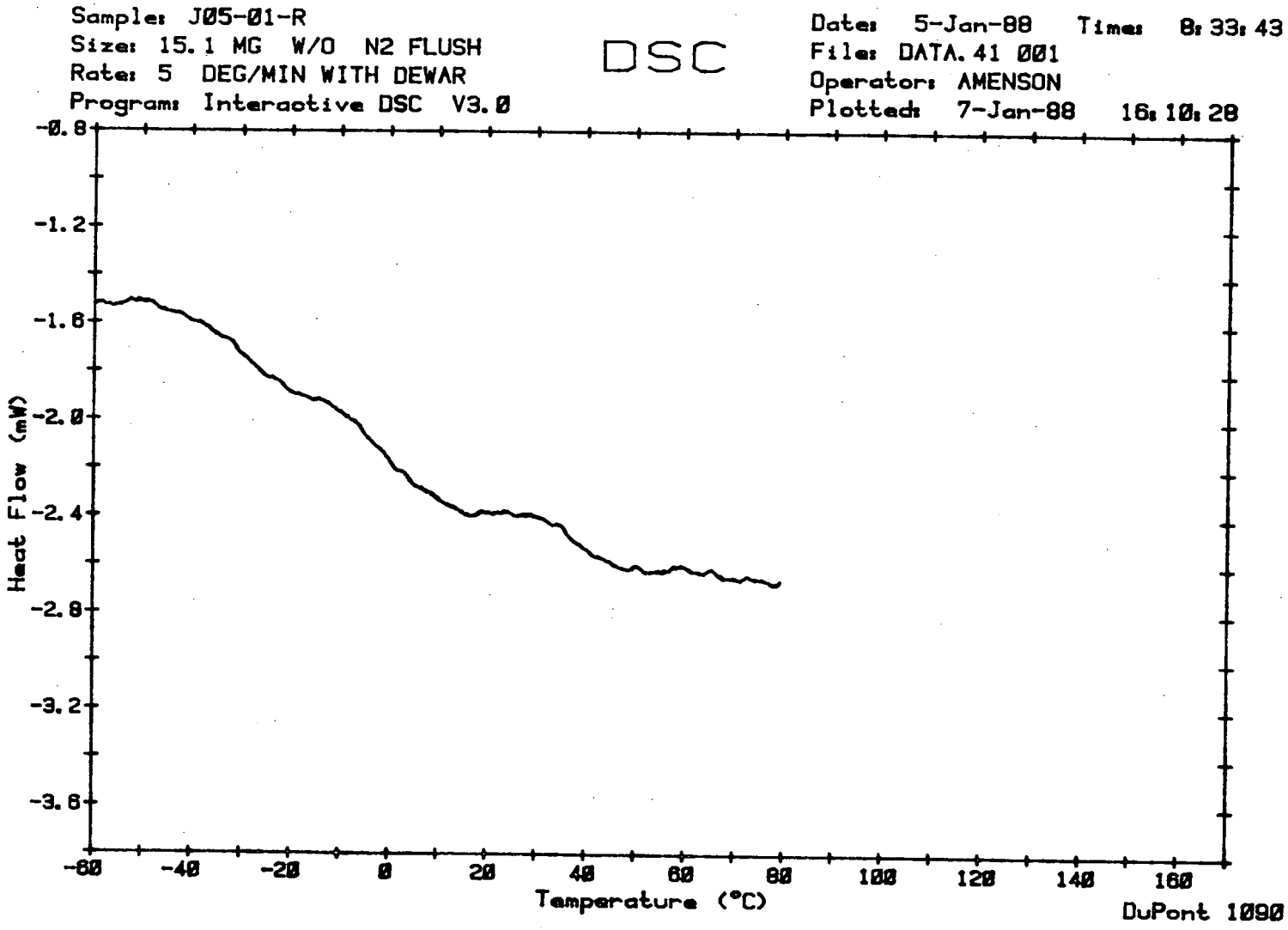
Sample: J05-01-R
Size: 15.1 MG W/O N2 FLUSH
Rate: 5 DEG/MIN WITH DEWAR
Program: Interactive DSC V3.0
DSC
Date: 5-Jan-88 Time: 8:33:43
File: DATA.41 001
Operator: AMENSON
Plotted: 7-Jan-88 16:10:28
-0.8
-1.2
-1.6
-2.0
-2.4
-2.8
-3.2
-3.6
Heat Flow (mW)
-60
-40
-20
0
20
40
60
80
100
120
140
160
Temperature (°C)
DuPont 1090

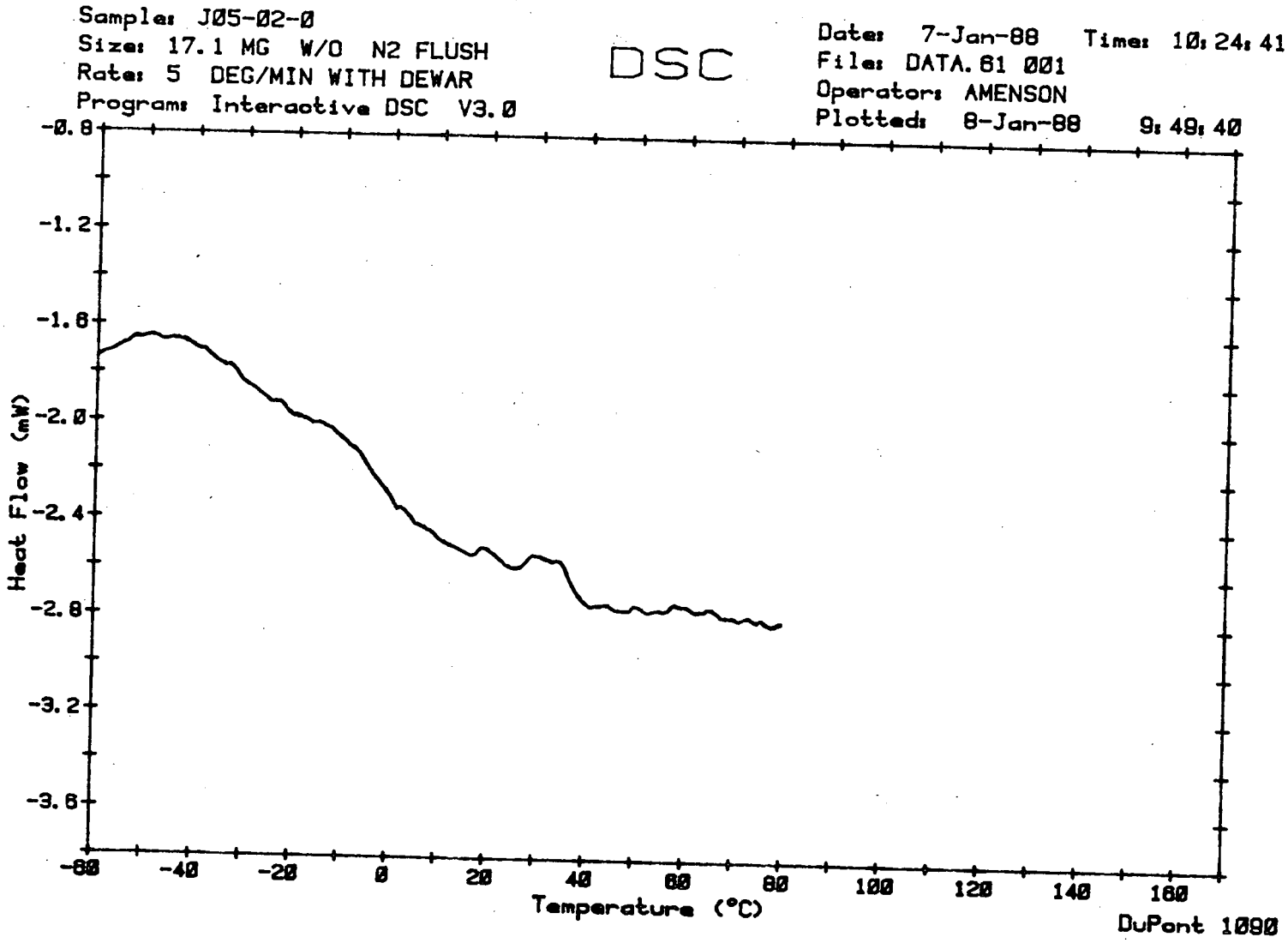
Sample: J05-02-0
Size: 17.1 MG W/O N2 FLUSH
Rate: 5 DEG/MIN WITH DEWAR
Program: Interactive DSC V3.0
DSC
Date: 7-Jan-88 Time: 10:24:41
File: DATA.61 001
Operator: AMENSON
Plotted: 8-Jan-88 9:49:40
-0.8
-1.2
-1.6
-2.0
-2.4
-2.8
-3.2
-3.6
Heat Flow (mW)
-60
-40
-20
0
20
40
60
80
100
120
140
160
Temperature (°C)
DuPont 1090

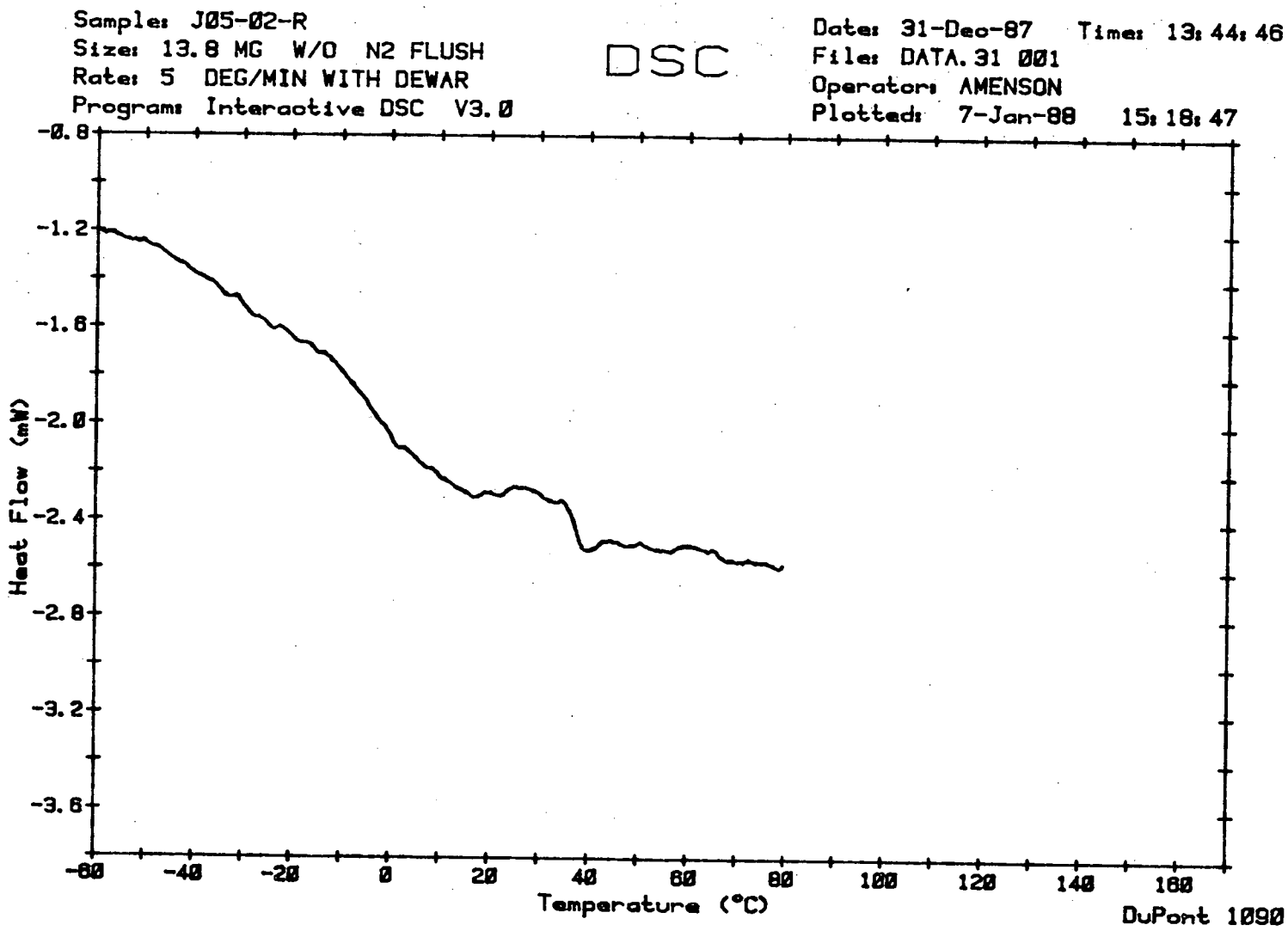
Sample: J05-02-R
Size: 13.8 MG W/O N2 FLUSH
Rate: 5 DEG/MIN WITH DEWAR
Program: Interactive DSC V3.0
DSC
Date: 31-Dec-87 Time: 13:44:46
File: DATA.31 001
Operator: AMENSON
Plotted: 7-Jan-88 15:18:47
-0.8
-1.2
-1.6
-2.0
-2.4
-2.8
-3.2
-3.6
Heat Flow (mW)
-60
-40
-20
0
20
40
60
80
100
120
140
160
Temperature (°C)
DuPont 1090

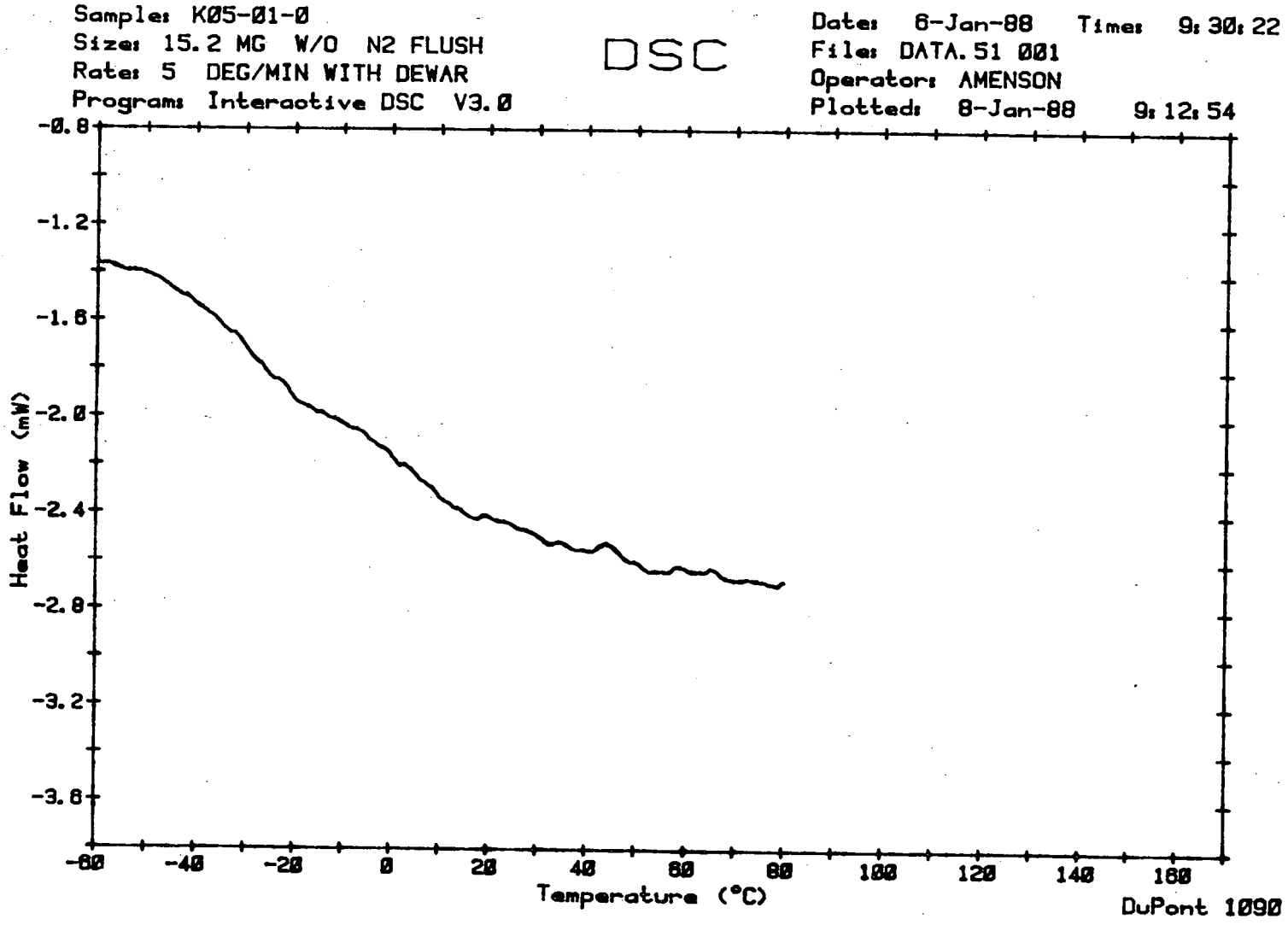
Sample: K05-01-0
Size: 15.2 MG W/O N2 FLUSH
Rate: 5 DEG/MIN WITH DEWAR
Program: Interactive DSC V3.0
DSC
Date: 6-Jan-88 Time: 9:30:22
File: DATA.51 001
Operator: AMENSON
Plotted: 8-Jan-88 9:12:54
-0.8
-1.2
-1.6
-2.0
-2.4
-2.8
-3.2
-3.6
Heat Flow (mW)
-60
-40
-20
0
20
40
60
80
100
120
140
160
Temperature (°C)
DuPont 1090

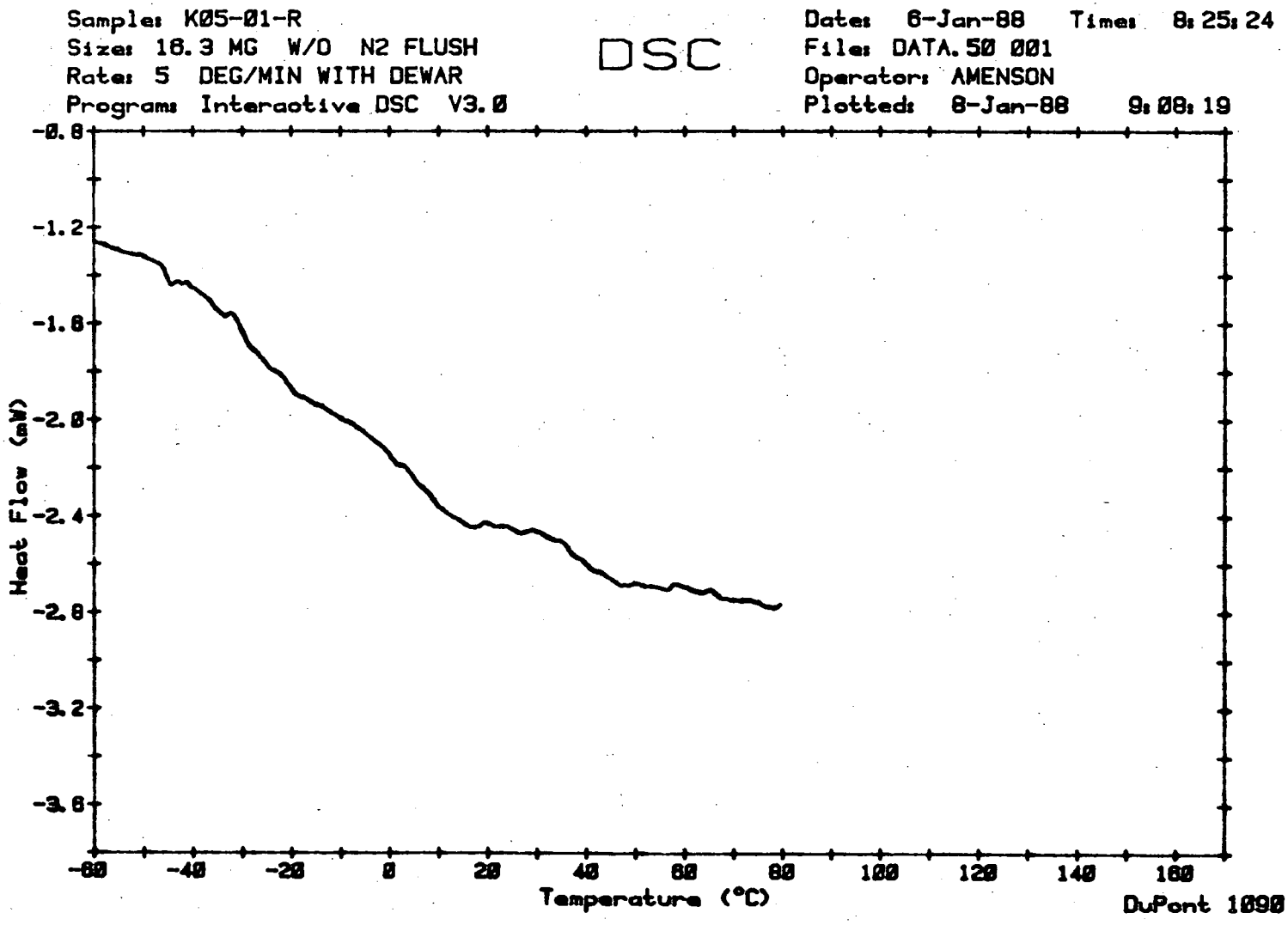
Sample: K05-01-R
Size: 16.3 MG W/O N2 FLUSH
Rate: 5 DEG/MIN WITH DEWAR
Program: Interactive DSC V3.0
DSC
Date: 6-Jan-88 Time: 8:25:24
File: DATA.50 001
Operator: AMENSON
Plotted: 8-Jan-88 9:08:19
-0.8
-1.2
-1.6
-2.0
-2.4
-2.8
-3.2
-3.6
Heat Flow (mW)
-60
-40
-20
0
20
40
60
80
100
120
140
160
Temperature (°C)
DuPont 1090

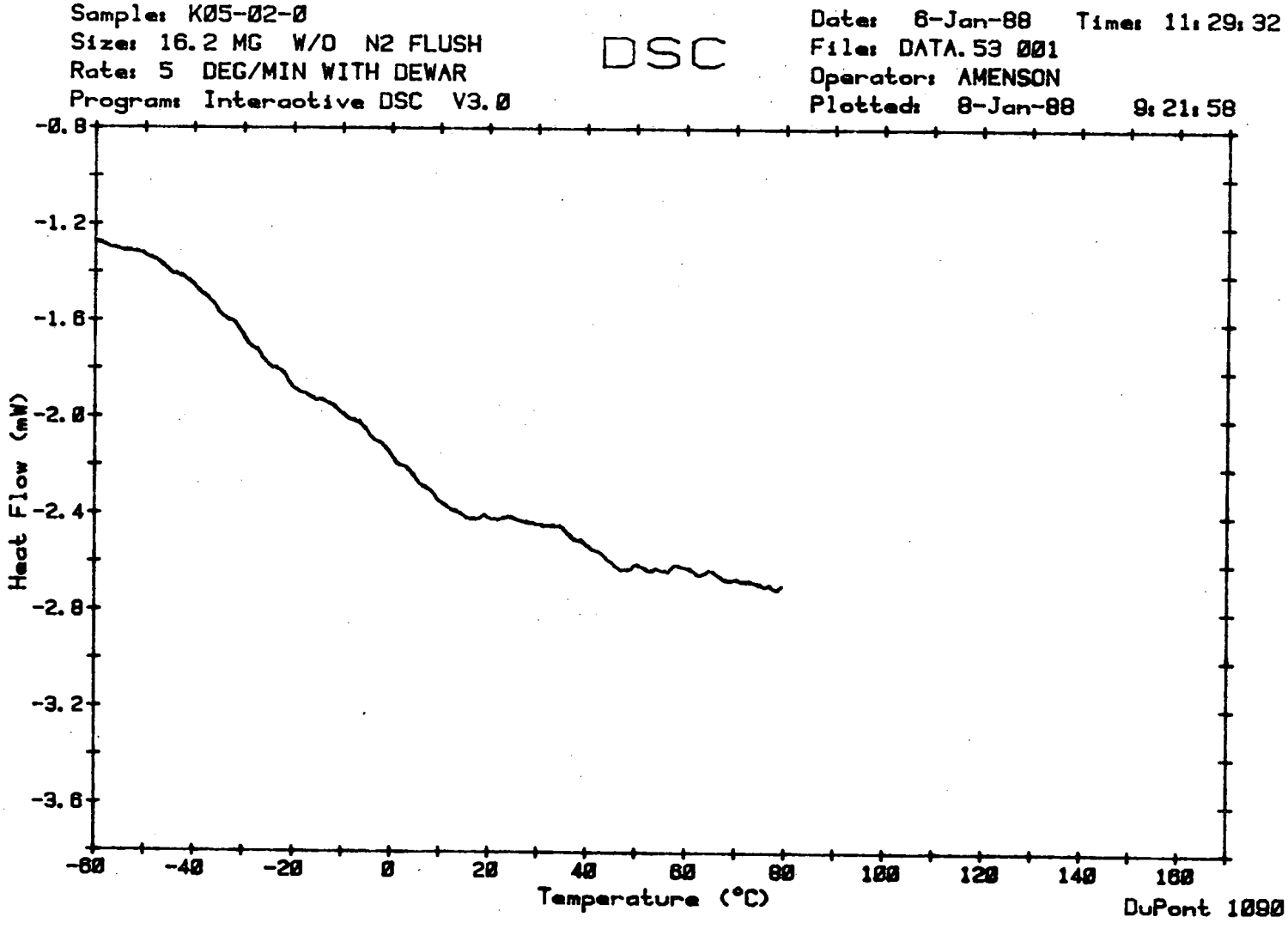
Sample: K05-02-0
Size: 16.2 MG W/O N2 FLUSH
Rate: 5 DEG/MIN WITH DEWAR
Program: Interactive DSC V3.0
DSC
Date: 6-Jan-88 Time: 11:29:32
File: DATA.53 001
Operator: AMENSON
Plotted: 8-Jan-88 9:21:58
-0.8
-1.2
-1.6
-2.0
-2.4
-2.8
-3.2
-3.6
Heat Flow (mW)
-60
-40
-20
0
20
40
60
80
100
120
140
160
Temperature (°C)
DuPont 1090

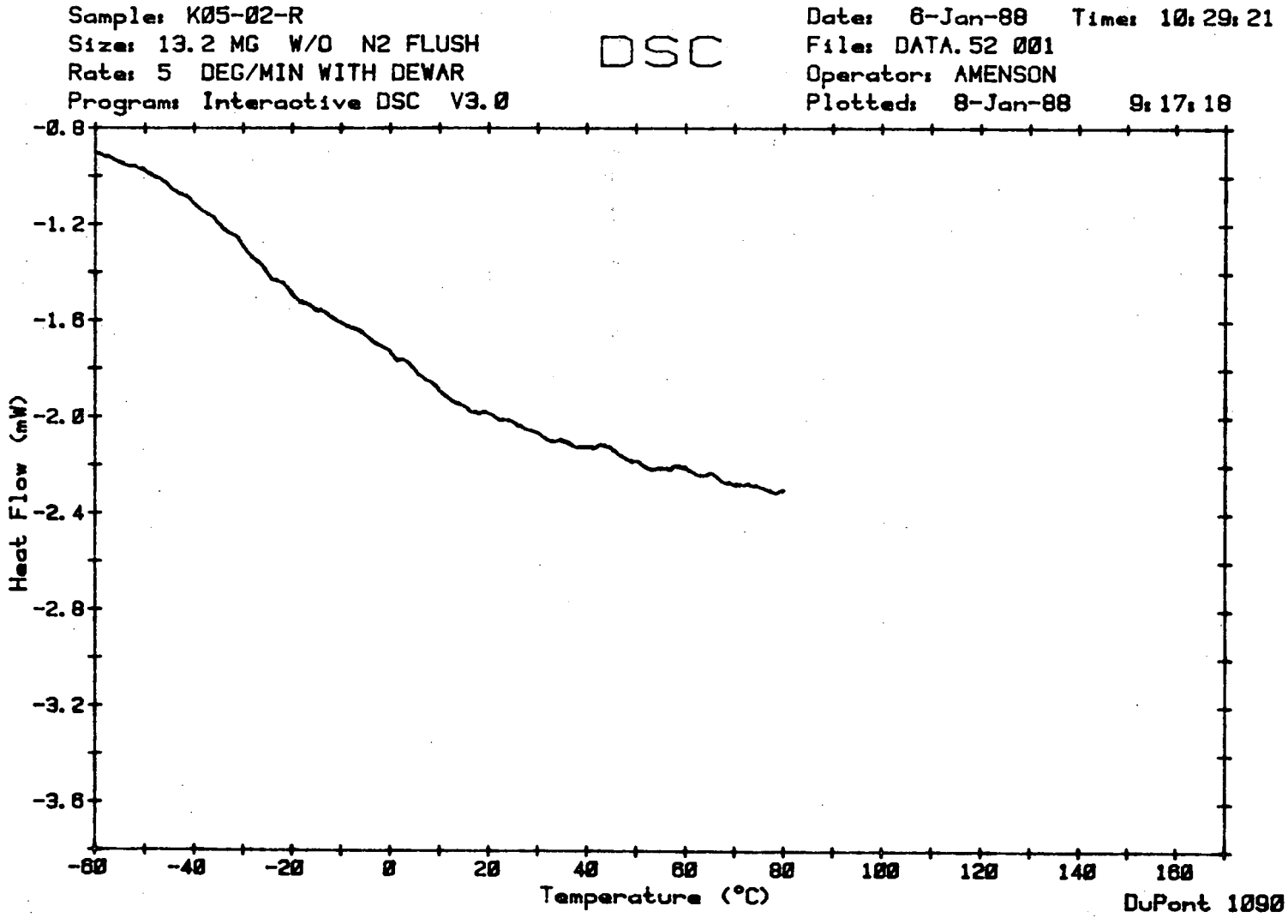
Sample: K05-02-R
Size: 13.2 MG W/O N2 FLUSH
Rate: 5 DEG/MIN WITH DEWAR
Program: Interactive DSC V3.0
DSC
Date: 6-Jan-88 Time: 10:29:21
File: DATA.52 001
Operator: AMENSON
Plotted: 8-Jan-88 9:17:18
-0.8
-1.2
-1.6
-2.0
-2.4
-2.8
-3.2
-3.6
Heat Flow (mW)
-60
-40
-20
0
20
40
60
80
100
120
140
160
Temperature (°C)
DuPont 1090

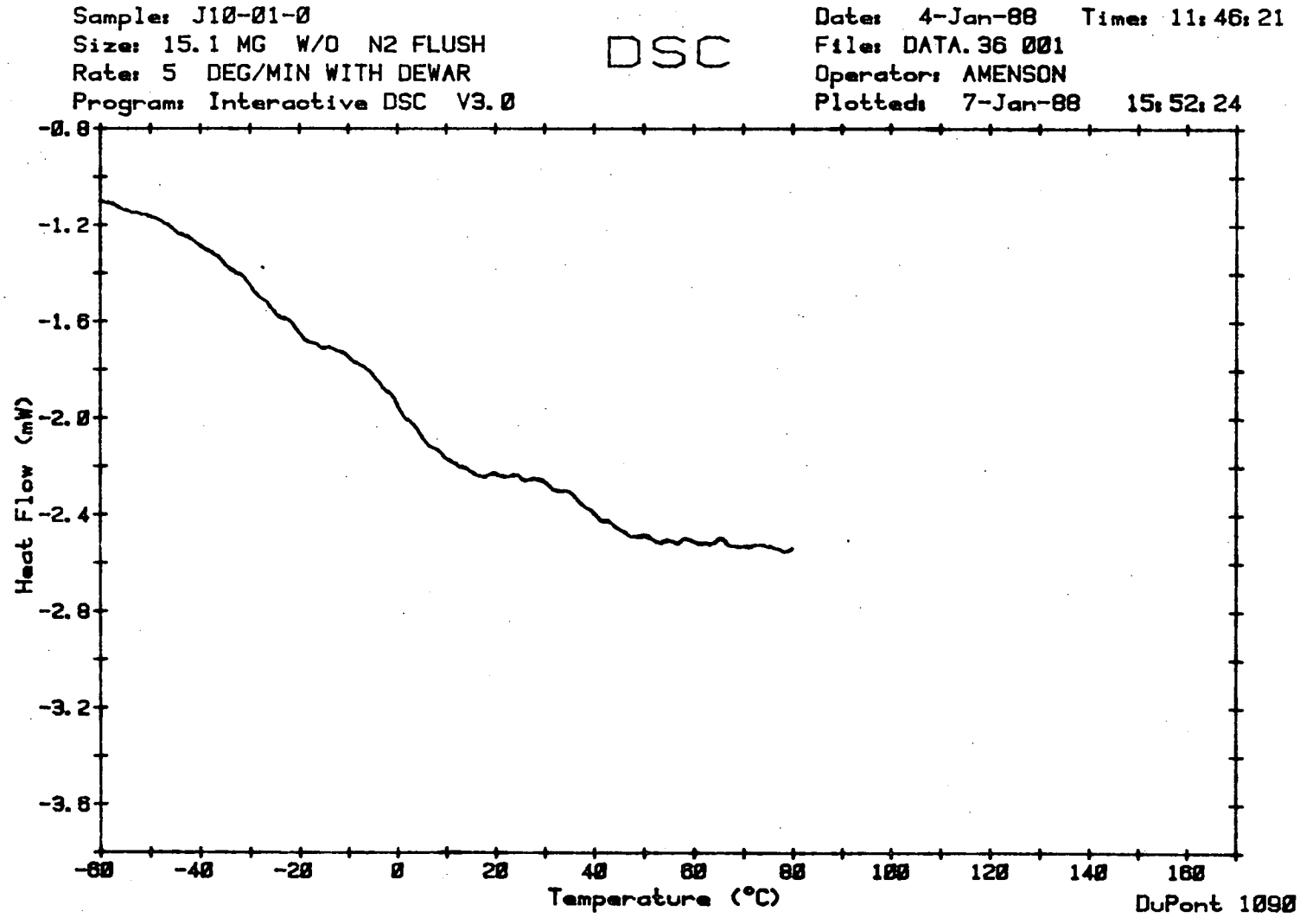
Sample: J10-01-0
Size: 15.1 MG W/O N2 FLUSH
Rate: 5 DEG/MIN WITH DEWAR
Program: Interactive DSC V3.0
DSC
Date: 4-Jan-88 Time: 11:46:21
File: DATA.36 001
Operator: AMENSON
Plotted: 7-Jan-88 15:52:24
-0.8
-1.2
-1.6
-2.0
-2.4
-2.8
-3.2
-3.6
Heat Flow (mW)
-60
-40
-20
0
20
40
60
80
100
120
140
160
Temperature (°C)
DuPont 1090

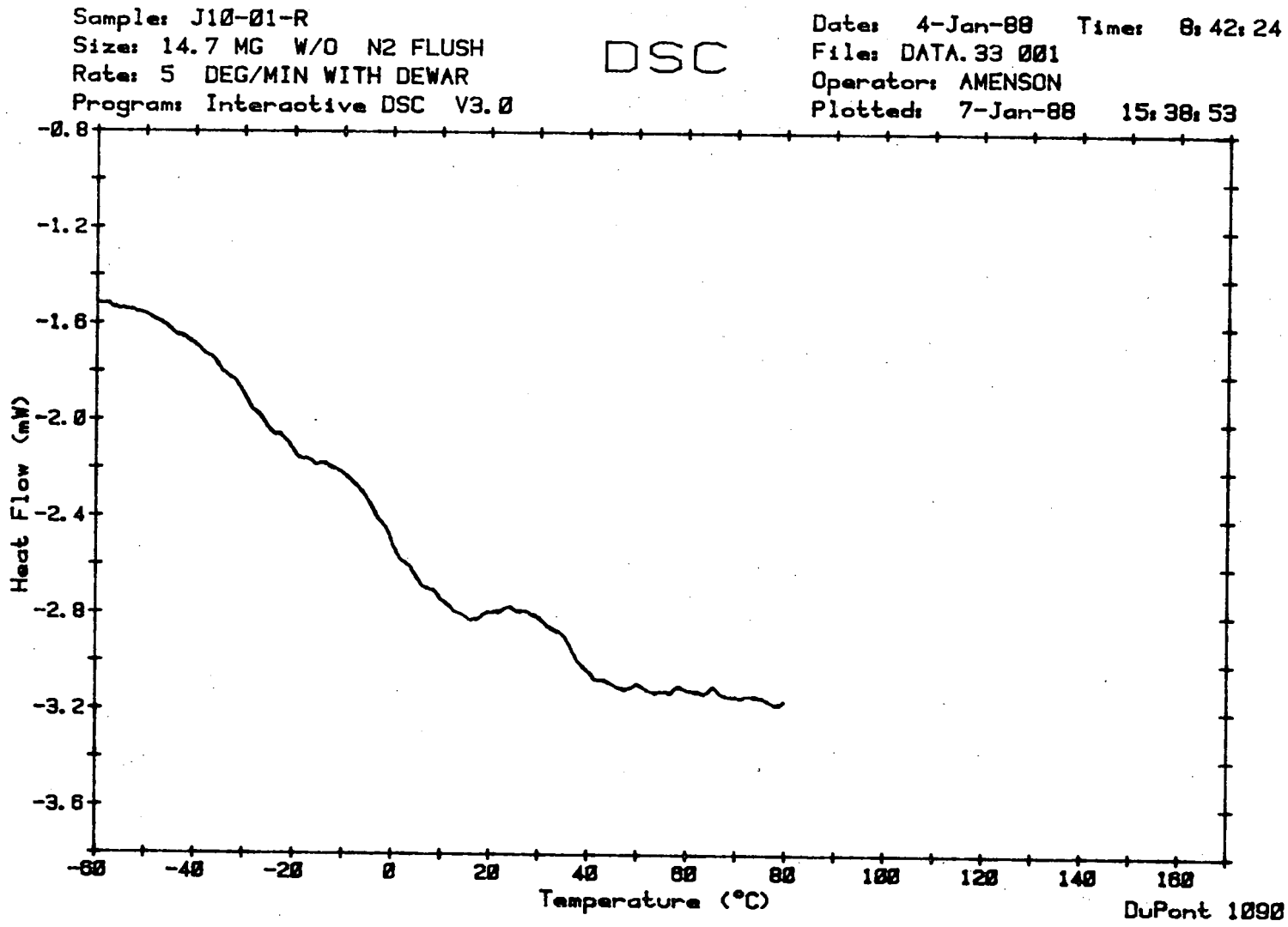
Sample: J10-01-R
Size: 14.7 MG W/O N2 FLUSH
Rate: 5 DEG/MIN WITH DEWAR
Program: Interactive DSC V3.0
DSC
Date: 4-Jan-88 Time: 8:42:24
File: DATA.33 001
Operator: AMENSON
Plotted: 7-Jan-88 15:38:53
-0.8
-1.2
-1.6
-2.0
-2.4
-2.8
-3.2
-3.6
Heat Flow (mW)
-60
-40
-20
0
20
40
60
80
100
120
140
160
Temperature (°C)
DuPont 1090

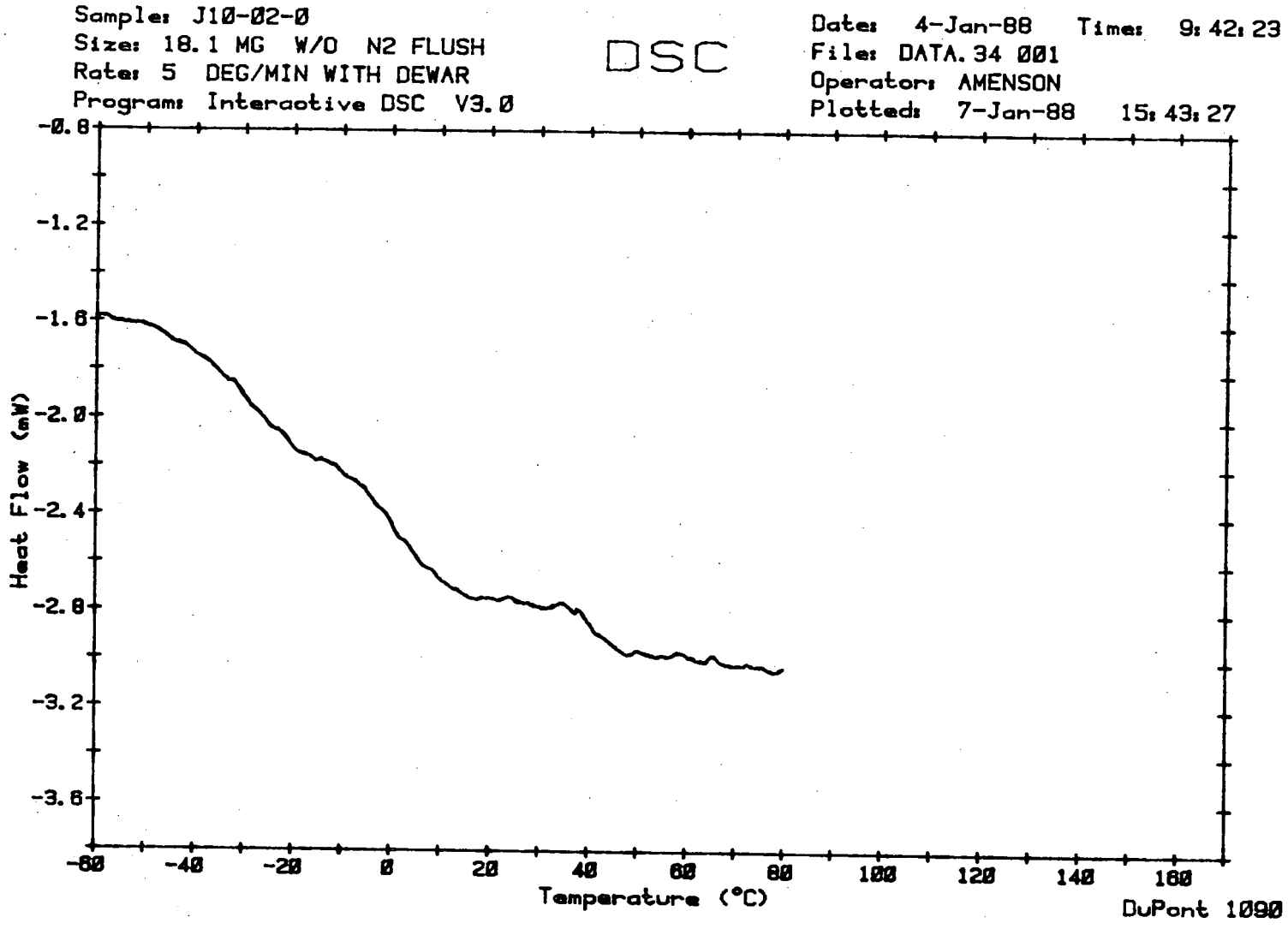
Sample: J10-02-0
Size: 18.1 MG W/O N2 FLUSH
Rate: 5 DEG/MIN WITH DEWAR
Program: Interactive DSC V3.0
DSC
Date: 4-Jan-88 Time: 9:42:23
File: DATA.34 001
Operator: AMENSON
Plotted: 7-Jan-88 15:43:27
-0.8
-1.2
-1.6
-2.0
-2.4
-2.8
-3.2
-3.6
Heat Flow (mW)
-60
-40
-20
0
20
40
60
80
100
120
140
160
Temperature (°C)
DuPont 1090

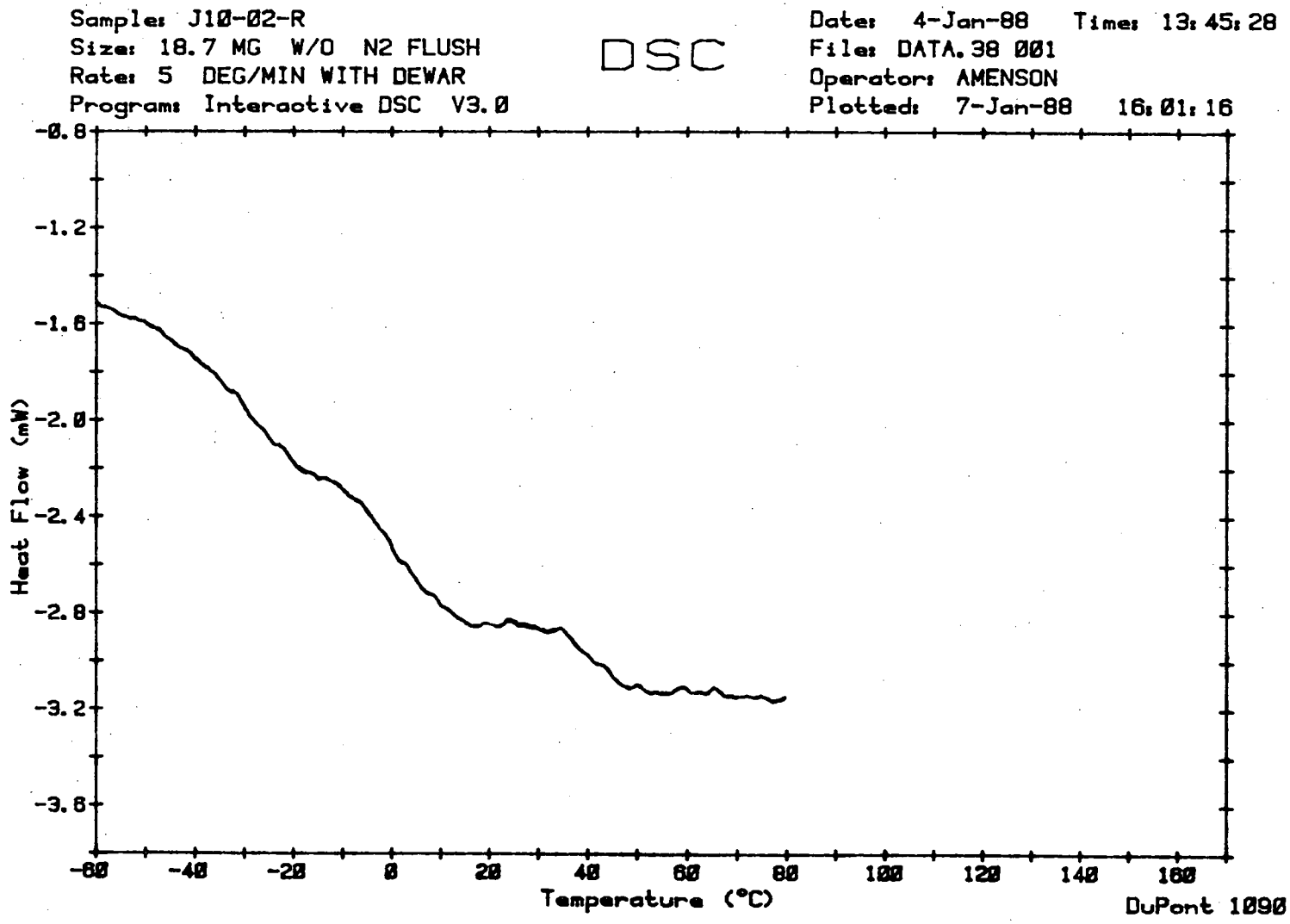
Sample: J10-02-R
Size: 18.7 MG W/O N2 FLUSH
Rate: 5 DEG/MIN WITH DEWAR
Program: Interactive DSC V3.0
DSC
Date: 4-Jan-88 Time: 13:45:28
File: DATA.38 001
Operator: AMENSON
Plotted: 7-Jan-88 16:01:16
-0.8
-1.2
-1.6
-2.0
-2.4
-2.8
-3.2
-3.6
Heat Flow (mW)
-60
-40
-20
0
20
40
60
80
100
120
140
160
Temperature (°C)
DuPont 1090

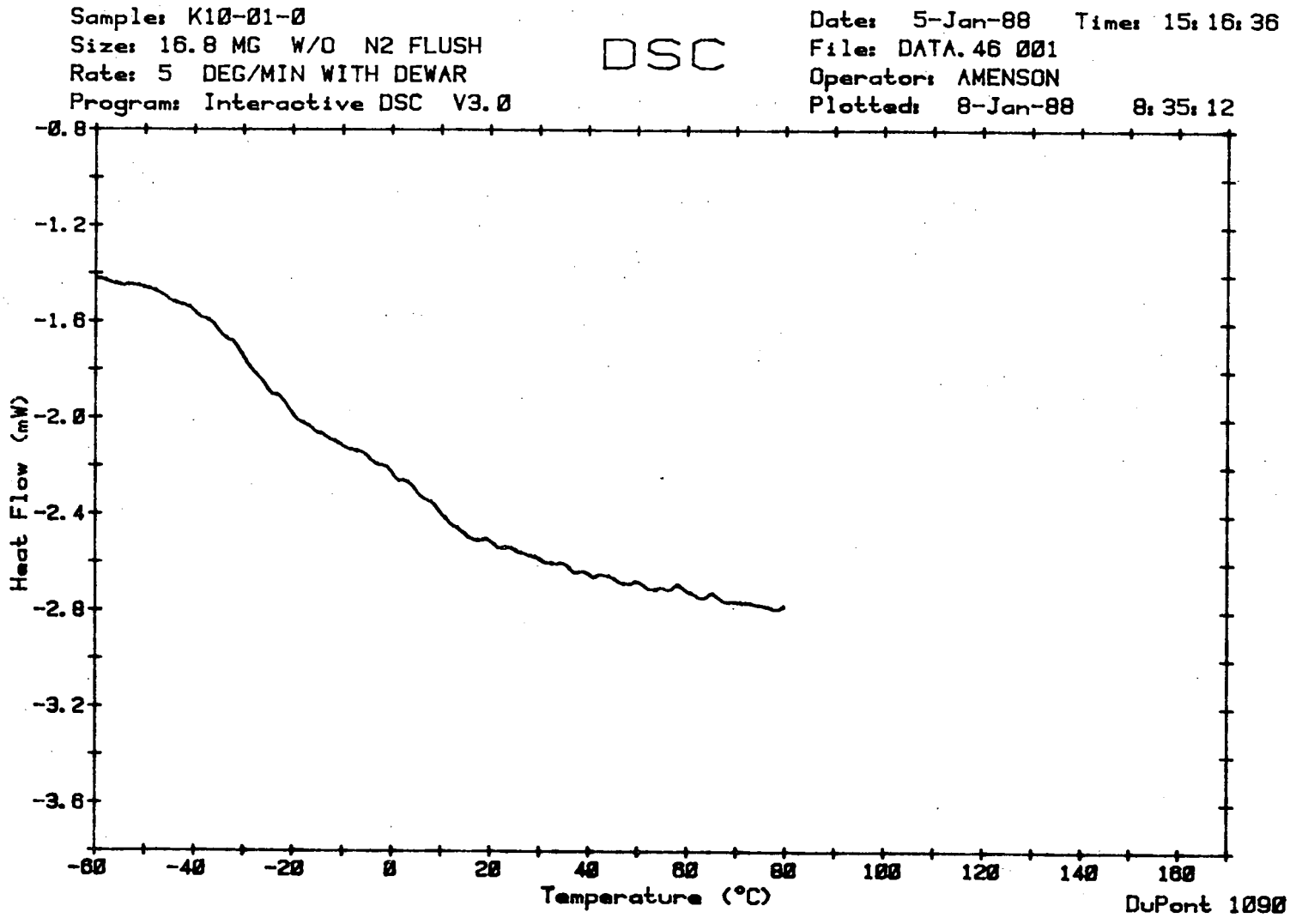
Sample: K10-01-0
Size: 16.8 MG W/O N2 FLUSH
Rate: 5 DEG/MIN WITH DEWAR
Program: Interactive DSC V3.0
DSC
Date: 5-Jan-88 Time: 15:16:36
File: DATA.46 001
Operator: AMENSON
Plotted: 8-Jan-88 8:35:12
-0.8
-1.2
-1.6
-2.0
-2.4
-2.8
-3.2
-3.6
Heat Flow (mW)
-60
-40
-20
0
20
40
60
80
100
120
140
160
Temperature (°C)
DuPont 1090

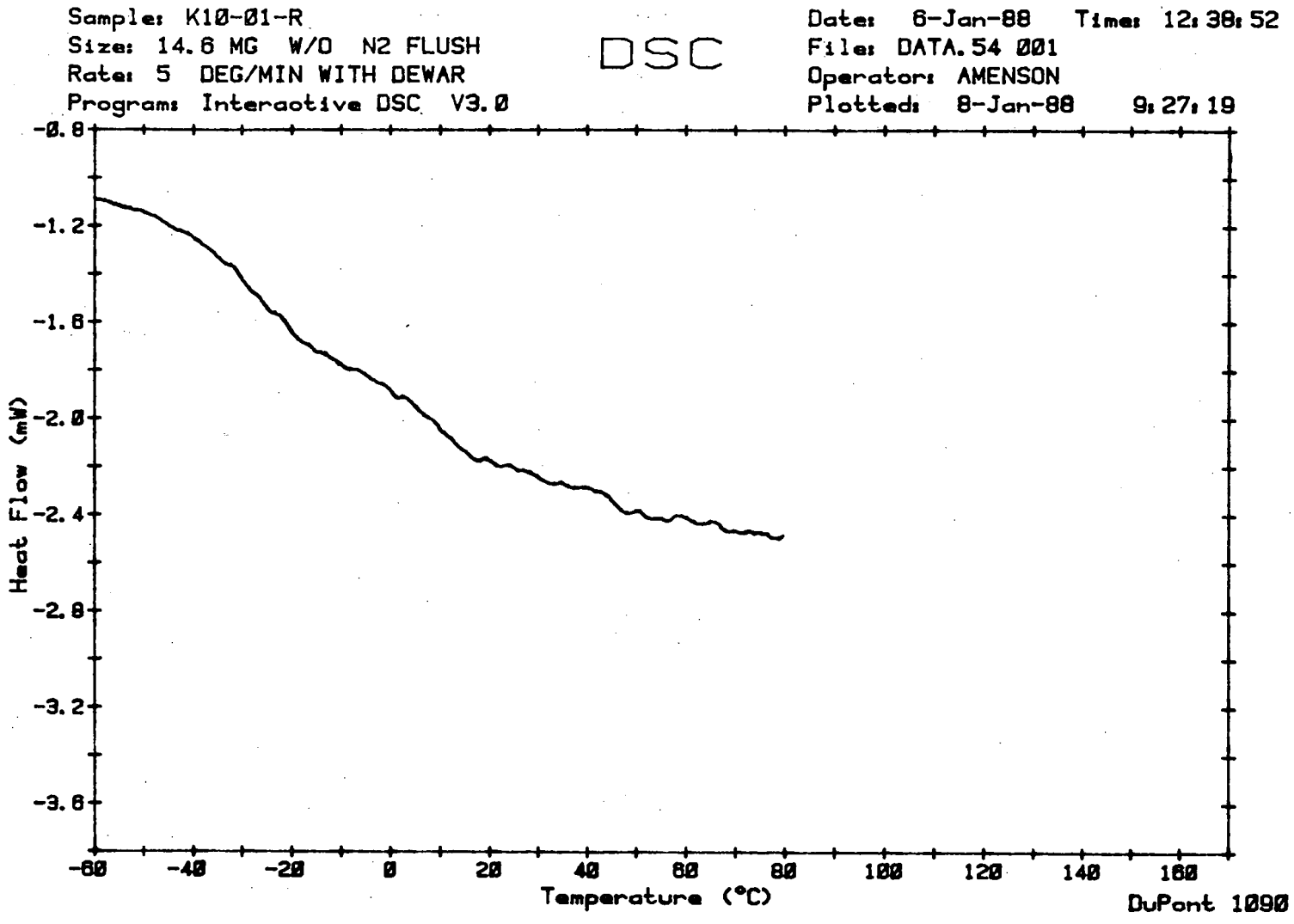
Sample: K10-01-R
Size: 14.6 MG W/O N2 FLUSH
Rate: 5 DEG/MIN WITH DEWAR
Program: Interactive DSC V3.0
DSC
Date: 6-Jan-88 Time: 12:38:52
File: DATA.54 001
Operator: AMENSON
Plotted: 8-Jan-88 9:27:19
-0.8
-1.2
-1.6
-2.0
-2.4
-2.8
-3.2
-3.6
Heat Flow (mW)
-60
-40
-20
0
20
40
60
80
100
120
140
160
Temperature (°C)
DuPont 1090

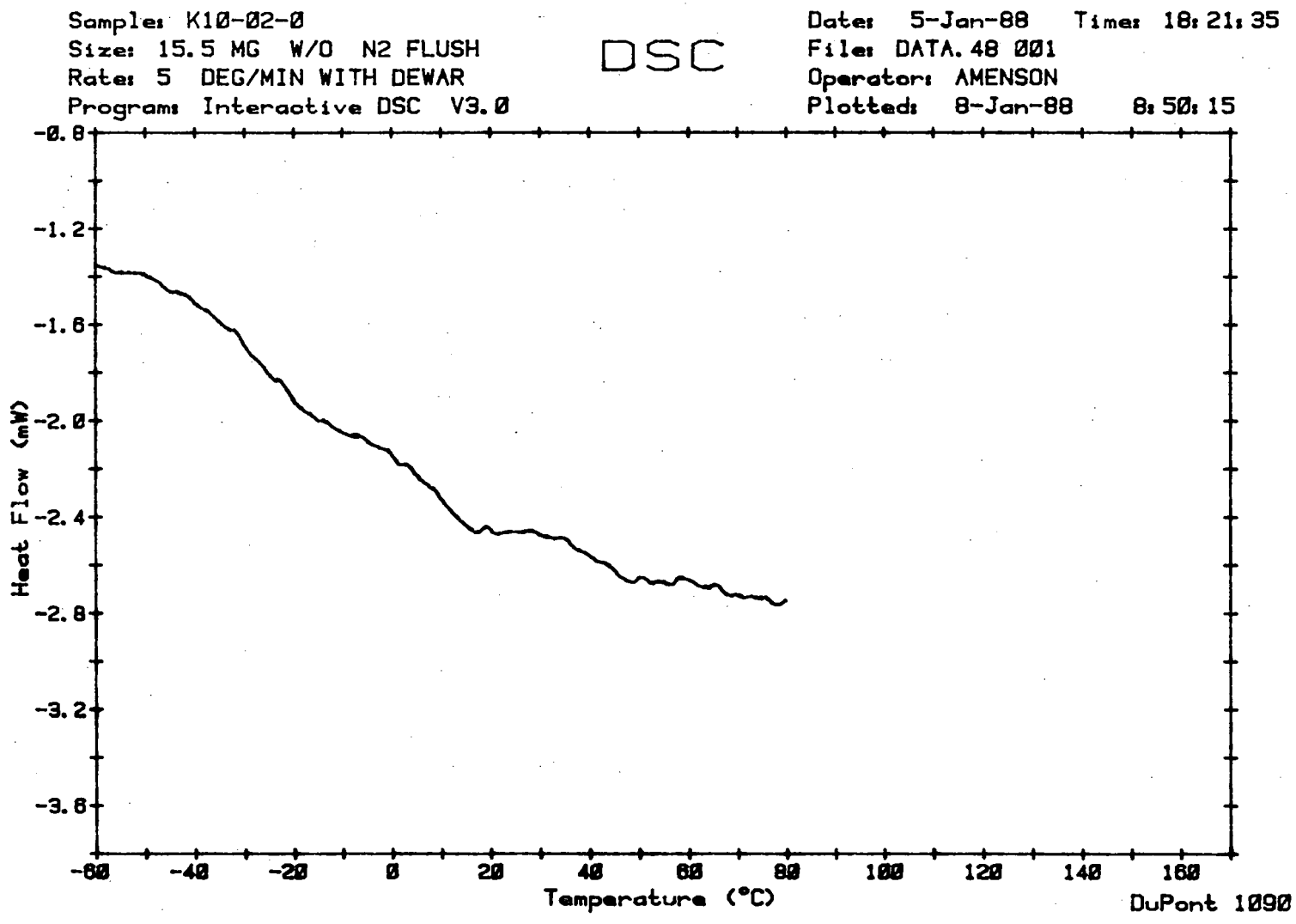
Sample: K10-02-0
Size: 15.5 MG W/O N2 FLUSH
Rate: 5 DEG/MIN WITH DEWAR
Program: Interactive DSC V3.0
DSC
Date: 5-Jan-88 Time: 18:21:35
File: DATA.48 001
Operator: AMENSON
Plotted: 8-Jan-88 8:50:15
-0.8
-1.2
-1.6
-2.0
-2.4
-2.8
-3.2
-3.6
Heat Flow (mW)
-60
-40
-20
0
20
40
60
80
100
120
140
160
Temperature (°C)
DuPont 1090

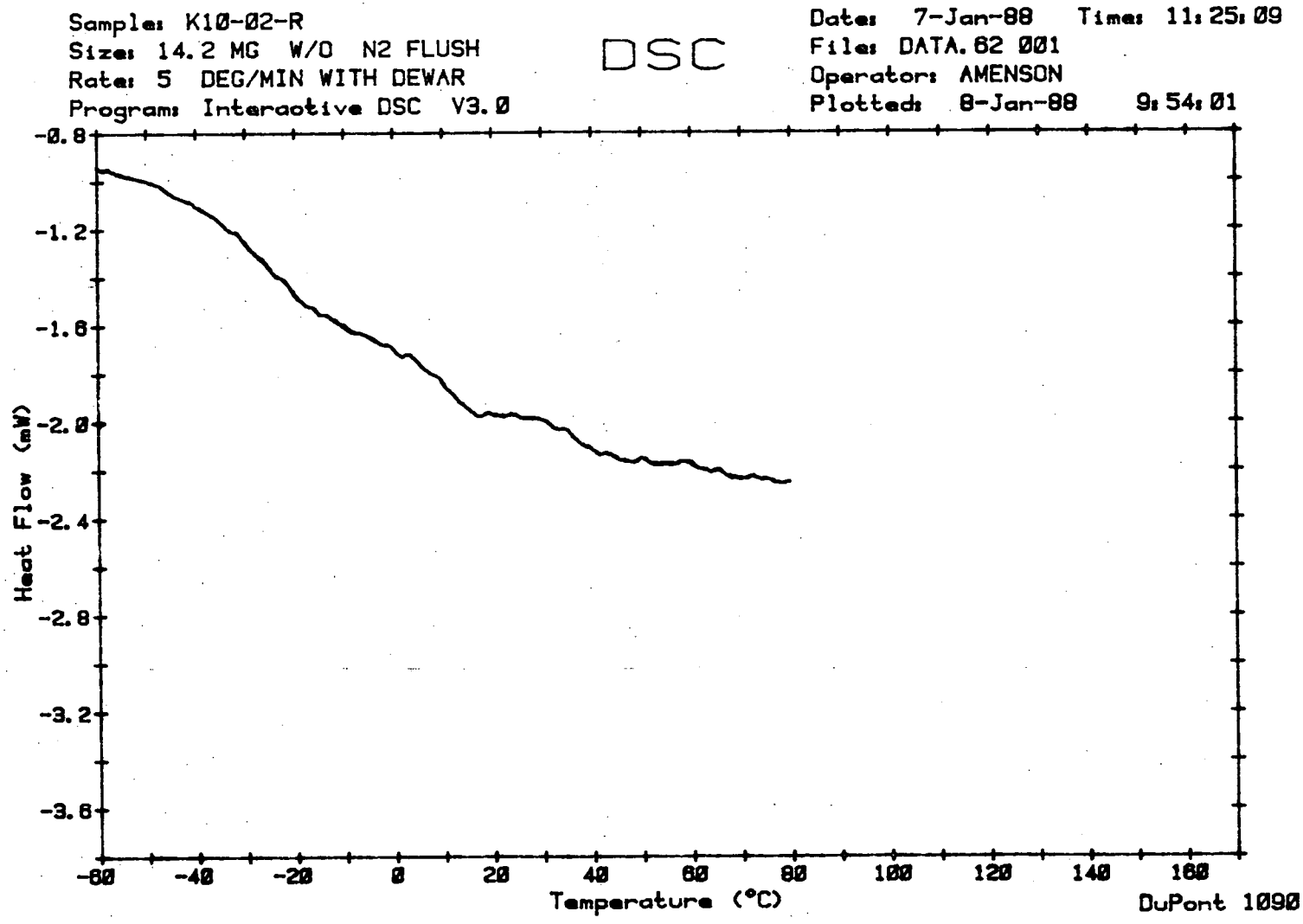
Sample: K10-02-R
Size: 14.2 MG W/O N2 FLUSH
Rate: 5 DEG/MIN WITH DEWAR
Program: Interactive DSC V3.0
DSC
Date: 7-Jan-88 Time: 11:25:09
File: DATA.62 001
Operator: AMENSON
Plotted: 8-Jan-88 9:54:01
-0.8
-1.2
-1.6
-2.0
-2.4
-2.8
-3.2
-3.6
Heat Flow (mW)
-60
-40
-20
0
20
40
60
80
100
120
140
160
Temperature (°C)
DuPont 1090

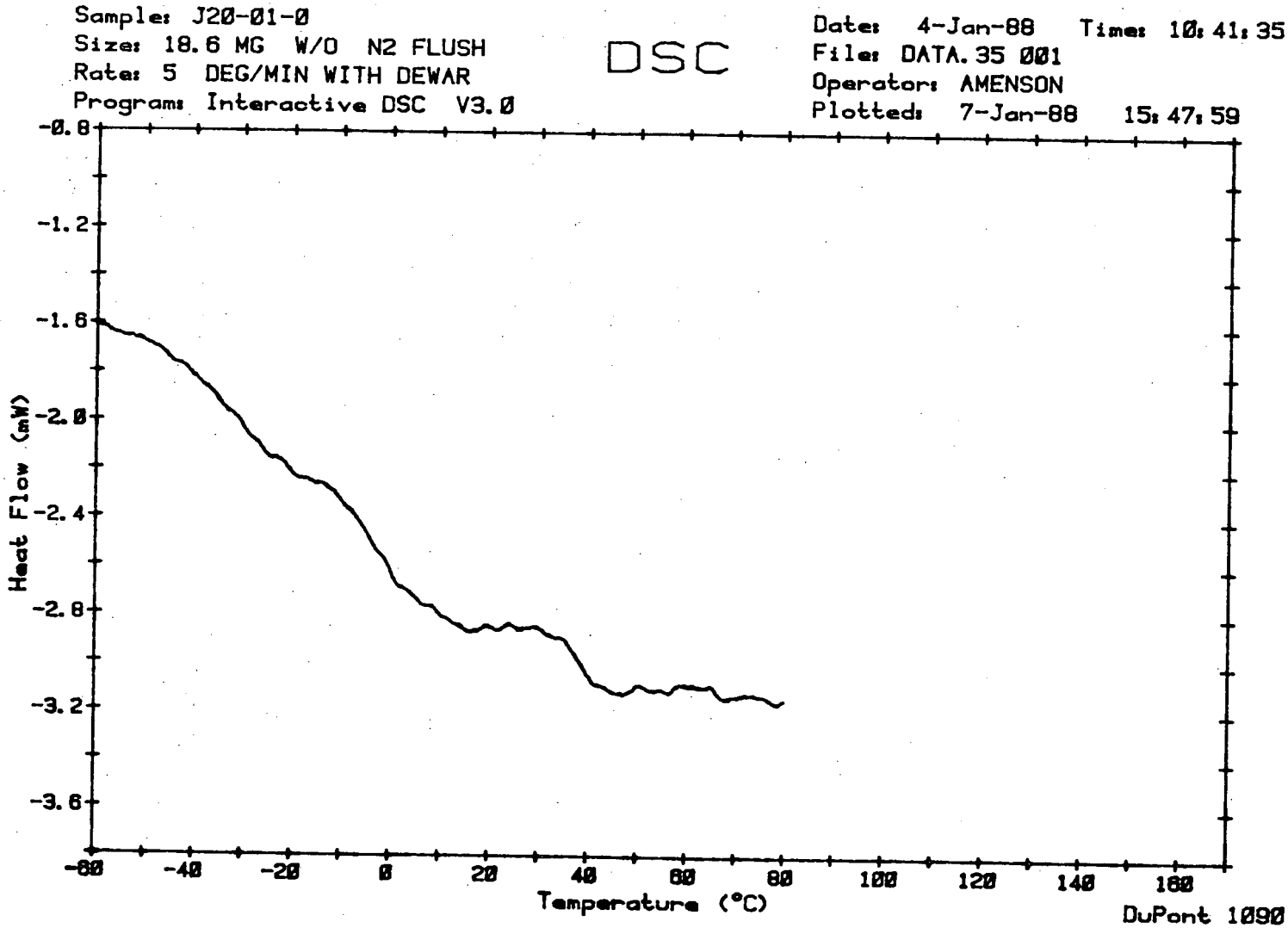
Sample: J20-01-0
Size: 18.6 MG W/O N2 FLUSH
Rate: 5 DEG/MIN WITH DEWAR
Programs: Interactive DSC V3.0
DSC
Date: 4-Jan-88 Time: 10:41:35
File: DATA.35 001
Operator: AMENSON
Plotted: 7-Jan-88 15:47:59
-0.8
-1.2
-1.6
-2.0
-2.4
-2.8
-3.2
-3.6
Heat Flow (mW)
-60
-40
-20
0
20
40
60
80
100
120
140
160
Temperature (°C)
DuPont 1090

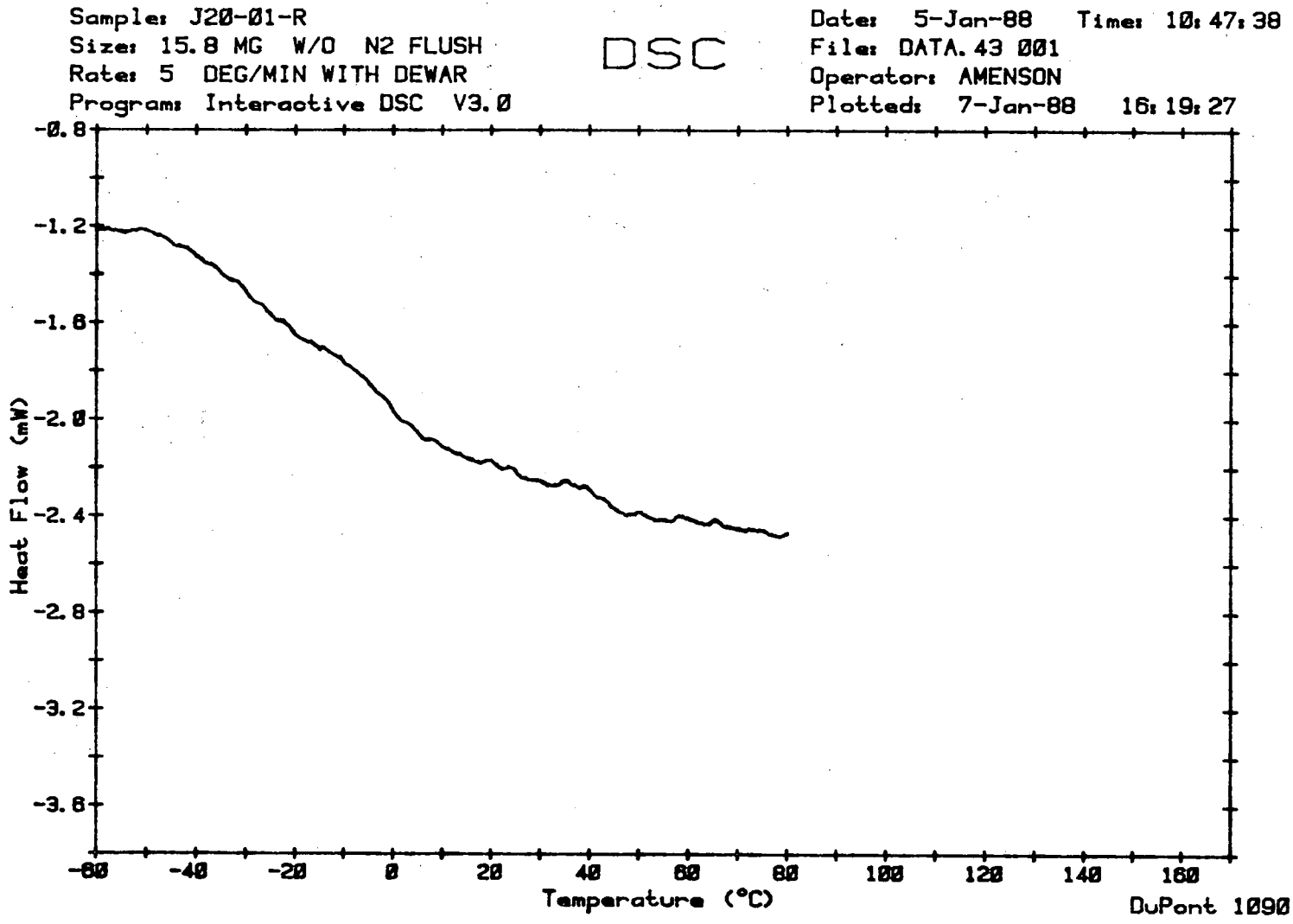
Sample: J20-01-R
Size: 15.8 MG W/O N2 FLUSH
Rate: 5 DEG/MIN WITH DEWAR
Program: Interactive DSC V3.0
DSC
Date: 5-Jan-88 Time: 10:47:38
File: DATA.43 001
Operator: AMENSON
Plotted: 7-Jan-88 16:19:27
-0.8
-1.2
-1.6
-2.0
-2.4
-2.8
-3.2
-3.6
Heat Flow (mW)
-60
-40
-20
0
20
40
60
80
100
120
140
160
Temperature (°C)
DuPont 1090

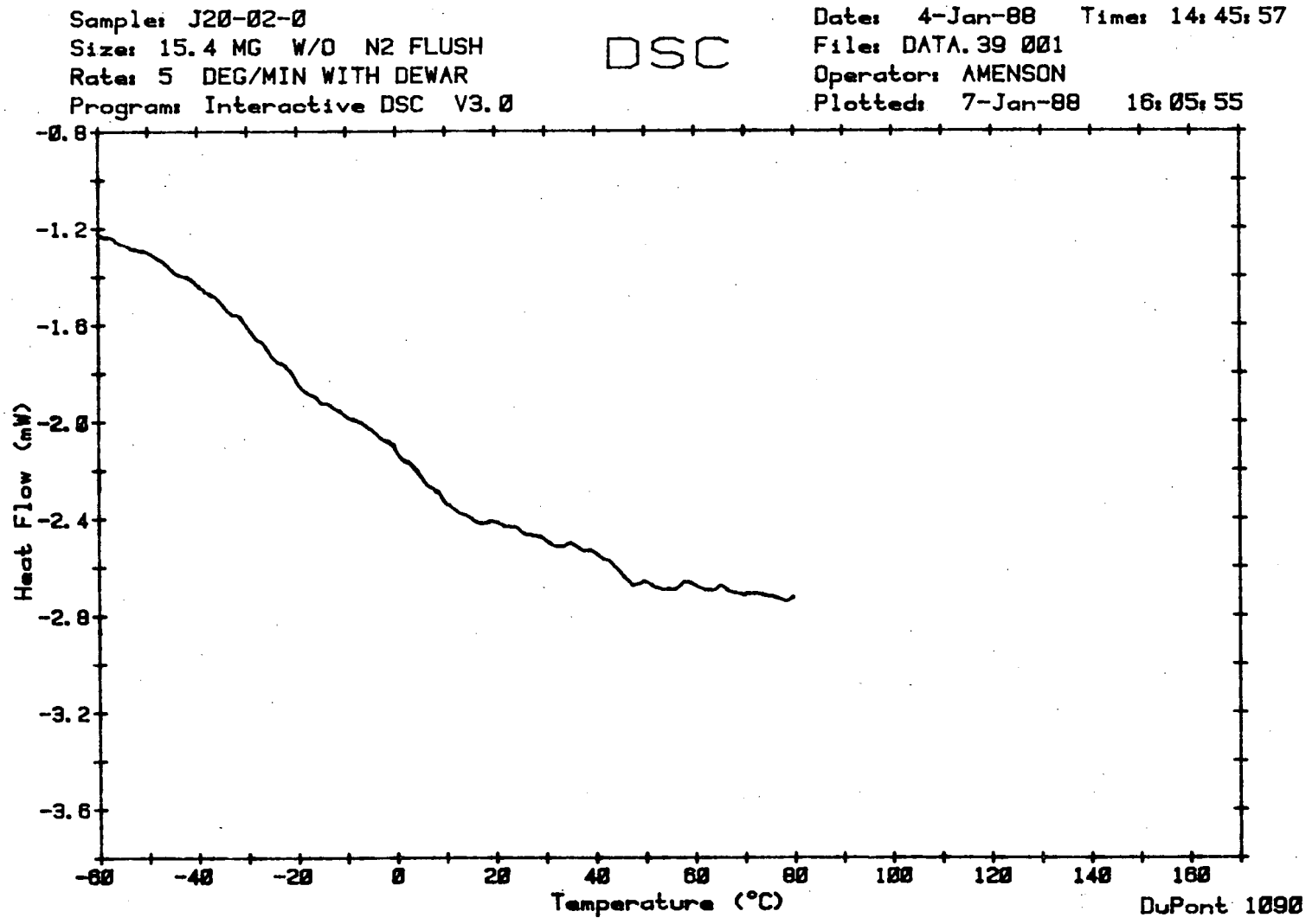
Sample: J20-02-0
Size: 15.4 MG W/O N2 FLUSH
Rate: 5 DEG/MIN WITH DEWAR
Program: Interactive DSC V3.0
DSC
Date: 4-Jan-88 Time: 14:45:57
File: DATA.39 001
Operator: AMENSON
Plotted: 7-Jan-88 16:05:55
-0.8
-1.2
-1.6
-2.0
-2.4
-2.8
-3.2
-3.6
Heat Flow (mW)
-60
-40
-20
0
20
40
60
80
100
120
140
160
Temperature (°C)
DuPont 1090

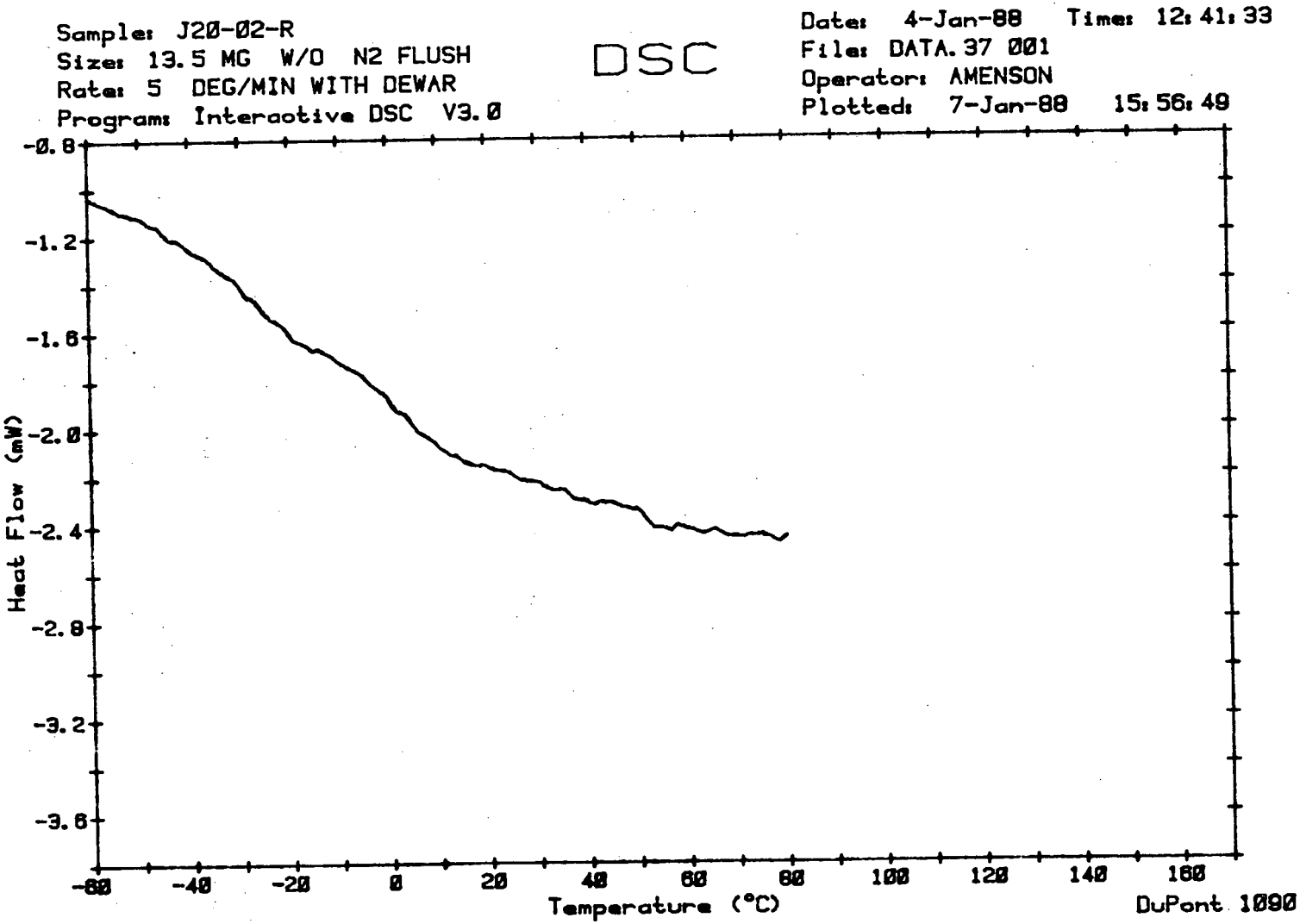
Sample: J20-02-R
Size: 13.5 MG W/O N2 FLUSH
Rate: 5 DEG/MIN WITH DEWAR
Program: Interactive DSC V3.0
DSC
Date: 4-Jan-88 Time: 12:41:33
File: DATA.37 001
Operator: AMENSON
Plotted: 7-Jan-88 15:56:49
-0.8
-1.2
-1.6
-2.0
-2.4
-2.8
-3.2
-3.6
Heat Flow (mW)
-60
-40
-20
0
20
40
60
80
100
120
140
160
Temperature (°C)
DuPont 1090

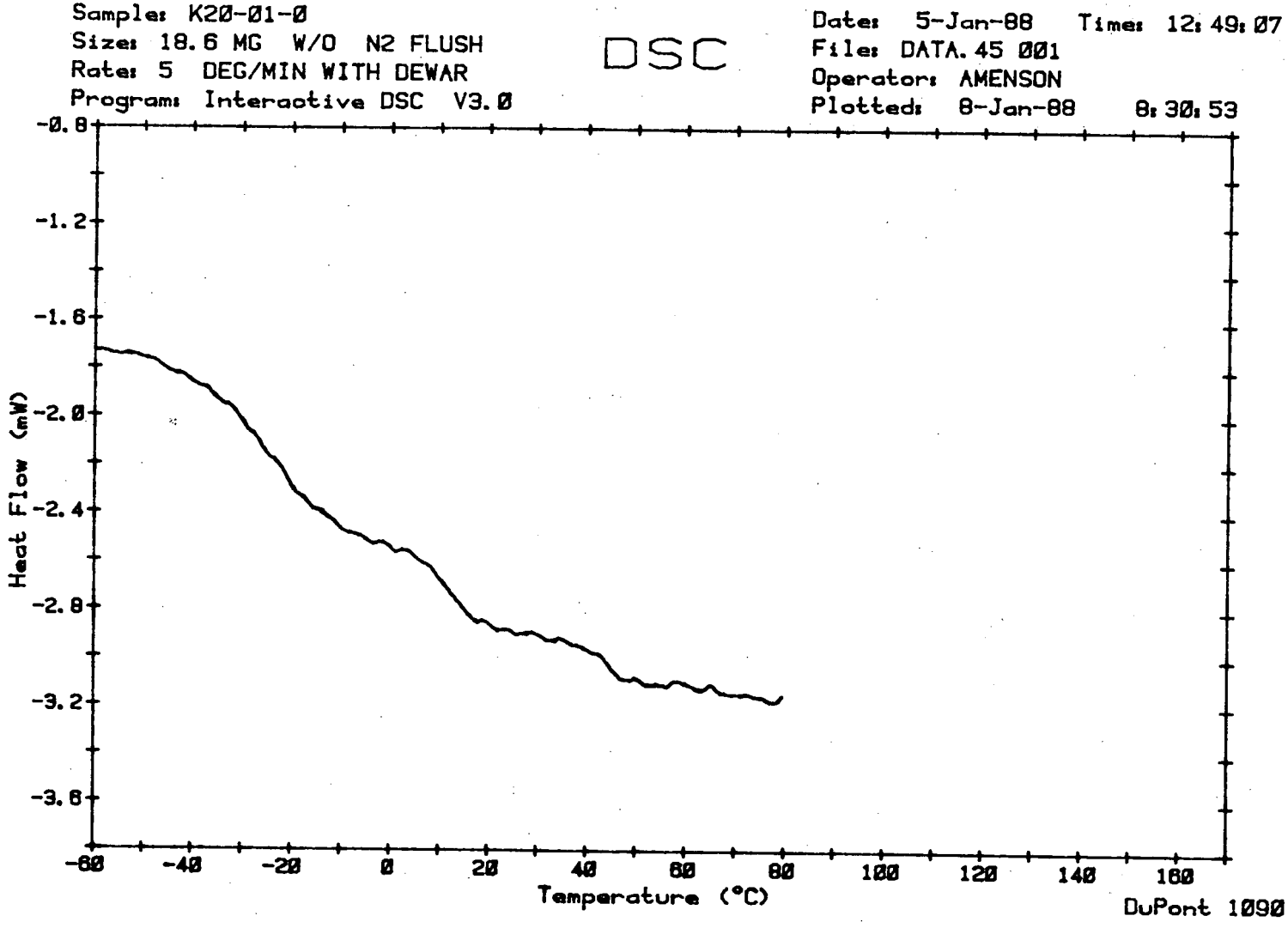
Sample: K20-01-0
Size: 18.6 MG W/O N2 FLUSH
Rate: 5 DEG/MIN WITH DEWAR
Program: Interactive DSC V3.0
DSC
Date: 5-Jan-88 Time: 12:49:07
File: DATA.45 001
Operator: AMENSON
Plotted: 8-Jan-88 8:30:53
-0.8
-1.2
-1.6
-2.0
-2.4
-2.8
-3.2
-3.6
Heat Flow (mW)
-60
-40
-20
0
20
40
60
80
100
120
140
160
Temperature (°C)
DuPont 1090

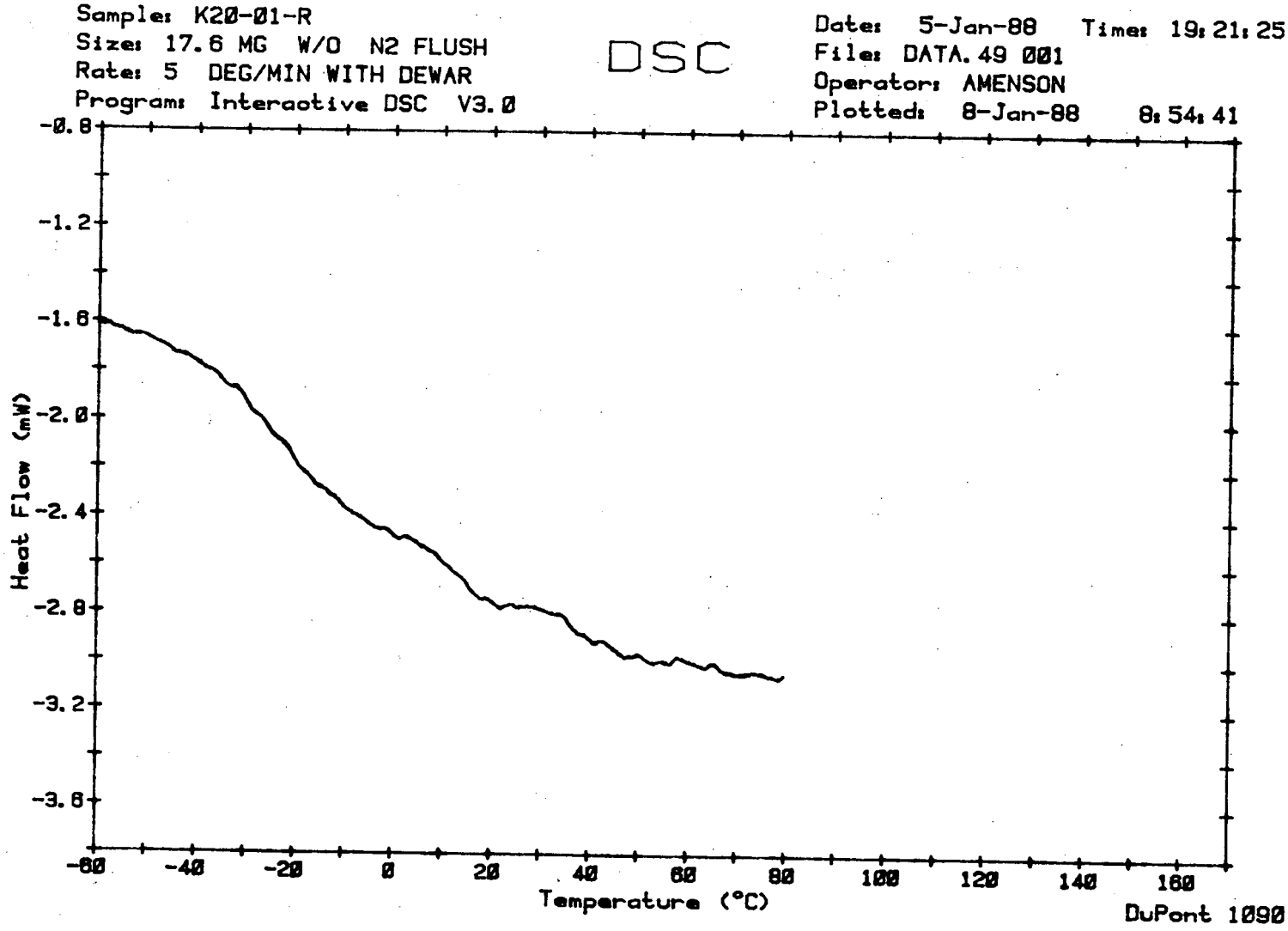
Sample: K20-01-R
Size: 17.6 MG W/O N2 FLUSH
Rate: 5 DEG/MIN WITH DEWAR
Program: Interactive DSC V3.0
DSC
Date: 5-Jan-88 Time: 19:21:25
File: DATA.49 001
Operator: AMENSON
Plotted: 8-Jan-88 8:54:41
-0.8
-1.2
-1.6
-2.0
-2.4
-2.8
-3.2
-3.6
Heat Flow (mW)
-60
-40
-20
0
20
40
60
80
100
120
140
160
Temperature (°C)
DuPont 1090

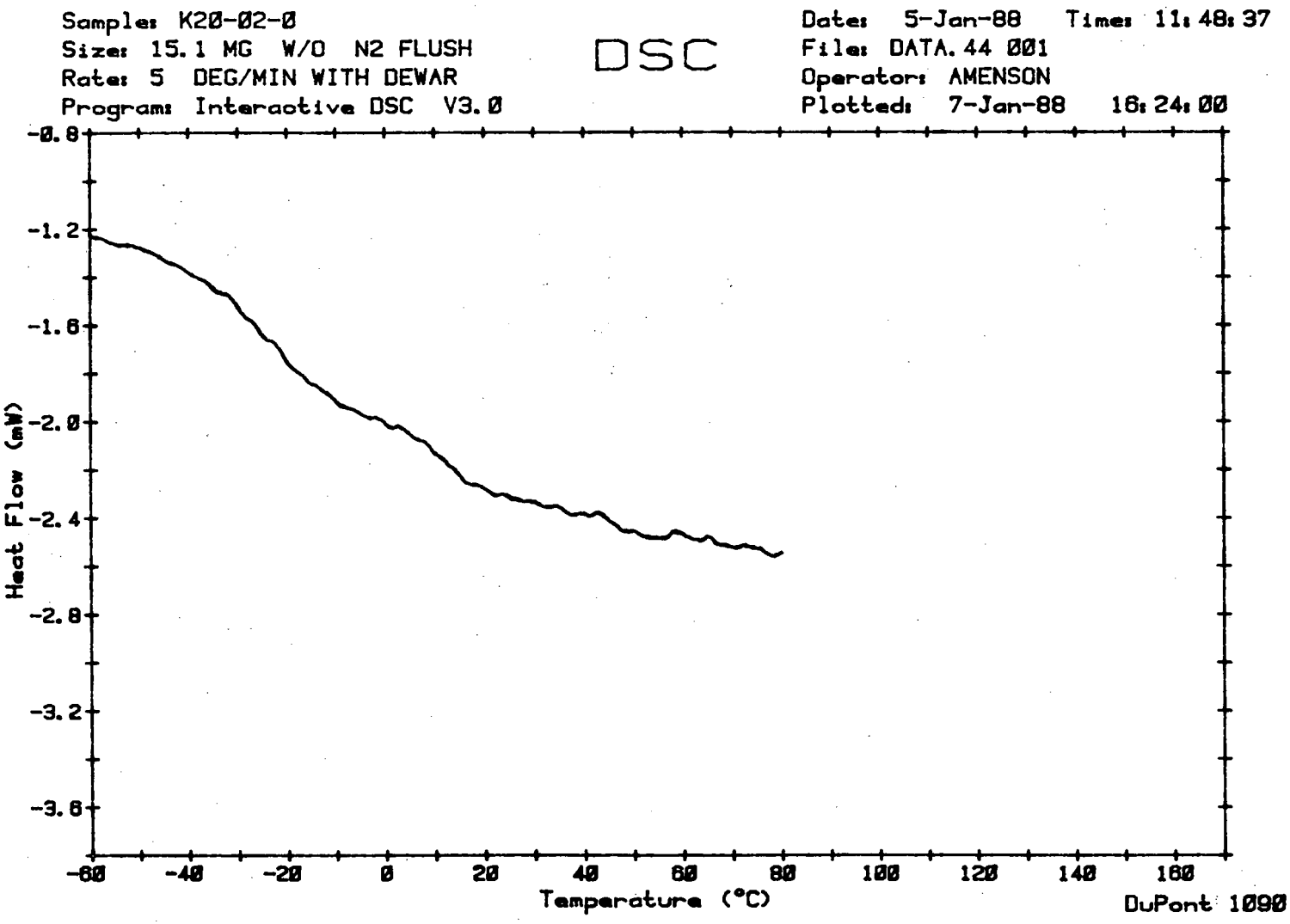
Sample: K20-02-0
Size: 15.1 MG W/O N2 FLUSH
Rate: 5 DEG/MIN WITH DEWAR
Program: Interactive DSC V3.0
DSC
Date: 5-Jan-88 Time: 11:48:37
File: DATA.44 001
Operator: AMENSON
Plotted: 7-Jan-88 16:24:00
-0.8
-1.2
-1.6
-2.0
-2.4
-2.8
-3.2
-3.6
Heat Flow (mW)
-60
-40
-20
0
20
40
60
80
100
120
140
160
Temperature (°C)
DuPont 1090

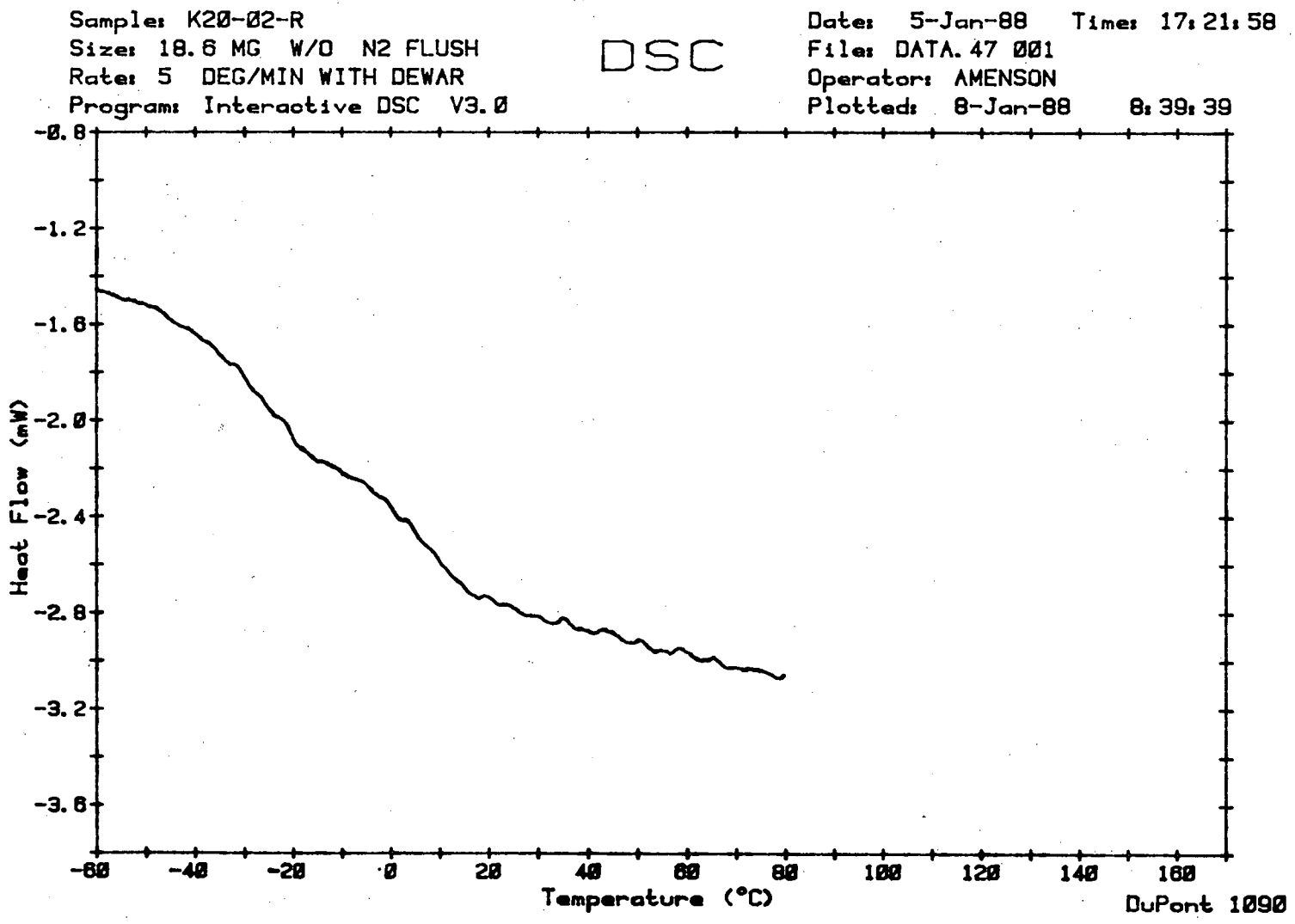
Sample: K20-02-R
Size: 18.6 MG W/O N2 FLUSH
Rate: 5 DEG/MIN WITH DEWAR
Program: Interactive DSC V3.0
DSC
Date: 5-Jan-88 Time: 17:21:58
File: DATA.47 001
Operator: AMENSON
Plotted: 8-Jan-88 8:39:39
-0.8
-1.2
-1.6
-2.0
-2.4
-2.8
-3.2
-3.6
Heat Flow (mW)
-60
-40
-20
0
20
40
60
80
100
120
140
160
Temperature (°C)
DuPont 1090

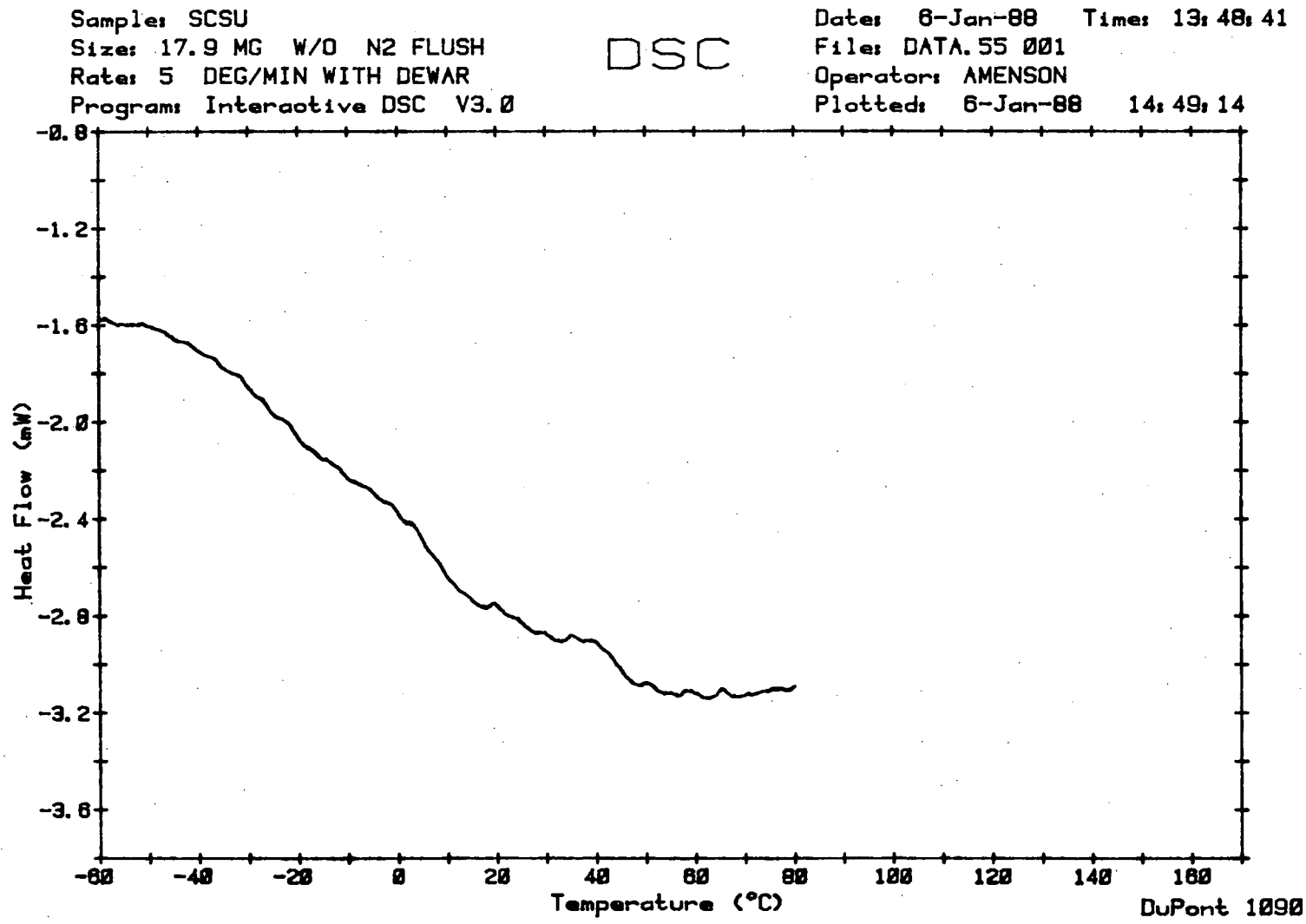
Sample: SCSU
Size: 17.9 MG W/O N2 FLUSH
Rate: 5 DEG/MIN WITH DEWAR
Program: Interactive DSC V3.0
DSC
Date: 6-Jan-88 Time: 13:48:41
File: DATA.55 001
Operator: AMENSON
Plotted: 6-Jan-88 14:49:14
-0.8
-1.2
-1.6
-2.0
-2.4
-2.8
-3.2
-3.6
Heat Flow (mW)
-60
-40
-20
0
20
40
60
80
100
120
140
160
Temperature (°C)
DuPont 1090

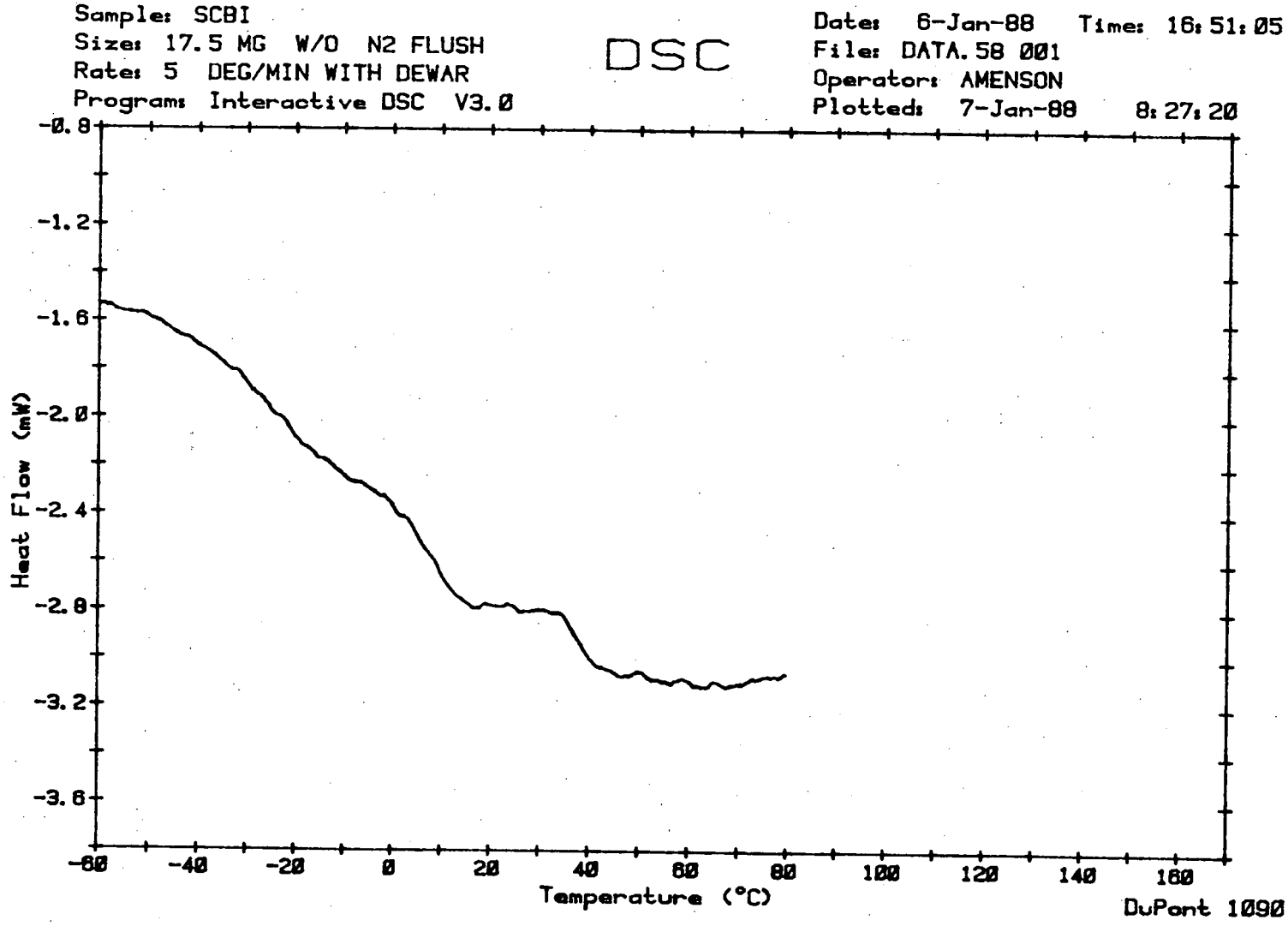
Sample: SCBI
Size: 17.5 MG W/O N2 FLUSH
Rate: 5 DEG/MIN WITH DEWAR
Programs Interactive DSC V3.0
DSC
Date: 6-Jan-88 Time: 16:51:05
File: DATA.58 001
Operator: AMENSON
Plotted: 7-Jan-88 8:27:20
-0.8
-1.2
-1.6
-2.0
-2.4
-2.8
-3.2
-3.6
Heat Flow (mW)
-60
-40
-20
0
20
40
60
80
100
120
140
160
Temperature (°C)
DuPont 1090

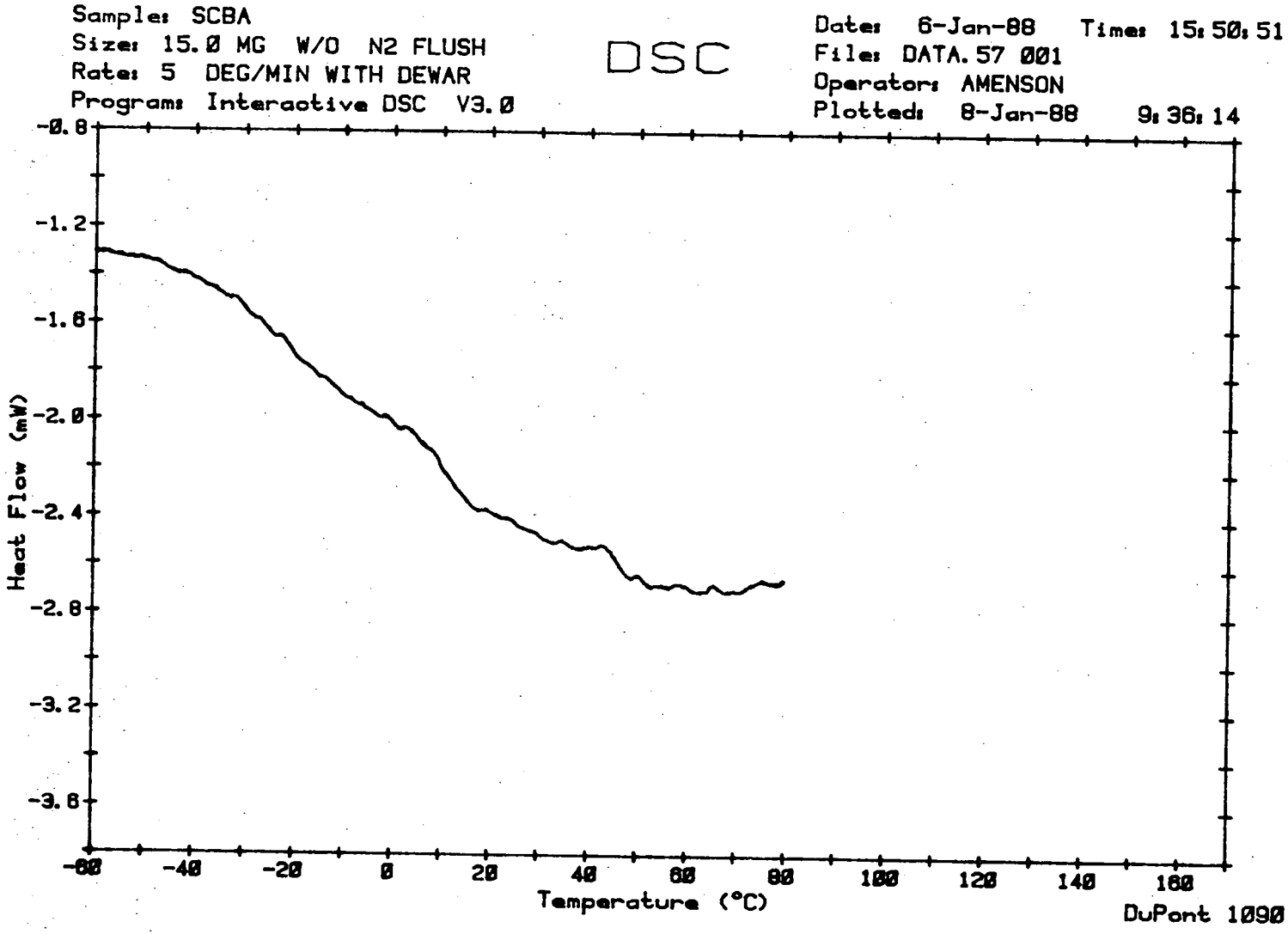
Sample: SCBA
Size: 15.0 MG W/O N2 FLUSH
Rate: 5 DEG/MIN WITH DEWAR
Program: Interactive DSC V3.0
DSC
Date: 6-Jan-88 Time: 15:50:51
File: DATA.57 001
Operator: AMENSON
Plotted: 8-Jan-88 9:36:14
-0.8
-1.2
-1.6
-2.0
-2.4
-2.8
-3.2
-3.6
Heat Flow (mW)
-60
-40
-20
0
20
40
60
80
100
120
140
160
Temperature (°C)
DuPont 1090

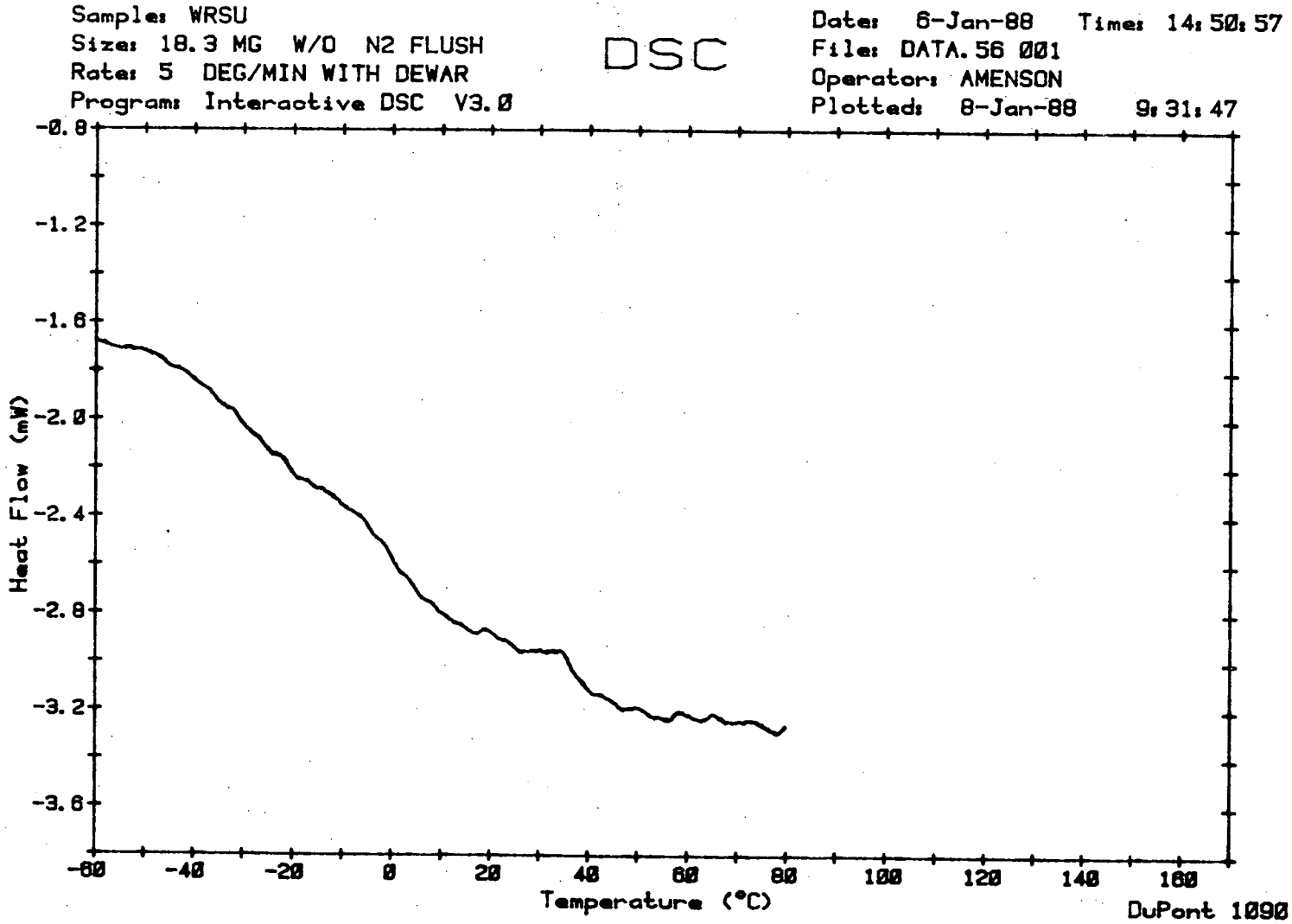
Sample: WRSU
Size: 18.3 MG W/O N2 FLUSH
Rate: 5 DEG/MIN WITH DEWAR
Program: Interactive DSC V3.0
DSC
Date: 6-Jan-88 Time: 14:50:57
File: DATA.56 001
Operator: AMENSON
Plotted: 8-Jan-88 9:31:47
-0.8
-1.2
-1.6
-2.0
-2.4
-2.8
-3.2
-3.6
Heat Flow (mW)
-60
-40
-20
0
20
40
60
80
100
120
140
160
Temperature (°C)
DuPont 1090

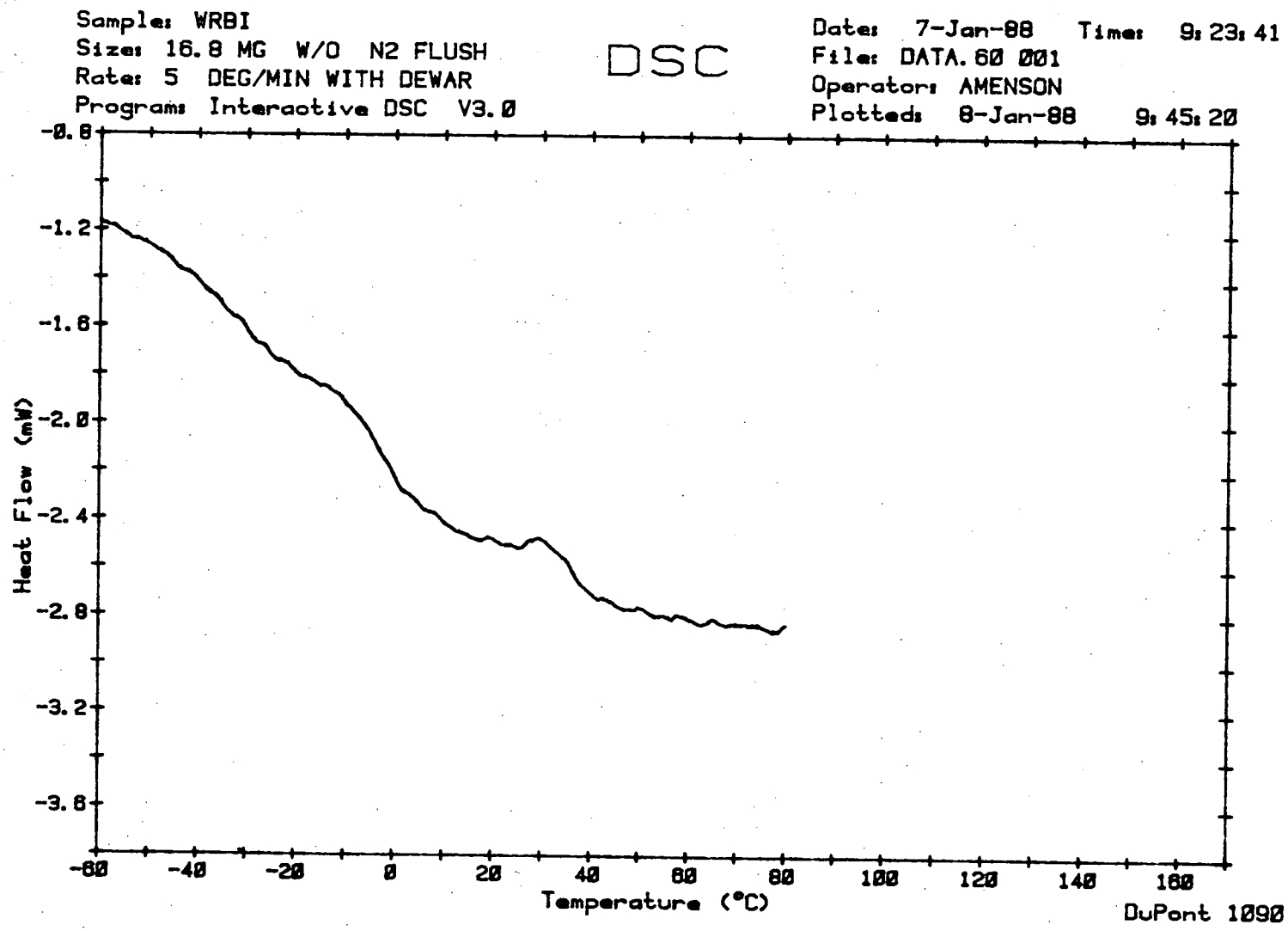
Sample: WRBI
Size: 16.8 MG W/O N2 FLUSH
Rate: 5 DEG/MIN WITH DEWAR
Programs: Interactive DSC V3.0
DSC
Date: 7-Jan-88 Time: 9:23:41
File: DATA.60 001
Operator: AMENSON
Plotted: 8-Jan-88 9:45:20
-0.8
-1.2
-1.6
-2.0
-2.4
-2.8
-3.2
-3.6
Heat Flow (mW)
-60
-40
-20
0
20
40
60
80
100
120
140
160
Temperature (°C)
DuPont 1090

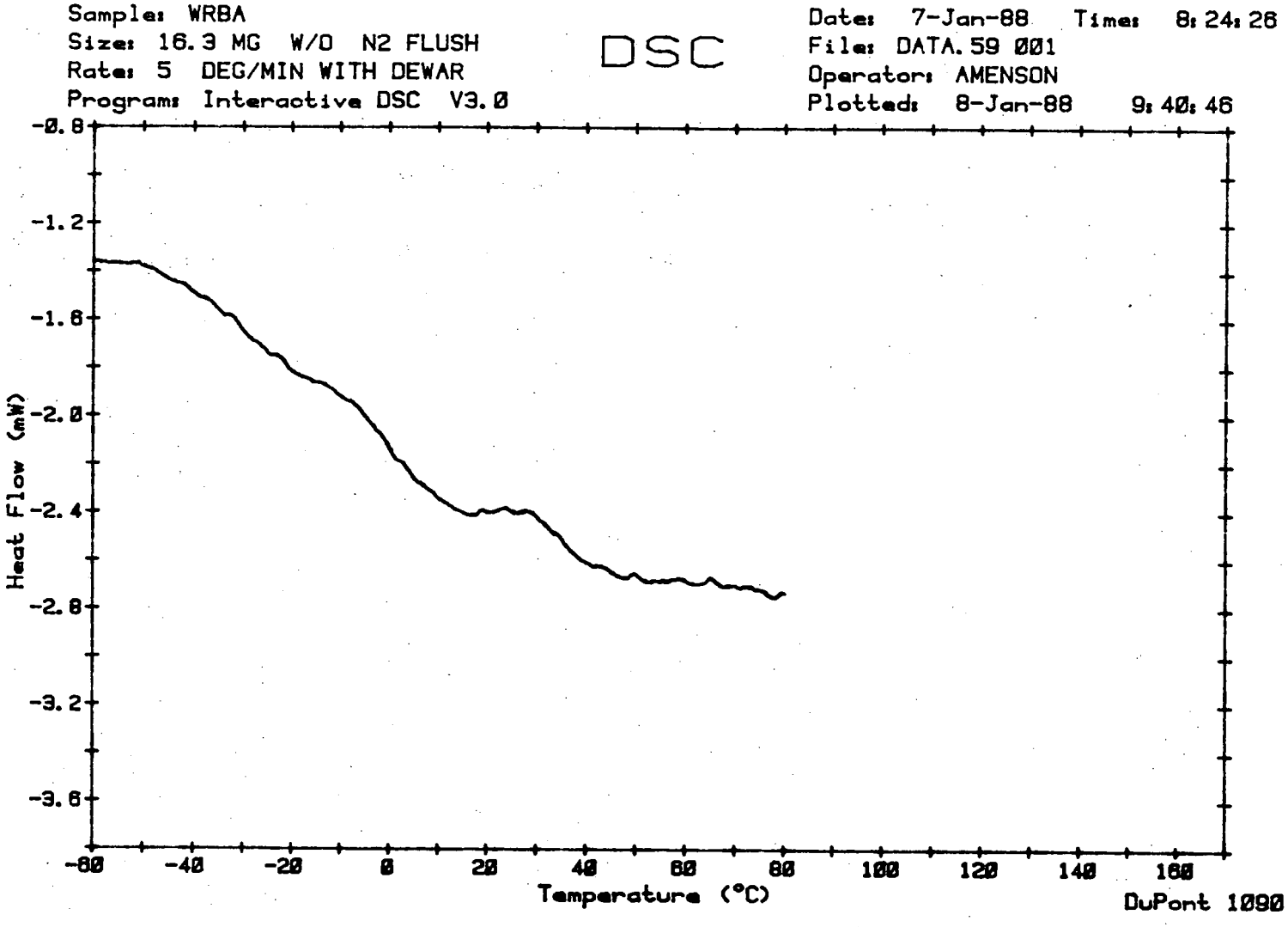
Sample: WRBA
Size: 16.3 MG W/O N2 FLUSH
Rate: 5 DEG/MIN WITH DEWAR
Program: Interactive DSC V3.0
DSC
Date: 7-Jan-88 Time: 8:24:26
File: DATA.59 001
Operator: AMENSON
Plotted: 8-Jan-88 9:40:46
-0.8
-1.2
-1.6
-2.0
-2.4
-2.8
-3.2
-3.6
Heat Flow (mW)
-80
-40
-20
0
20
40
60
80
100
120
140
160
Temperature (°C)
DuPont 1090

APPENDIX III

X-RAY DIFFRACTION SPECTRA

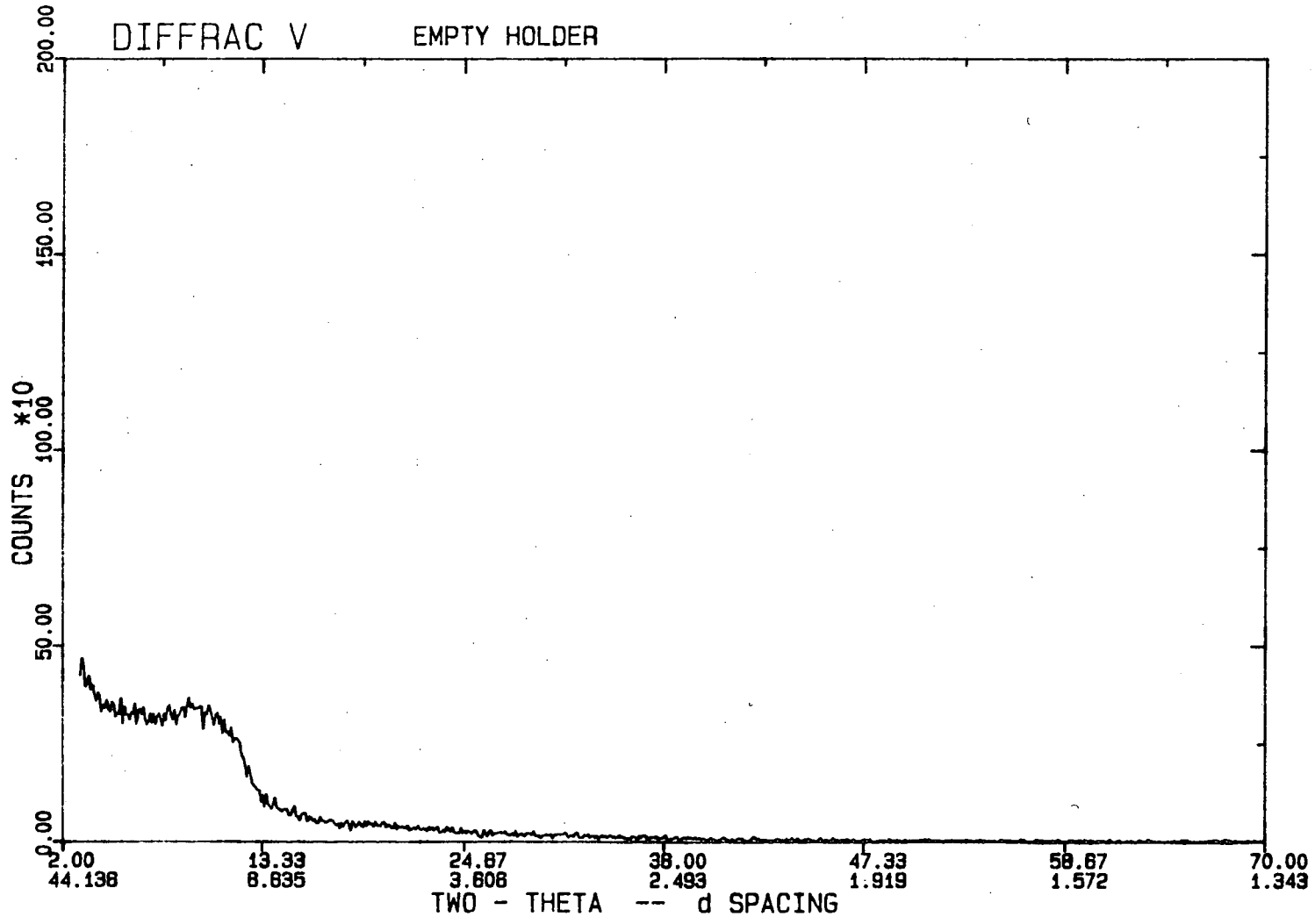
DIFFRAC V
EMPTY HOLDER
200.00
150.00
100.00
50.00
0.00
COUNTS *10
2.00
44.138
13.33
6.635
24.67
3.608
36.00
2.493
47.33
1.919
58.67
1.572
70.00
1.343
TWO - THETA -- d SPACING

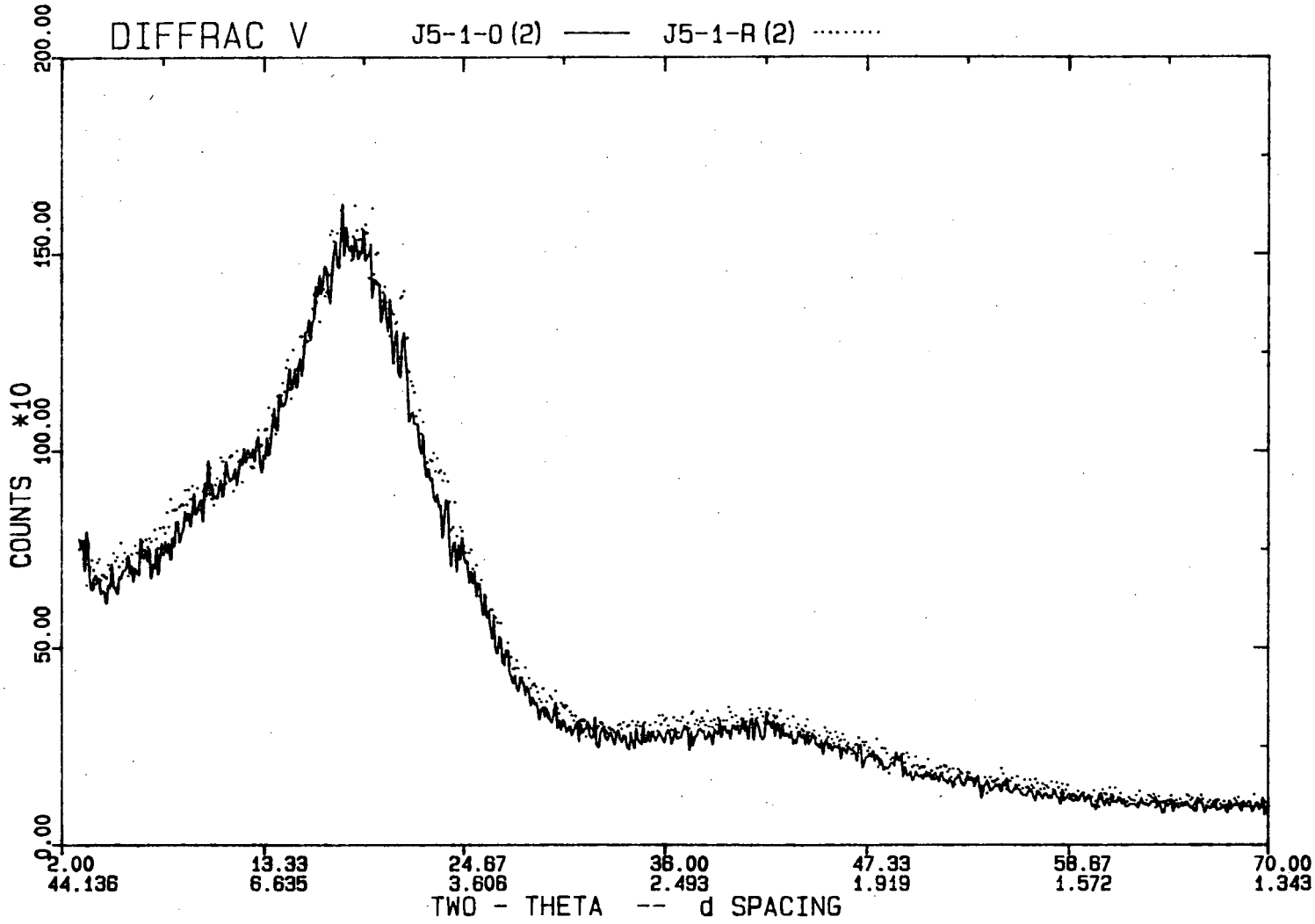
DIFFRAC V
J5-1-0 (2)
J5-1-R (2)
200.00
150.00
100.00
50.00
0.00
COUNTS *10
2.00
44.136
13.33
6.635
24.67
3.606
36.00
2.493
47.33
1.919
58.67
1.572
70.00
1.343
TWO - THETA -- d SPACING

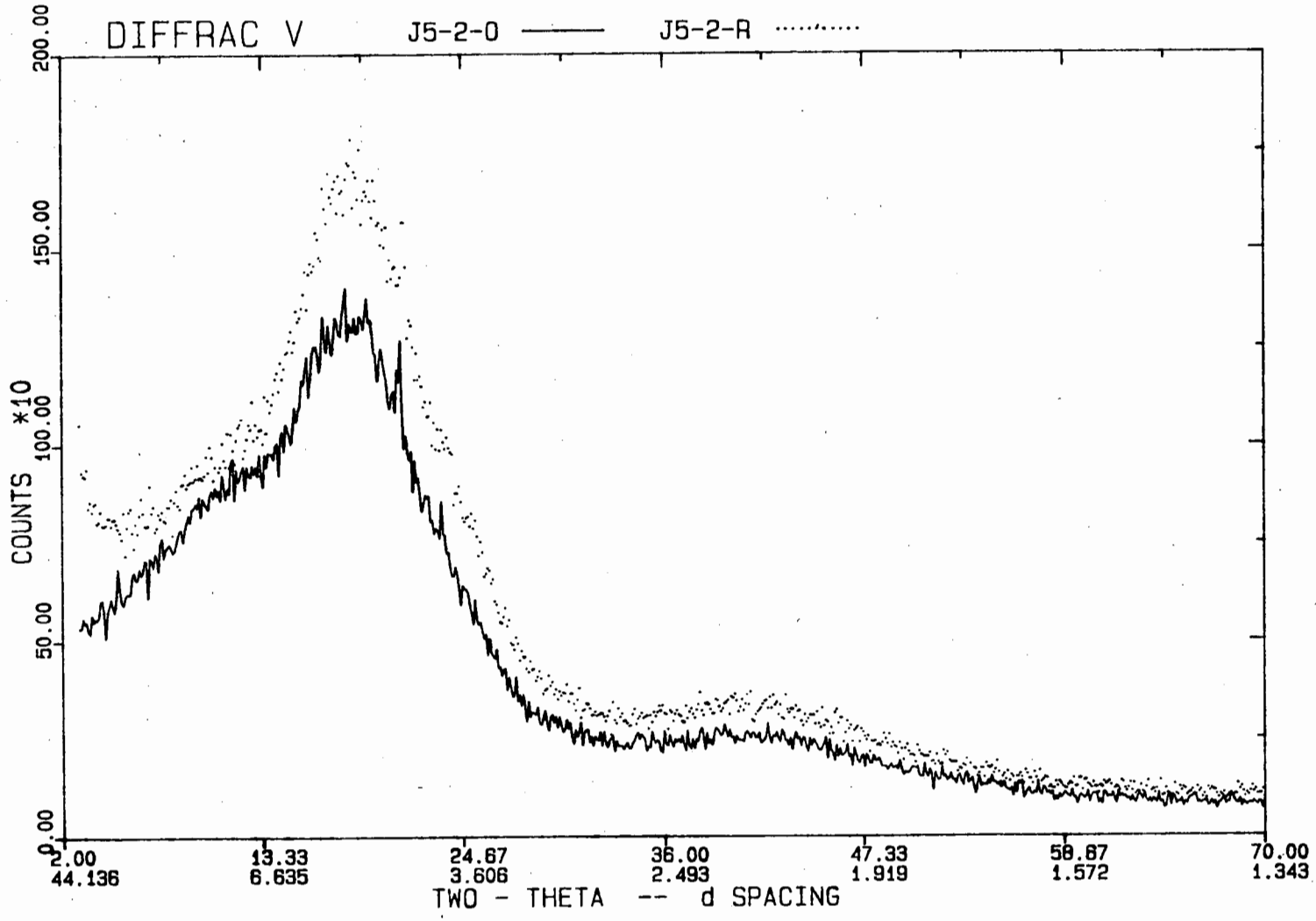
DIFFRAC V
J5-2-0
J5-2-R
200.00
150.00
100.00
50.00
0.00
COUNTS *10
2.00
44.136
13.33
6.635
24.67
3.606
36.00
2.493
47.33
1.919
58.67
1.572
70.00
1.343
TWO - THETA -- d SPACING

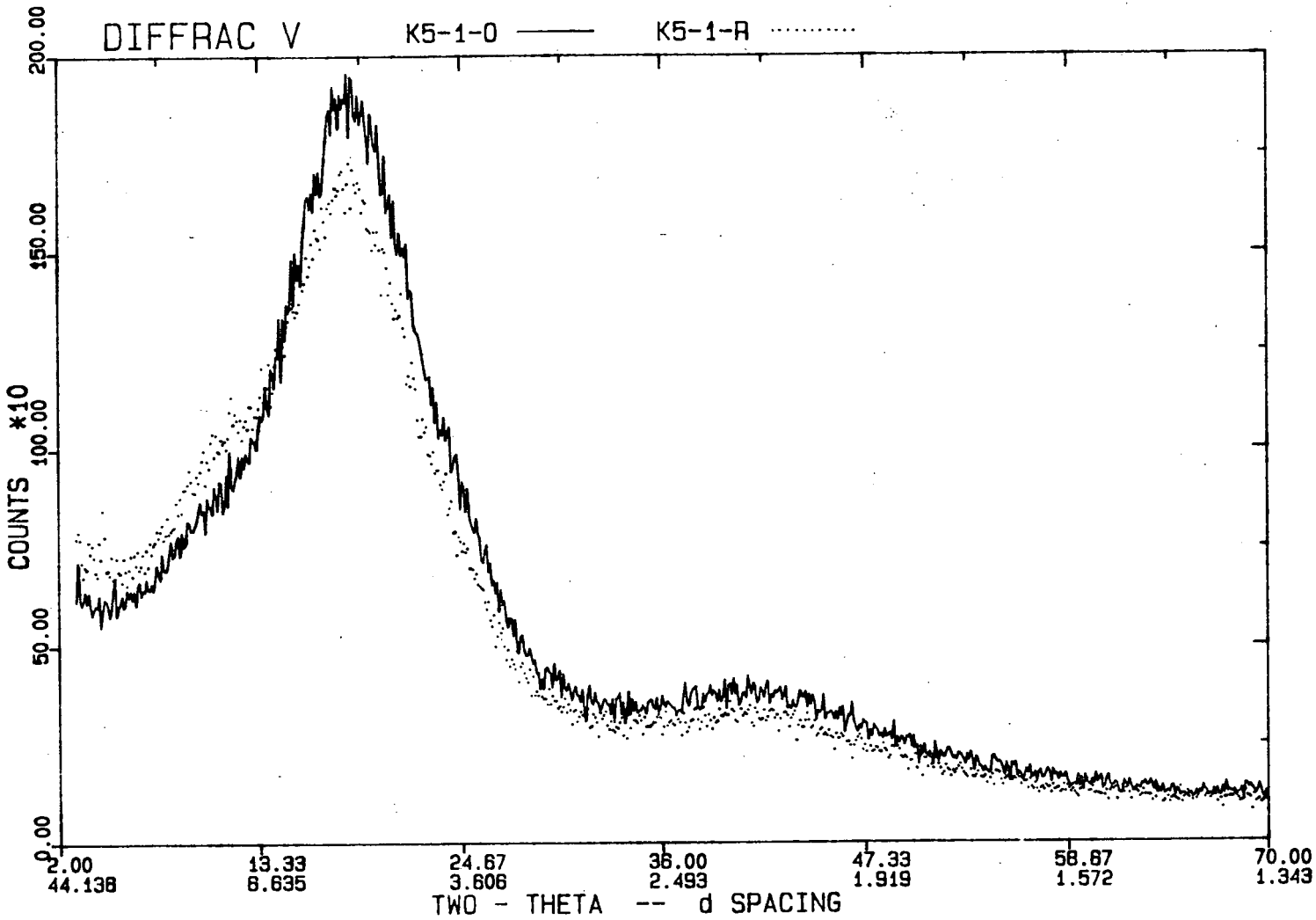
DIFFRAC V
K5-1-0
K5-1-R
200.00
150.00
100.00
50.00
0.00
COUNTS *10
2.00
44.138
13.33
6.635
24.67
3.606
36.00
2.493
47.33
1.919
58.67
1.572
70.00
1.343
TWO - THETA -- d SPACING

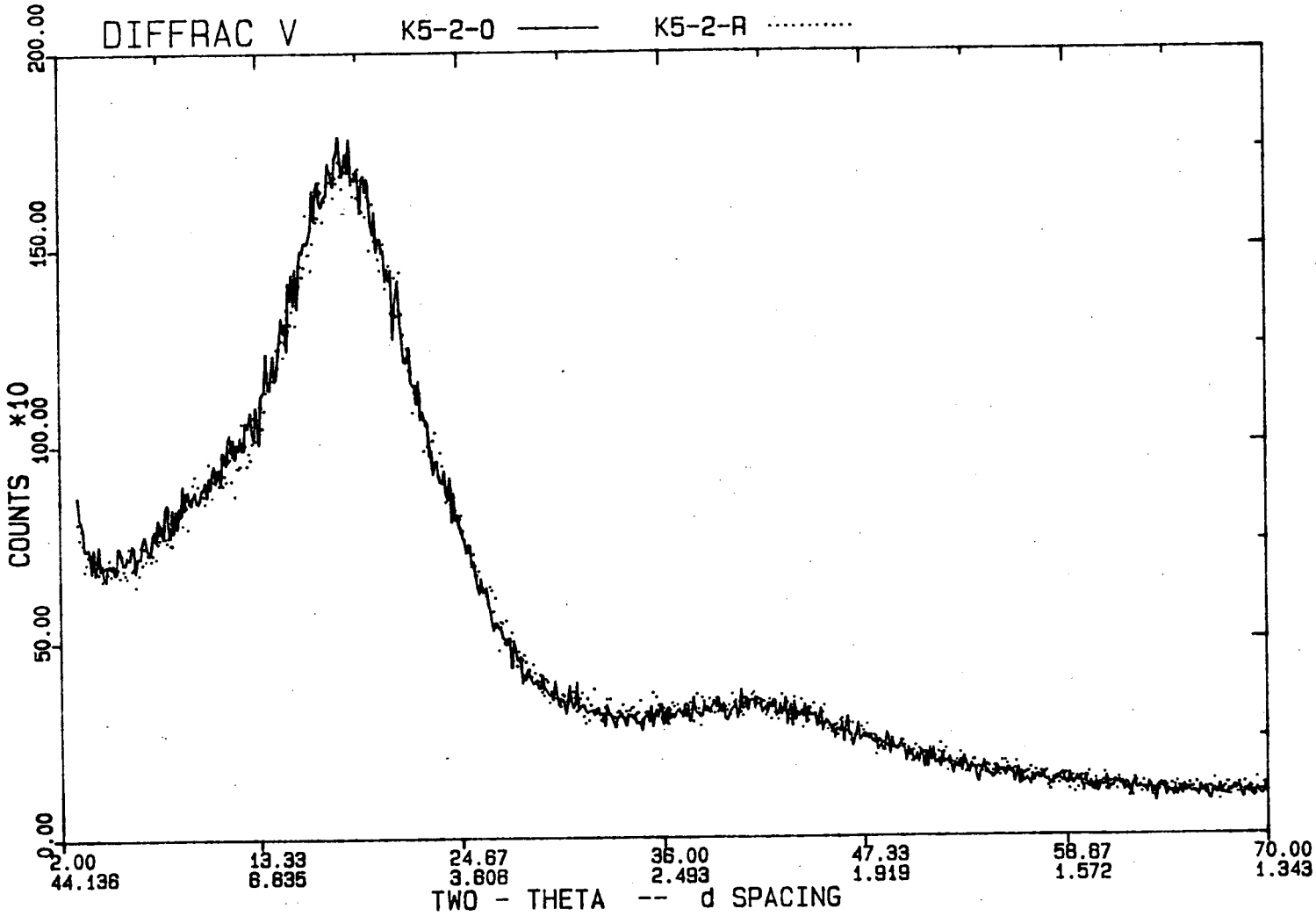
DIFFRAC V
K5-2-0
K5-2-R
COUNTS *10
200.00
150.00
100.00
50.00
0.00
2.00
44.136
13.33
6.635
24.67
3.606
36.00
2.493
47.33
1.919
58.67
1.572
70.00
1.343
TWO - THETA -- d SPACING

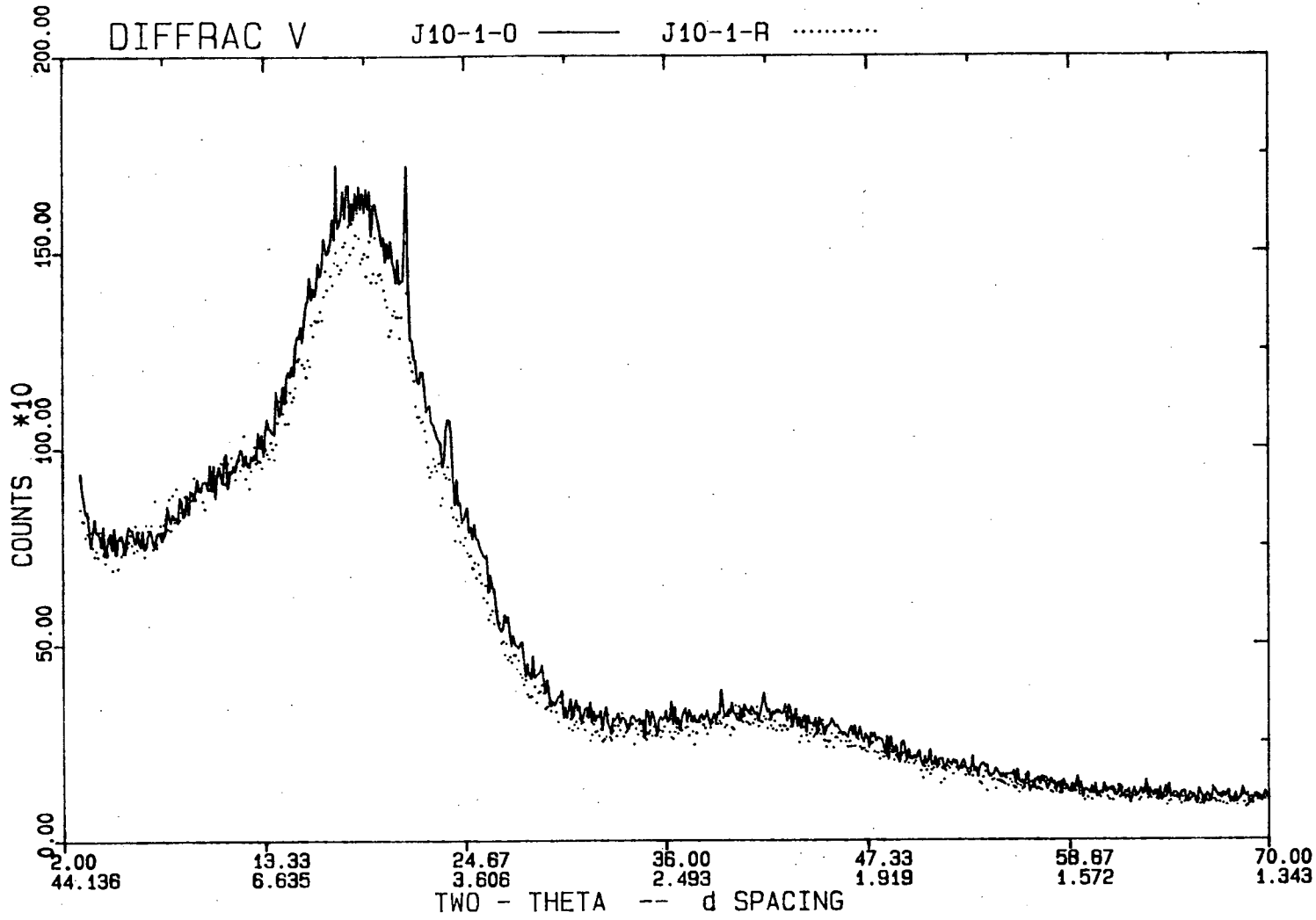
DIFFRAC V
J10-1-0
J10-1-R
200.00
150.00
100.00
50.00
0.00
COUNTS *10
2.00
44.136
13.33
6.635
24.67
3.606
36.00
2.493
47.33
1.919
58.67
1.572
70.00
1.343
TWO - THETA -- d SPACING

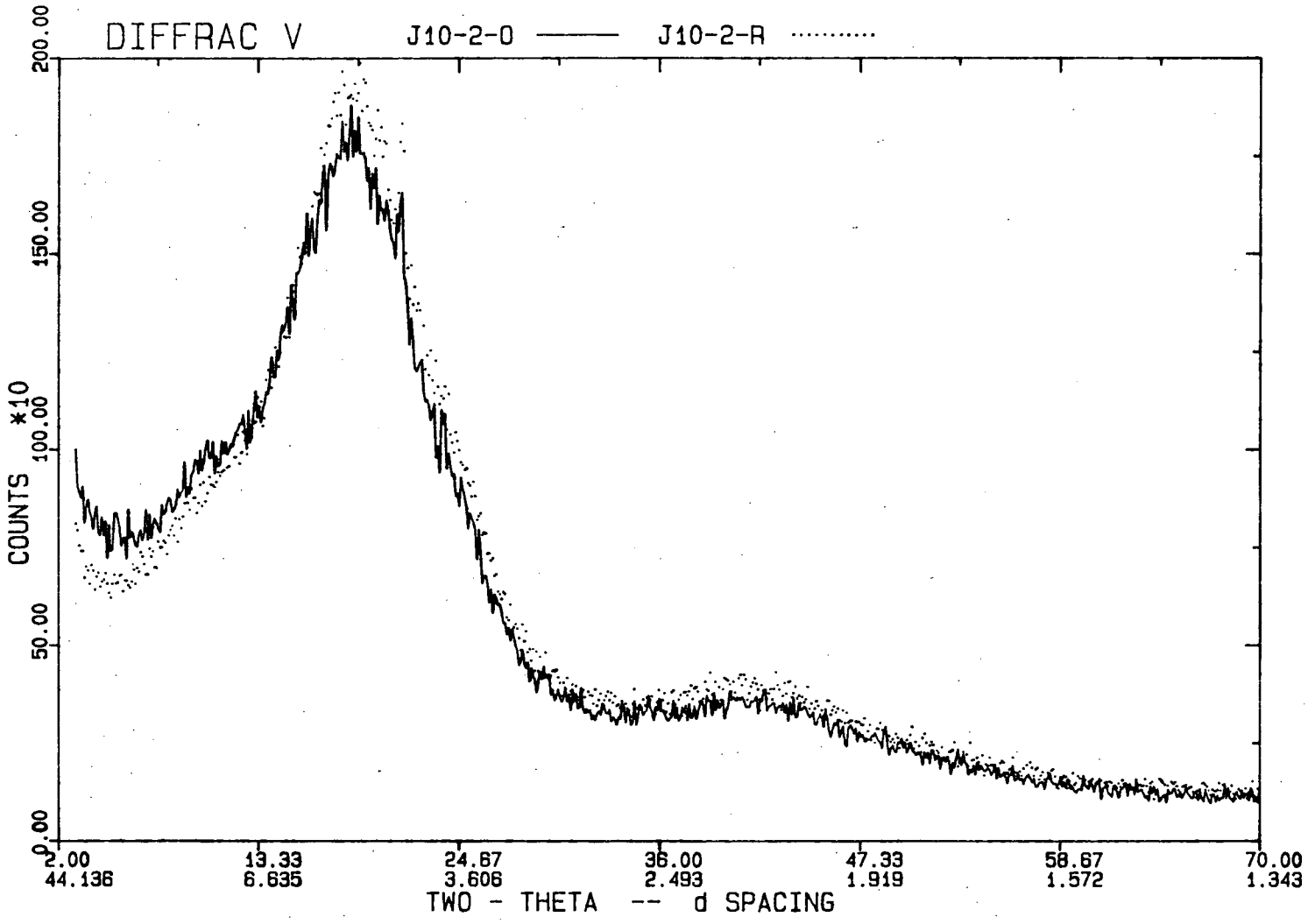
DIFFRAC V
J10-2-0
J10-2-R
200.00
150.00
100.00
50.00
0.00
COUNTS *10
2.00
44.136
13.33
6.635
24.67
3.606
36.00
2.493
47.33
1.919
58.67
1.572
70.00
1.343
TWO - THETA -- d SPACING

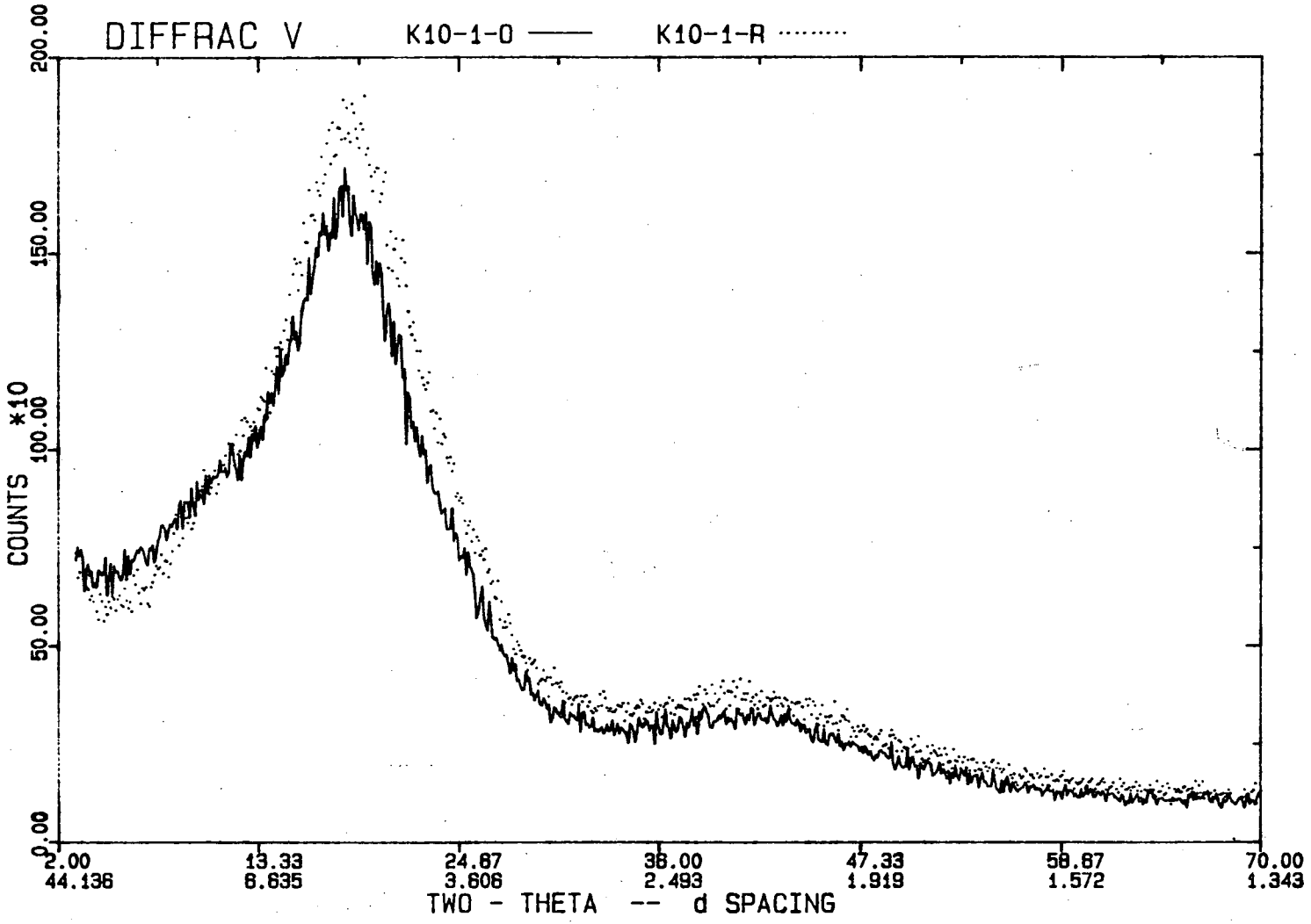
DIFFRAC V
K10-1-0
K10-1-R
200.00
150.00
100.00
50.00
0.00
COUNTS *10
2.00
44.136
13.33
6.635
24.67
3.606
36.00
2.493
47.33
1.919
58.67
1.572
70.00
1.343
TWO - THETA -- d SPACING

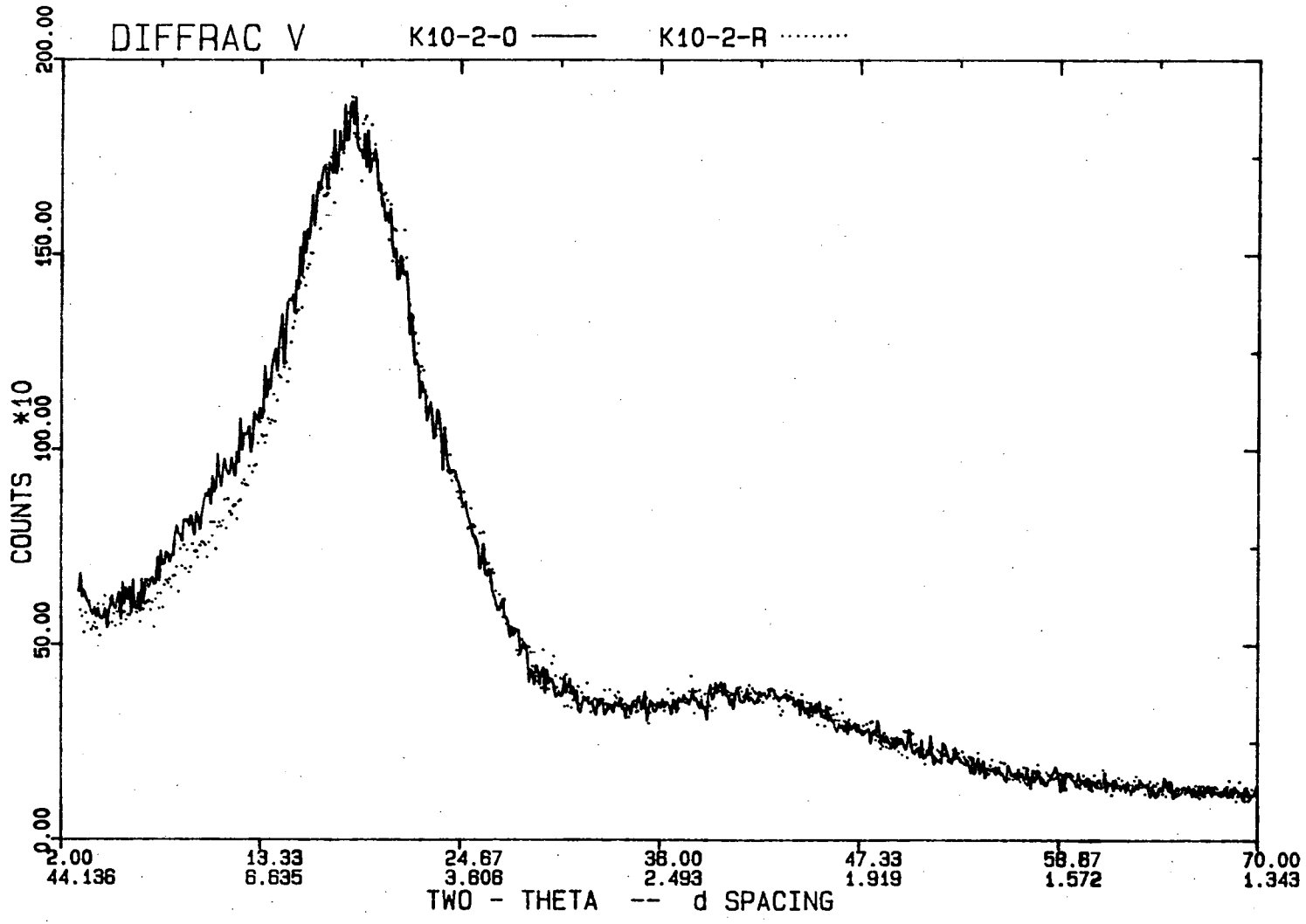
DIFFRAC V
K10-2-0
K10-2-R
COUNTS *10
200.00
150.00
100.00
50.00
0.00
2.00
44.136
13.33
6.635
24.67
3.608
36.00
2.493
47.33
1.919
58.67
1.572
70.00
1.343
TWO - THETA -- d SPACING

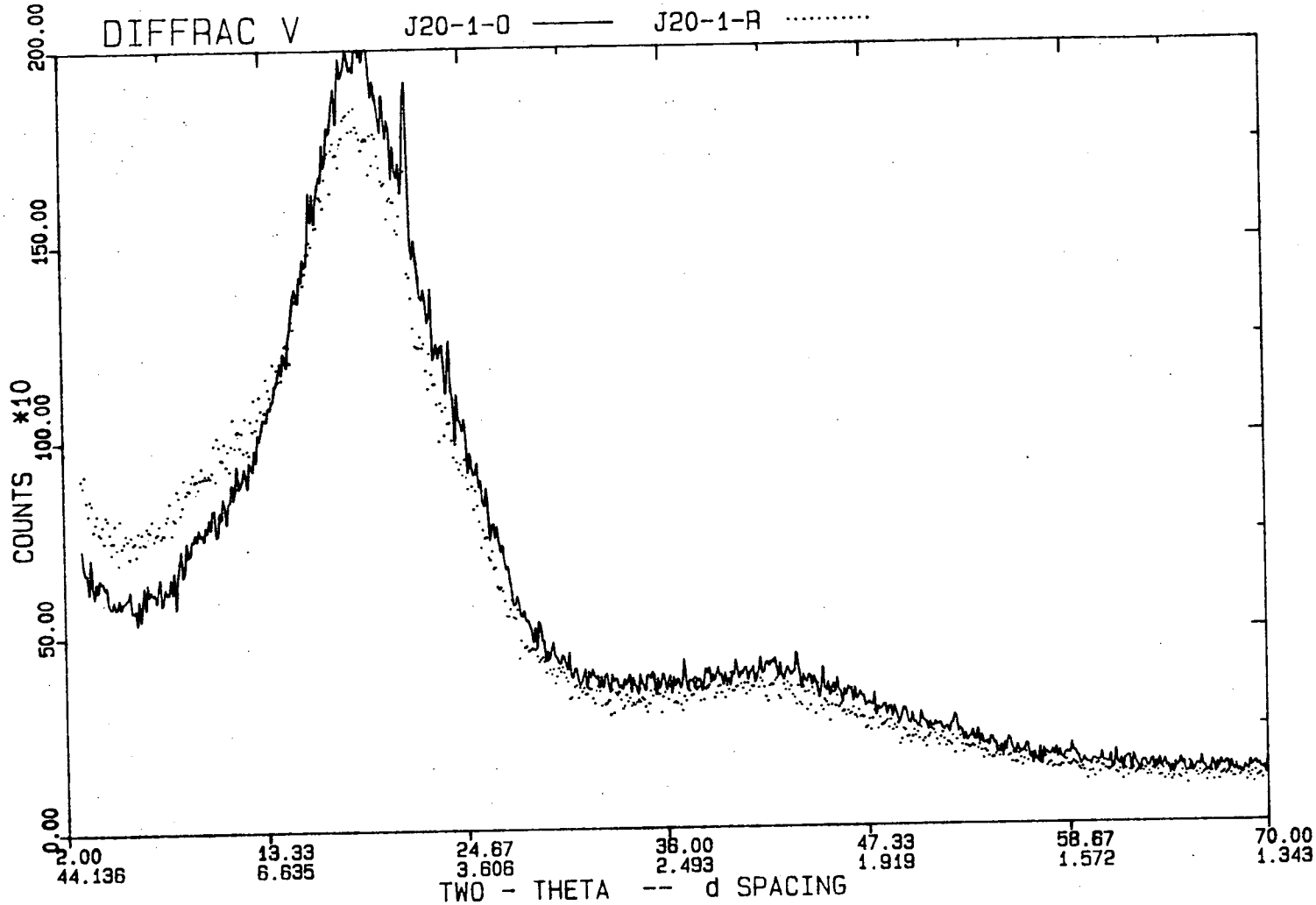
DIFFRAC V
J20-1-0
J20-1-R
200.00
150.00
100.00
50.00
0.00
COUNTS *10
2.00
44.136
13.33
6.635
24.67
3.606
36.00
2.493
47.33
1.919
58.67
1.572
70.00
1.343
TWO - THETA -- d SPACING

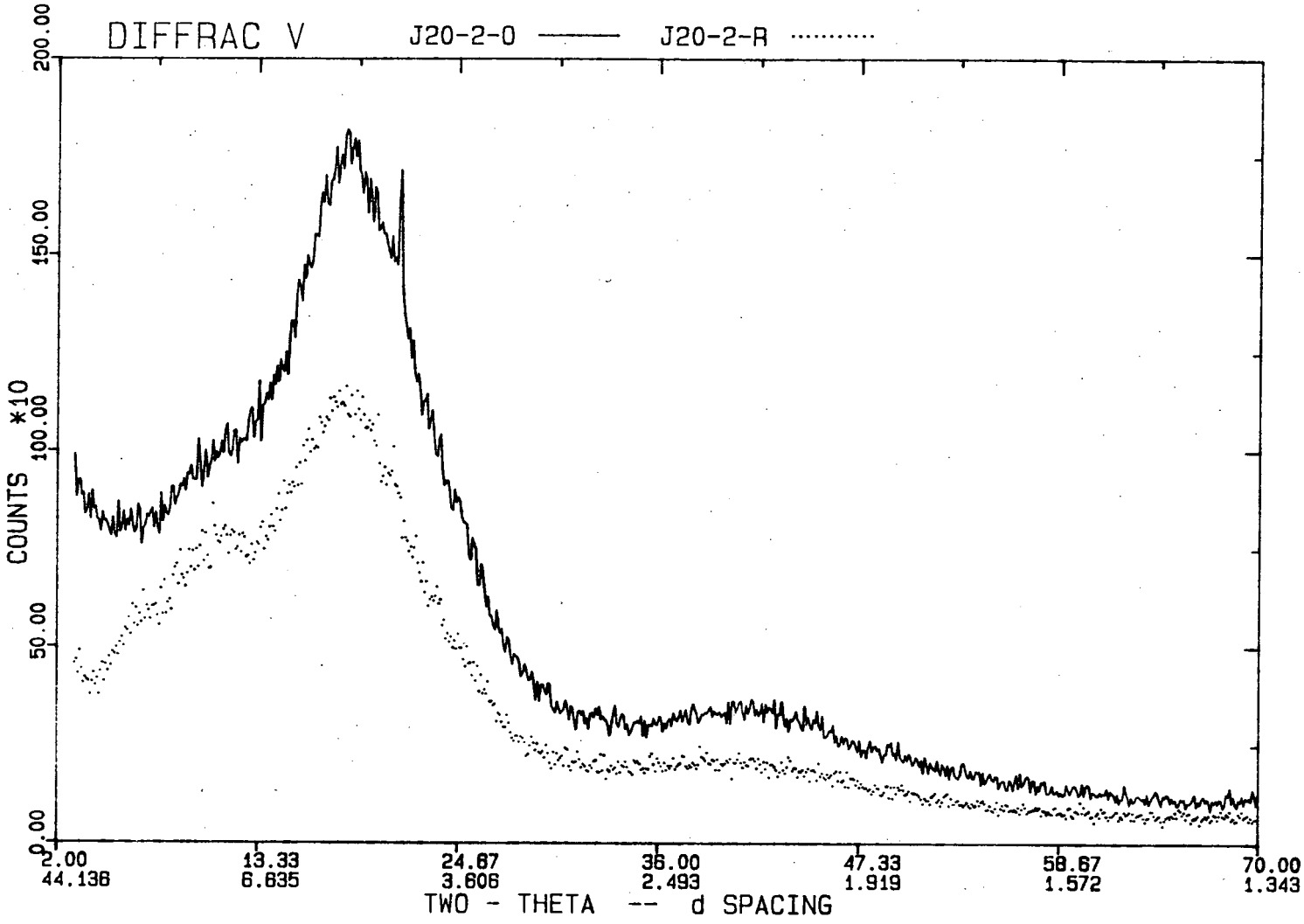
DIFFRAC V
J20-2-0
J20-2-R
COUNTS *10
200.00
150.00
100.00
50.00
0.00
2.00
44.136
13.33
6.635
24.67
3.606
36.00
2.493
47.33
1.919
58.67
1.572
70.00
1.343
TWO - THETA -- d SPACING

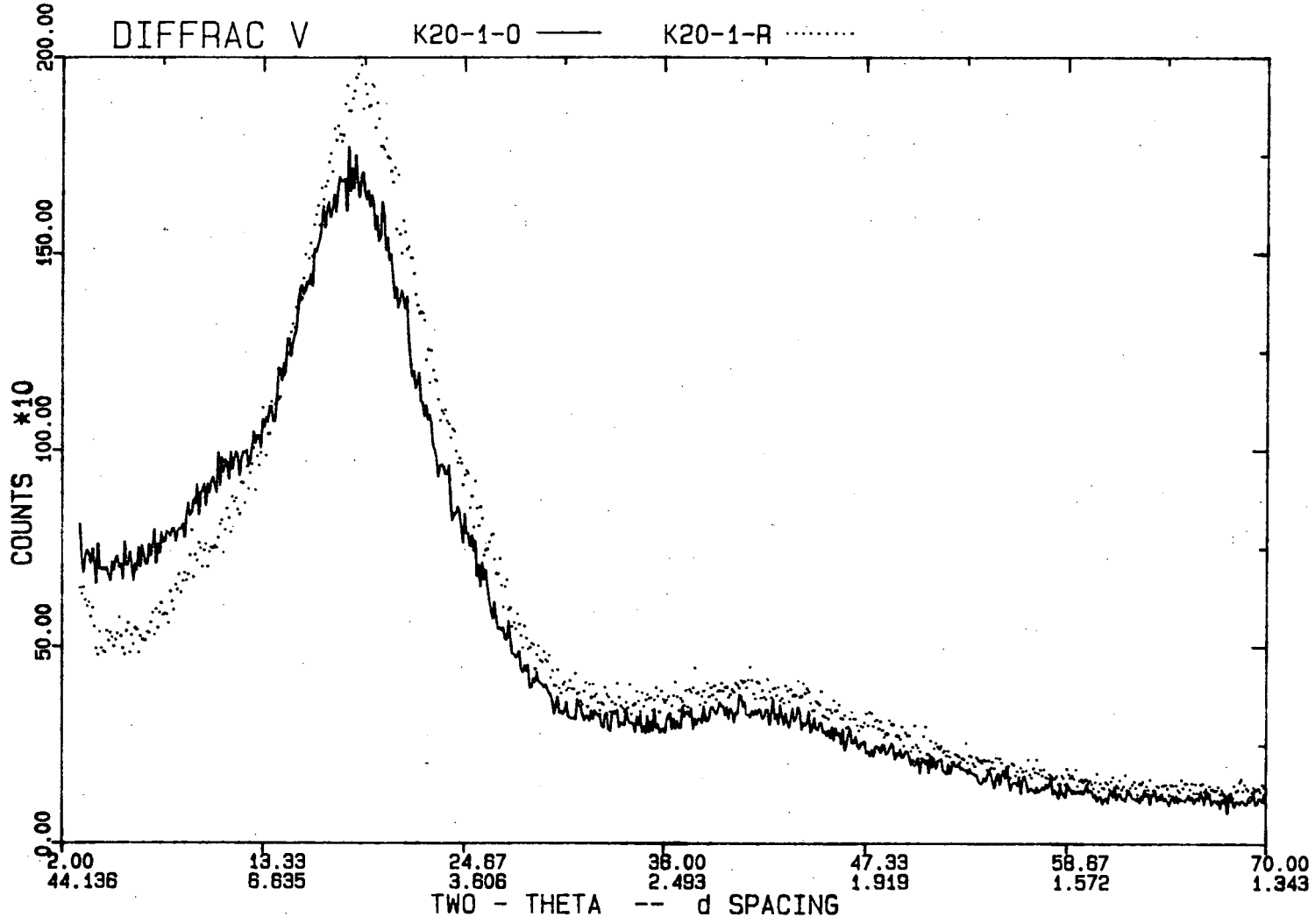
DIFFRAC V
K20-1-0
K20-1-R
COUNTS *10
200.00
150.00
100.00
50.00
0.00
2.00
44.136
13.33
6.635
24.67
3.606
36.00
2.493
47.33
1.919
58.67
1.572
70.00
1.343
TWO - THETA -- d SPACING

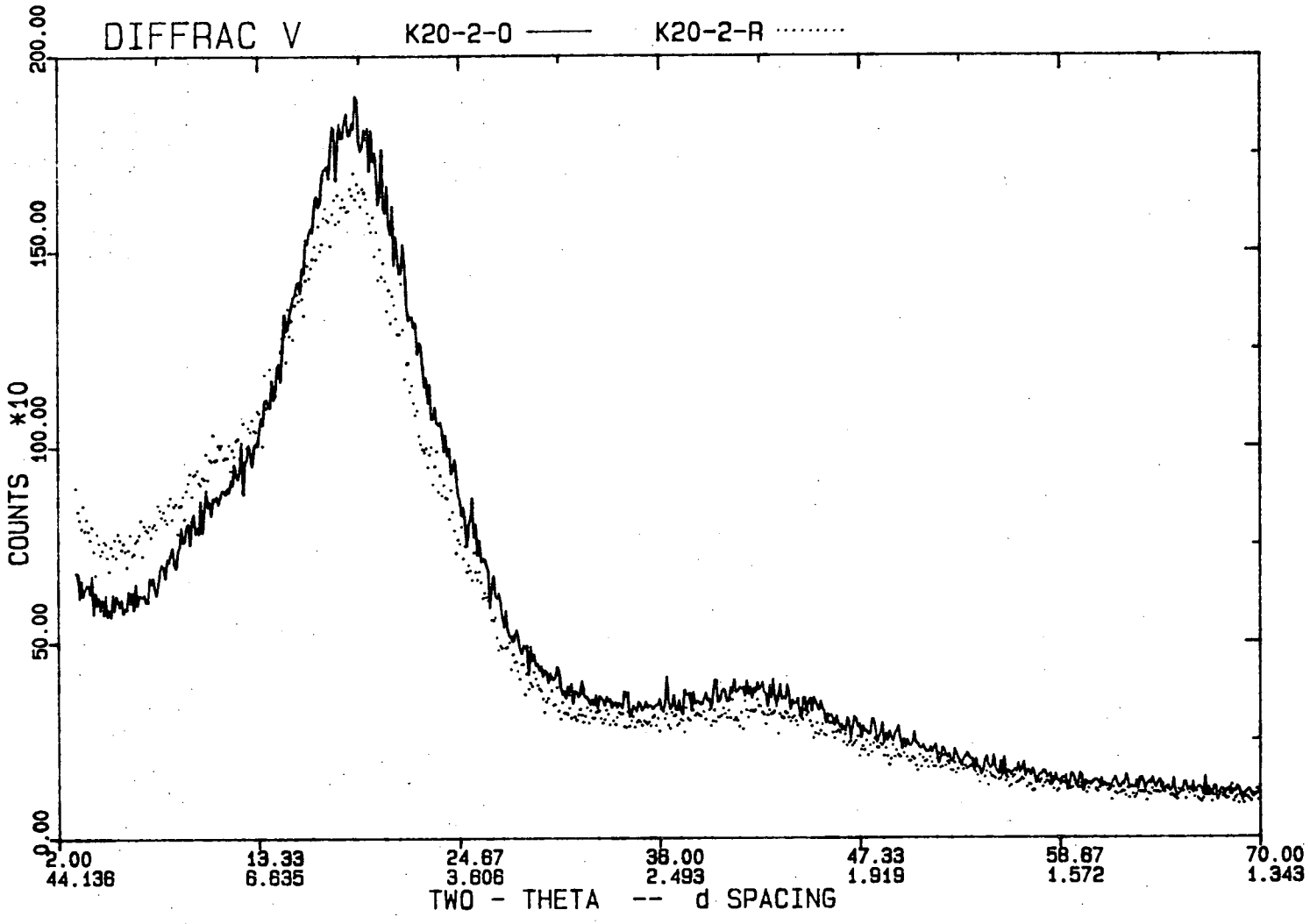
DIFFRAC V
K20-2-0
K20-2-R
200.00
150.00
100.00
50.00
0.00
COUNTS *10
2.00
44.136
13.33
6.635
24.67
3.606
36.00
2.493
47.33
1.919
58.67
1.572
70.00
1.343
TWO - THETA -- d SPACING